Fuel Processing Technology 233 (2022) 107310

Contents lists available at ScienceDirect

Fuel Processing Technology

journal homepage: www.elsevier.com/locate/fuproc

A review on the valorization of CO_2. Focusing on the thermodynamics and catalyst design studies of the direct synthesis of dimethyl ether

A. Ateka *, P. Rodriguez-Vega, J. Ereña, A.T. Aguayo, J. Bilbao

Department of Chemical Engineering, University of the Basque Country UPV/EHU, P.O. Box 644, 48080 Bilbao, Spain

ARTICLE INFO

Keywords:
DME
Syngas
Fuels
Bifunctional catalyst
Thermodynamics
Core-shell catalyst

ABSTRACT

The direct synthesis of dimethyl ether (DME) on bifunctional catalysts is highly attractive for valorizing CO_2 and syngas derived from biomass gasification and is a key process to reduce greenhouse gas emissions. DME economy (conventionally based on its use as fuel) arouses growing interest, in parallel with the development of different routes for its conversion into hydrocarbons (fuels and chemicals) and H_2 production. This review, after analyzing different routes and catalytic processes for the valorization of CO_2, focuses on studies regarding the thermodynamics of the direct synthesis of DME and the advances in the development of new catalysts. Compared to the synthesis of methanol and the synthesis of DME in two stages, carrying out the reactions of methanol synthesis and its dehydration to DME in the same reactor favors the formation of DME from CO_2 and from CO_2 co-fed with syngas. Starting from the experience for syngas feedstocks, numerous catalysts have been studied. The first catalysts were physical mixtures or composites prepared by extrusion of methanol synthesis catalysts (CuO-ZnO with different carriers and promoters) and dehydration catalysts (mainly γ-Al_2O_3 and HZSM-5 zeolite). The performance of the catalysts has been progressively improved with different modifications of the composition and properties of the components to upturn the activity (lower for the hydrogenation of CO_2 than for CO) and selectivity, and to minimize the deactivation by coke and by sintering of the metallic function. The core-shell configuration of the bifunctional catalyst allows physically separating the environments of the reactions of methanol synthesis and its conversion into DME. The confinement facilitates the extent of both reactions and improves the stability of the catalyst, since the synergies of the deactivation mechanisms are eliminated.

Abbreviations: Al MAS-NMR, Al magic-angle spinning nuclear magnetic resonance; BTX, Benzene, toluene and xylenes; C_1-C_5, Hydrocarbons containing 1 to 5 carbon atoms; C_{5+}, Aliphatic; CCS, Carbon capture and storage; CI, Compression ignition; CIZO, Cu-In-Zr-O metallic catalyst; CNG, Compressed natural gas; CNT, Carbon nano tubes; CO-FTS, Fisher Tropsch synthesis from CO; CO_2-FTS, Fischer Tropsch synthesis from CO_2; CO_X, CO + CO_2 mixture; CZA, CuO-ZnO-Al_2O_3 metallic catalyst; CZMn, CuO-Zn-MnO metallic catalyst; CZZr, CuO-ZnO-ZrO_2 metallic catalyst; DAC, Direct air capture; DEA, Diethanolamine; DGA, Diglycolamine; DIPA, Diisopropanolamine; DMC, Dimethyl carbonate; DME, Dimethyl ether; DS, Dimethyl ether synthesis; DTG, Dimethyl ether to gasoline; DTO, Dimethyl ether to olefins; EB, Ethylbenzene; ECBM, Enhanced coal-bed-methane; EDR, Ethanol dry reforming; EGR, Enhanced gas recovery; EOR, Enhanced oil recovery; ESR, Ethanol steam reforming; FCC, Fluid catalytic cracking; FE, Ferrierite; FT, Fischer-Tropsch; GDR, Glycerol dry reforming; GHG, Greenhouse gases; GTL, Gas to liquid; HCCI, Homogeneous charge compression ignition; IPCC, Intergovernmental panel on climate change; LHHW, Langmuir-Hinshelwood-Hougen-Watson; LHV, Low heating value; HPAs, Heteropolyacids; LPG, Liquefied petroleum gases; MA, Methyl acetate; MDEA, Methyl-diethanolamine; MDR, Methane dry reforming; MEA, Monoethanolamine; MeOH, Methanol; MFTS, Modified Fischer-Tropsch synthesis; MOF, Metal organic framework; MOR, Mordenite; MS, Methanol synthesis; MSR, Methane steam reforming; MTBE, Methyl tertbuthyl ether; MTD, Methanol to dimethyl ether; MTG, Methanol to gasoline; MTO, Methanol to olefins; MTP, Methanol to paraffins; NG, Natural gas; OCM, Oxidative coupling of methane; ODE, Oxidative dehydrogenation of ethane; ODP, Oxidative dehydrogenation of paraffins; OX/ZEO, Metal oxide and zeolite composed catalyst; PEM, Proton exchange membrane; PEMFC, Proton exchange membrane fuel cells; PMMA, Polymethyl-methacrylate; POM, Partial oxidation of methane; SAPO, Silicoaluminophosphates; SOFC, Solid oxide fuel cells; TEA, Triethanolamine; TOS, Time on stream; TPO, Temperature programmed oxidation; TRL, Technological readiness level; WGS, rWGS, Water gas shift and reverse water gas shift reactions, respectively; XPS, X-ray photoelectron spectroscopy.

* Corresponding author.
E-mail address: ainara.ateka@ehu.eus (A. Ateka).

https://doi.org/10.1016/j.fuproc.2022.107310
Received 9 February 2022; Received in revised form 3 May 2022; Accepted 3 May 2022
Available online 14 May 2022

1. Introduction

The increasing estimates of CO_2 emissions, at a rate of 33 GT/year, a concentration forecast of 570 ppm by the end of the 21st century, and the serious consequences of climate change, as numerous natural disasters (heat waves, hurricanes, wildfires, droughts, sea level rise), are some of the most pressing problems for humanity. In this scenario, a deep transition period towards a zero-emissions energy model, based on the increasing utilization of renewable energy sources, may be expected. The taxes to the countries for CO_2 emissions [1] and the economic consequences of climate change (valued at a loss of 31 billion-dollar in 2017 [2]) are also an incentive to take measures aimed at reducing the net emissions of CO_2.

The technologies for CO_2 capture and storage/sequestration (CCS) have received extensive attention [3]. The physical absorption (where CO_2 is scrubbed from the flue gas) is common for high CO_2 partial pressure. It is carried out at low temperature, with low energy requirement and it is favored using commercial solvents. Using chemical absorption, CO_2 present in low concentration can be separated reacting with alkanolamines or dissolved alkaline salts. Among the former, MEA (monoethanolamine), DEA (diethanolamine), TEA (triethanolamine), MDEA (methyldiethanolamine), DIPA (diisopropanolamine) and DGA (diglycolamine) are used. KOH is commonly used as alkaline reactant. Separating CO_2 using membranes requires lower capital cost and the equipment occupies smaller space. The membranes used are prepared with different materials: zeolites, carbon nanotubes (CNT), polyamides, polyether sulfone or polydimethyl phenylene oxide, among others [4].

Adsorption is effective for low CO_2 concentrations using zeolites, silica based-materials (microporous as SAPO-34 or mesoporous as MCM-41 or SBA-15), activated carbon, graphene, metal-organic frameworks (MOFs), lithium orthosilizate (Li_4SiO_4), lithium zirconate (Li_2ZrO_3) and other porous materials as adsorbents. For chemical adsorption, materials (mainly carbons) functionalized by polymeric amines (polyethylenimine, polypropylenimine, polyallylamine, polyaniline, amino dendrimers, and hyperbranched polyamines) are used [5,6]. In general, the capture capacity is higher for adsorption than for absorption (88–176 kg of CO_2 per kg of adsorbent, and 0.4–1.2 kg of CO_2 per kg of absorbent, respectively). Cryogenic distillation produces high purity liquid CO_2, and is an interesting method to treat gas at high pressure. However, the cost of this technology is high, due to the energy requirement for refrigeration. Electrochemical technology is another emerging alternative for CO_2 capture from mediums of different concentration. The characteristics of this technology and the development state have been explained by Sharifian et al. [7]. Using the "pH swing" concept, CO_2 can be captured and recovered, which facilitates its subsequent online valorization. Given the higher cost of this technology over others commonly used (and in particular with respect to absorption with amines), its economic viability requires using renewable energies and developing low-cost membranes.

CCS technologies for stationary sources contemplate the [8]: i) Direct air capture (DAC) for CO_2 removal from small sources and from the transport sector, responsible of 1/3 to 1/2 of total emissions, and; ii) moving to remote sites for large-scale CO_2 sequestration. To finance the expensive investments required by these technologies, it is essential to promote CO_2 upgrading generating an economic benefit. Among the CO_2 utilization technologies [9–24], two objectives are distinguished, the direct use (pure or in solution), and its use as feedstock for the production of chemicals and fuels (use after transformation). The direct use of CO_2 for carbonated drinks is associated to the origin of the commercialization of soft drinks. It is also used as fire extinguisher, refrigerant, anesthetic gas, dry ice, solvent, process fluid and welding medium. Other routes directly using CO_2 on a larger scale comprise methods for the extraction of mineral sources: EOR (enhanced oil recovery), ECBM (enhanced coal-bed methane) recovery, and EGR (enhanced gas recovery). The use of CO_2 in micro-algae cultivation along with free sunlight has the advantage of operating at mild conditions, but requires controlling the pH (in the 6.6–10.5 range) and a sealed reactor.

The transformation of CO_2 into chemicals and fuels is difficult, given the thermodynamic stability of the molecule due to its structure, constituted by a carbon atom with its four electrons bonded to oxygen atoms through covalent double bonds (O=C=O). Moreover, the Gibbs free energy of CO_2 ($\Delta G^0 = -394$ kJ mol^{-1}) is much lower than that of the possible products of its transformation. Consequently, the challenges of the processes for this transformation are very demanding. Among them [11]: i) Great energy supply from renewable and carbon-neutral sources; ii) the use of high temperature and/or pressure, or; iii) the intervention of catalysts active sites, organisms or biological species capable for activating the reactions involved. In Fig. 1 different routes for the transformation of CO_2 are gathered.

The processes for CO_2 transformation through chemical and electrochemical reactions have multiple technological alternatives. As to the electrochemical reduction regards, two possible routes are distinguished [25], with CO_2 as intermediate to produce formic acid, or CO and hydrocarbons (mainly methane). Jiang et al. [26] have summarized the recent advances in understanding the reaction mechanism and exploring cathode materials. The external energy source in these processes can be thermal, electrocatalytic or photocatalytic, providing the opportunity to these processes to be integrated with renewable energy production (solar, wind and marine). In the artificial photosynthesis strategy, semiconductor catalysts convert CO_2 into hydrocarbons with solar energy through a multielectron transfer mechanism. In this mechanism, TiO_2 (commonly used as catalyst) absorbs light upon illumination and generates a pair of photo-excited electrons and holes. These initiators interact with H_2O and CO_2 molecules to produce methane and other products by selecting appropriate catalyst (usually prepared by doping TiO_2) and conditions [27].

However, the chemical reactions occur at a high rate and are carried out in an easier-to-scale reactor. Some authors classify the chemical transformation pathways according to their energy requirements [13]. Kamkeng et al. [11] make a comparison of the CO_2 transformation routes according to different criteria (technological maturity, cost considerations, market analysis and amount of CO_2 used). Taking into account the technological readiness level (TRL) tool (Fig. 2), synthesis of methane and methanol have high TRL values (7–9). The main advantages of hydrogenation processes focus on the market interest of CO_2-derived fuels and raw materials (gasoline, methanol, DME, methane, olefins, aromatics), and on the amount of CO_2 used in their production (2.6 t fuel/t CO_2 in Fischer-Tropsch synthesis). Nonetheless, in terms of cost per ton of product, the interest of these processes is conditioned by the price of H_2.

2. Catalytic processes for CO_2 conversion

The different catalytic and electrocatalytic processes for CO_2 conversion into fuels and chemical products have been reviewed several times [10,13,28–31], and these are schematized in Fig. 3. It can be observed that some products are, at the same time, raw materials for other processes. That is, oxygenates (methanol and DME) with interest as fuels, are converted into olefins (MTO and DTO processes, respectively) [32,33], into hydrocarbons in the gasoline range (MTG and DTG processes, respectively) [34,35], or in BTX aromatics [36]. These reactions proceed according to the dual cycle mechanism, with arenes and olefins as intermediates [37], and the product distribution is dependent on the acidity and shape selectivity of the catalyst (based on SAPO-34 in the MTO process and based on HZSM-5 zeolite in the other processes). Besides, methanol and DME are hydrogen vectors (through reforming) [38,39]. Methanol (MeOH) can also be selectively dehydrogenated towards formaldehyde [40], which will be used in polymers and resin production.

Furthermore, CO_2 allows for the production of synthesis gas (H_2/CO) through the reverse Water-Gas-Shift (rWGS) reaction (where CO_2 takes

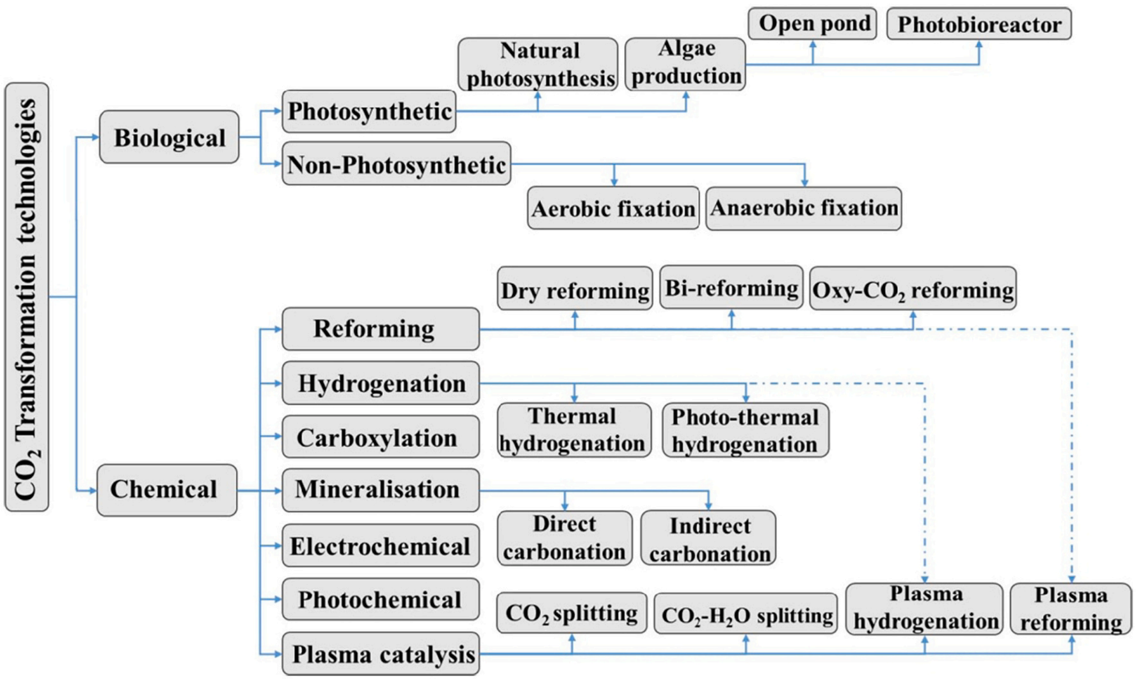

Fig. 1. Routes for the transformation of CO_2 through chemical, biological and electrochemical processes. Adapted from the work by Kamkeng et al. [11]. Copyright 2021, Elsevier.

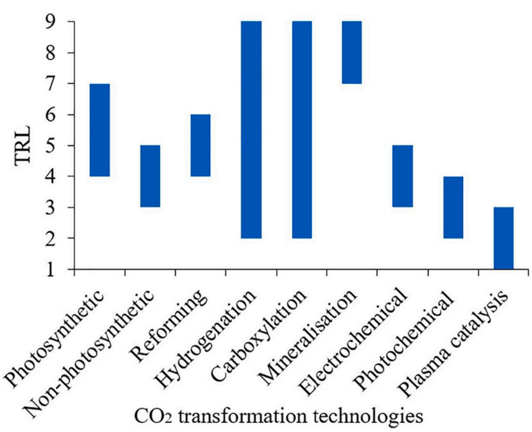

Fig. 2. Technology readiness level (TRL) of CO_2 transformation technologies. Reproduced from the work by Kamkeng et al. [11]. Copyright 2021, Elsevier.

the role of H_2 acceptor) [41] or by dry reforming of methane, hydrocarbons or oxygenates (where CO_2 acts as oxidant agent) [42]. In addition, synthesis gas or CO_2 directly can be converted into a hydrocarbons mixture, either through the Fischer-Tropsch (FT) route [43] or with MeOH/DME as intermediates, over bifunctional catalysts [44,45]. These reactions can be controlled by choosing selective acidic functions for the production of C_{2+} alcohols, isoparaffinic gasoline or aromatics. From the energy requirement point of view, the reactions in which the second reactant has a higher Gibbs free energy have lower energy requirement and so, are more favorable. However, CO_2 hydrogenation reactions require a large amount of external energy and the use of a catalyst to overcome the activation barrier. According to this classification, already suggested by De et al. [46], the characteristics of the CO_2 conversion processes are described in the next sections, distinguishing those not requiring H_2 as reactant (Section 2.1) and hydrogenation processes (Section 2.2).

2.1. Reactions without H_2 as reactant

These reactions are of greater interest in an energy transition state like the current one, prior to the availability of H_2 produced from sustainable sources and using renewable energies.

2.1.1. Oxidative dehydrogenation

2.1.1.1. Methane as reactant. The direct conversion of methane into ethane (Eq. (1)) or into ethylene (Eq. (2)), through oxidative coupling (OCM) forming C-C bonds, has a growing interest in valorizing burgeoning natural gas reserves, in which CO_2 content may reach 10%.

$$2CH_4 + CO_2 \rightarrow CH_3CH_3 + CO + H_2O \quad (1)$$

$$2CH_4 + 2CO_2 \rightarrow CH_2CH_2 + 2CO + 2H_2O \quad (2)$$

These reactions occur through the following mechanism [47]: 1) Cleavage of methane C-H bonds in the active sites of the catalyst, forming CH_3* and CH_2* radicals; 2) dissociation of CO_2 towards CO and O* active oxygen; 3) coupling of these radicals; 4) recombination of CH_3* and CH_2* radicals; 5) dehydrogenation, either oxidative or radical, of ethane to ethylene. The catalysts must be selective, avoiding the formation of syngas by dry reforming. The strong basic metallic oxide catalysts used can be grouped into [19,48]: 1) Pure oxides of the lanthanide series, of which La_2O_3 shows the greatest performance; 2) basic oxides loaded with Group 1 or 2 cations (Li/MgO, Ba/MgO, and Sr/La_2O_3); 3) transition metal oxides containing Group 1 cations, and; 4) redox catalysts, like CeO_2 modified by Group 1 and 2 cations. Over ZrO_2/TiO_2 catalysts acetic acid is formed by the insertion of the adsorbed CO_2 into the CH_3* species, followed by the hydrogenation with H* in the adsorption of methane [49].

2.1.1.2. Paraffins as reactants. The production of light olefins through oxidative dehydrogenation of their corresponding paraffins (ODP) (Eq. (3)) is an upgrade. In this manner, raw materials are obtained for the production of polyolefins and, at the same time, the high-energy requirement of steam cracking, as well as the rapid deactivation of the

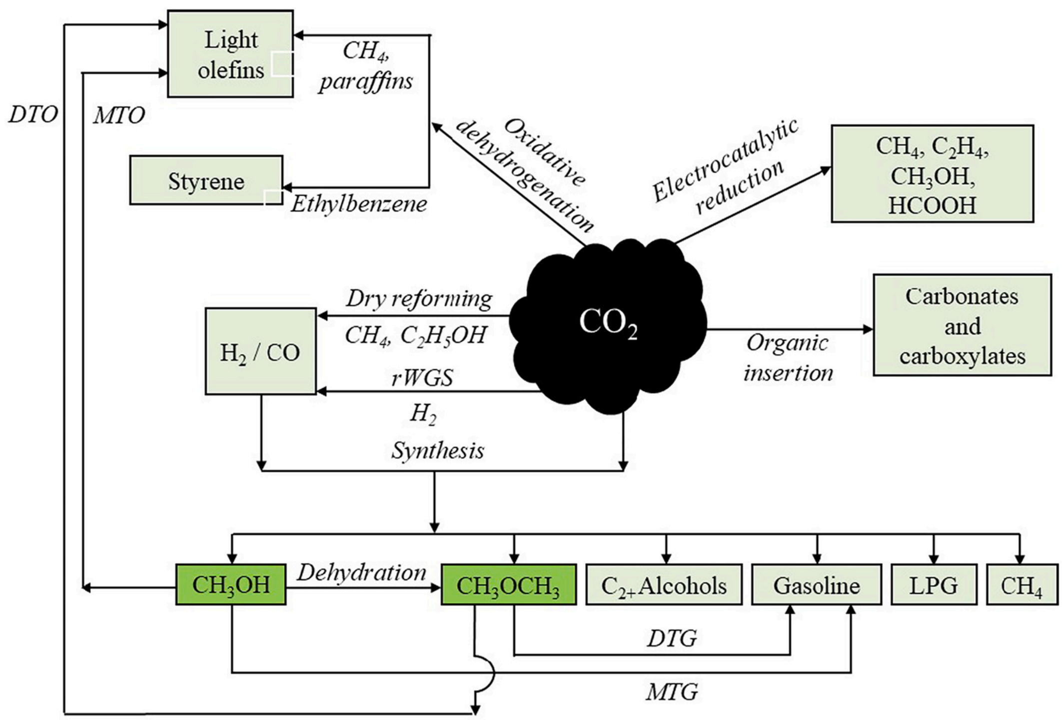

Fig. 3. Catalytic and electrocatalytic routes for obtaining fuels and raw materials from CO_2.

catalyst due to coke deposition (attenuated by the gasification capacity of CO_2) are avoided.

$$C_nH_{2n+2} + CO_2 \rightarrow C_nH_{2n} + CO + H_2O \quad (3)$$

The most studied catalysts for ODP are based on redox properties, principally MoO_3, Cr_2O_3 and V_2O_5. CeO_2 (with well-established redox properties), ZrO_2, TiO_2, SiO_2 and zeolites (HZSM-5, MCM-41) have been used as supports, since the mesoporosity of the latter is known to favor the dispersion of metallic oxides [50]. The basic character of these catalysts favors CO_2 adsorption and olefins desorption, while paraffins dehydrogenation is activated by the presence of the acidic sites.

ODP mechanism [51] considers the rWGS (Eq. (5)) reaction, where H_2, product of the dehydrogenation, is oxidized by CO_2. Furthermore, paraffin dry reforming (Eq. (6)) and coke deposits oxidation through reverse Boudouard reaction (Eq. (7)) are considered.

$$C_nH_{2n+2} \rightleftharpoons C_nH_{2n} + H_2 \quad (4)$$

$$H_2 + CO_2 \rightleftharpoons CO + H_2O \quad (5)$$

$$C_nH_{2n+2} + nCO_2 \rightarrow 2nCO + (n+1)H_2 \quad (6)$$

$$CO_2 + C \rightleftharpoons 2CO \quad (7)$$

The thermodynamic analysis of the CO_2 assisted dehydrogenation of ethane (ODE) shows the need for reaction temperatures above 550 °C for a good compromise between the extent of the hydrogenation and rWGS reactions according to Najari et al. [52]. These authors review the advances in this reaction, comparing the behavior of the most used catalysts. The catalysts are based on Ni, Ni-Fe, Cr_2O_3, Ga_2O_3, or CoO_x, and use acidic supports as γ-Al_2O_3, SiO_2, CeO_2, ZrO_2, TiO_2, SBA and zeolites (being HZSM-5 the most common).

Jiang et al. [53] classify the catalysts for CO_2 assisted dehydrogenation of propane (ODP) according to the nature of their metallic function, distinguishing: i) Redox-type catalysts (those based on CrO_x are the most used ones). The redox cycle is described in Eqs. (8)–(10) [54]; ii) non-redox type catalysts (Ga_2O_3 polymorphs, Ga_2O_3-Al_2O_3 solid solutions and mixed GaO_2-ZrO_2), and iii) other transition metal catalysts (Fe_2O_3, Fe-Ni, Mo_2C). As supports, the afore-mentioned ones for ODE, mesoporous zeolites (such as MCM-41) and activate carbons have been tested.

$$C_3H_8 + CrO_x \rightleftharpoons CrO_{x-1} + C_3H_6 + H_2O \quad (8)$$

$$CO_2 + CrO_{x-1} \rightleftharpoons CO + CrO_x \quad (9)$$

$$H_2 + CrO_x \rightleftharpoons Cr_{x-1} + H_2O \quad (10)$$

It should be pointed out that the dehydrogenation of C_{5+} paraffins is not viable due to the fast catalyst deactivation by coke deposition.

2.1.1.3. Ethylbenzene as reactant. The oxidative dehydrogenation of ethylbenzene (ODE) to styrene is of great interest to avoid selectivity limitations and catalyst deactivation by coke in the conventional industrial process without oxidant agent, which require an excess of vapor. ODE with CO_2 as dehydrogenating agent, with the steps described in Eqs. (11), (12) and (5), results in a styrene selectivity of 97% and its energy demand is of approximately a tenth of that of the conventional process. Therefore, it offers an attractive option for satisfying the growing demand of styrene (yearly production of 14.6 Mt) in the production of synthetic rubber, polystyrene and styrene-acrylonitrile copolymers.

$$C_6H_5CH_2CH_3 + CO_2 \rightarrow C_6H_5CH = CH_2 + H_2O + CO \quad (11)$$

$$C_6H_5CH_2CH_3 \rightarrow C_6H_5CH = CH_2 + H_2 \quad (12)$$

Fe_2O_3/CeO_2 catalyst has a high activity attributable to the redox activity of the Ce sites (changing Ce^{4+} and Ce^{3+}), promoted by Fe^{3+} and whose presence improves the oxygen storage capacity of Ce [55]. The relevance of both the redox efficiency and the mesoporous structure of the support has been proven by Burri et al. [56] using CeO_2-ZrO_2 supported on SBA-15. VO_x, MoO_x, WO_x, CrO_x-based catalysts have also been studied, either supported on SiO_2, mesoporous zeolite (MCM-41) or active carbon incorporated in hydrotalcite (Mg-V-Al structures) [57]. With the latter, Sakurai et al. [58] obtained an ethylbenzene (EB) conversion of 67.1% and styrene selectivity of 80%. Different mechanisms have been proposed for ODE from EB, considering the three step mechanism the most favorable thermodynamically [59]:

$$C_8H_{10} + os \rightleftharpoons C_8H_{10} - os \tag{13}$$

$$C_8H_{10} - os + rs \rightarrow C_8H_8^{\bullet} + 2H - os \tag{14}$$

$$H - os + H - os \rightarrow H_2 + 2os \tag{15}$$

$$CO_{2\ (g)} + rs \rightleftharpoons CO_{(g)} + O - rs \tag{16}$$

$$H_{2\ (g)} + O - rs \rightleftharpoons H_2O_{(g)} + rs \tag{17}$$

$$C_8H_8 - rs \rightarrow C_8H_8 + rs \tag{18}$$

where "*os*" refers to the oxidizing sites and "*rs*" to the reducing sites.

2.1.2. Dry reforming

Beyond CO_2 transformation, the lower energy requirement of dry reforming than that of steam reforming is a remarkable advantage, although H_2 yield and the resulting H_2/CO ratio are lower. Its application has extended to the conversion of fossil sources (methane) and sources derived from biomass (as ethanol, glycerol and bio-oil).

2.1.2.1. Methane as reactant. Methane dry reforming (MDR, Eq. (19)) is the principal route for the current production of H_2. Although CH_4 is a fossil source, the process has good future prospects for biogas feedstocks (with CH_4 and CO_2 as major components) derived from the anaerobic digestion of organic waste materials [60].

$$CH_4 + CO_2 \rightarrow 2H_2 + 2CO \tag{19}$$

The reaction steps of MDR on the catalyst surface involve:

1. Methane adsorption and abstraction of hydrogen:

$$CH_4 \rightarrow CH_4^* \rightarrow CH_{4-x}^* + \chi H^* \tag{20}$$

2. CO_2 adsorption and abstraction of an oxygen atom:

$$CO_2 \rightarrow CO_2^* \rightarrow CO^* + O^* \tag{21}$$

3. The formation of CO and hydrogen on the surface:

$$CH^* + O^* \rightarrow CO^* + H^* \tag{22}$$

4. The formation of H_2O:

$$O + H^* \rightarrow OH^* + H^* \rightarrow H_2O^* \rightarrow H_2O \tag{23}$$

5. The recombination of hydrogen on the surface and desorption:

$$H^* + H^* \rightarrow H_2^* \rightarrow H_2 \tag{24}$$

In addition, the WGS reaction (Eq. (5)), the coke formation reactions by decomposition of CH_4 (Eq. (25)) and formation/gasification of coke by the Boudouard reaction (Eq. (7)) take place.

$$CH_4 \rightarrow C + 2H_2 \tag{25}$$

The main limitations of MDR are the high-energy requirement (even being lower than for steam reforming, MSR) (heats of 247 kJ mol^{-1} and 228 kJ mol^{-1}, respectively), since temperature above 800 °C is required; and catalyst stability, affected by sintering and coke formation. The energy demand is reduced and coke formation is attenuated by combining MDR with MSR and POM (partial oxidation of methane). For that purpose, according to the tri-reforming concept, methane is co-fed with H_2O and O_2 [61]. Li et al. [62] have made a review on the advances on the technologies for heat supply, alternative to fossil fuels, including photochemical and electrochemical, plasma-assisted, solar energy, operating in solid oxide fuel cells, coupled with inorganic membranes and chemical looping reforming.

Noble metal and transition metal based-catalysts have been exhaustively studied [63–67]. According to activity they can be ordered as follows [68]: Ru ≈ Rh > Ni ≈ Ir > Pt > Pd > Co. Ni catalysts are generally used regarding their high activity and low cost. Anyhow, sintering and coke formation is quite fast for these catalysts. A great deal of effort has been addressed to improve the stability of Ni catalysts in MDR. Thus, various strategies have been used for attenuating sintering through strengthening the metal-support interactions: forming bimetallic catalysts, where metal is dispersed in nanoparticles [69], incorporated within perovskites [68] or with spinel and core-shell configurations [62]. The stability of Ni catalysts has also been upgraded incorporating in the support (Al_2O_3, SiO_2) basic promoters as alkaline metals (Li, Na, K), rare earth metal oxides (La_2O_3, CeO_2, Y_2O_3, Sm_2O_3) and reducible transition metal oxides (ZrO_2, TiO_2, MnO_2, MoO_3). These materials promote Ni dispersion, metal-support interaction, oxygen mobility and CO_2 and H_2O adsorption, attenuating coke formation [70–72]. A strategy to avoid catalyst deactivation by coke in the dry reforming of methane is to carry out the reaction without catalyst, with acetylene as intermediate. However, very high temperature is required for this approach (1400–1800 °C) [73].

2.1.2.2. Oxygenates as reactants. Although the stoichiometry of ethanol dry reforming (EDR) corresponds to Eq. (26), in parallel, the steam reforming (ESR) reaction will also take place, because the H_2O content in the ethanol (bio-ethanol) obtained from hydrolysis/fermentation of biomass is remarkable. This coexistence of dry and steam reforming also occurs for other bio-alcohols (such as butanol) and biomass-derived oxygenates, such as glycerol and oxygenates in bio-oil (product of the fast pyrolysis of biomass), whose stoichiometry of dry reforming ideally corresponds to Eqs. (27) and (28) respectively. Furthermore, all these bio-oxygenates undergo decomposition and dehydrogenation reactions, which require a catalyst and suitable reaction conditions to reform the by-products (CH_4, olefins and aldehydes) and to minimize the formation of coke.

$$C_2H_5OH + CO_2 \rightarrow 3CO + 3H_2 \tag{26}$$

$$C_3H_8O_3 + CO_2 \rightarrow 4CO + 3H_2 + H_2O \tag{27}$$

$$C_xH_yO_z + CO_2 \rightarrow CO + H_2 \tag{28}$$

These reactions have received less attention than bio-oxygenates steam reforming and the main challenge has been achieving catalyst stability [74]. In EDR catalysts based on noble and transition metals have been studied. Da Silva et al. [75] propose a mechanism for the Rh/CeO_2 catalyst involving the role of oxygen vacancies in the CeO_2. As to attenuate coke deactivation high values of temperature (around 1073 K) and an ethanol/CO_2 ratio (around 3) are required [76]. The combination of SBA-15 (with high specific surface) with CeO_2 (redox capacity) in the support improves the activity of the catalyst [77]. Comparing different supports, Drif et al. [78] determined the following activity: Rh/NiO-Al_2O_3 > > Rh/Al_2O_3 ≈ Rh/MgO-Al_2O_3 ≈ Rh/CeO_2-Al_2O_3 > Rh/ZrO_2-Al_2O_3 ≈ Rh/La_2O_3-Al_2O_3 at 1073 K. The high activity of Rh/NiO-Al_2O_3 was attributed to the smaller Rh particle size and to the presence of $NiAl_2O_4$ spinel phase, which limited the migration of Rh in Al_2O_3. Ir/CeO_2 catalyst has also shown a good behavior in the EDR reaction at 973 K, with the complete elimination of coke formation on the catalyst [79].

Ni-based catalysts are also very active, according to CO_2 conversions following the order: Ni/CeO_2 ≈ Ni/Al_2O_3 > Ni/MgO ≈ Ni/ZrO_2. To attenuate sintering and coke deactivation, the interest of incorporating Co and promoters with redox capacity has been assessed [80,81]. The activity of Cu and Co as primary catalysts and the effect of promoters with redox capacity for enhancing their stability has also been studied [82,83].

The studies on glycerol dry reforming (GDR) are focused on Ni-based catalysts, with particular emphasis on the influence of types of supports and promoters. As CO_2 and glycerol are adsorbed at different sites of the bifunctional catalyst, the reaction is controlled by the glycerol adsorption step. The complex mechanism of glycerol conversion explains the fast deactivation by coke, whose precursors are the by-products of the reaction (CO, CH_4, aldehydes, hydrocarbons). To attenuate coke deactivation, limiting the acidity of the support is essential. Thus, γ-Al_2O_3 catalyst is very active, but undergoes fast deactivation mainly due to the deposition of whisker type of carbon on the catalyst surface [84]. The deposition of La_2O_3 on the Al_2O_3 support prior to Ni, increases Ni dispersion and attenuates coke formation [85]. Several attempts have been made to optimize the Ni-based catalysts for higher activity and stability. Among these the use of CaO [86] or SiO_2 [87] or ternary oxides (Al_2O_3–ZrO_2–TiO_2) [74] as supports, the addition of Re to the catalyst [88] or Ag as promoter [87].

Precious metal (Rh, Ru, Ir, Pd and Pt) catalysts with MgO stabilized Al_2O_3 as support were also tested for their activity towards GDR by Tavanarad et al. [89]. It should be noted, that after the fast initial deactivation due to whisker carbon, these catalysts maintain a pseudosteady state.

2.1.3. Chemicals production

Acetic acid production is an example of an opportunity to valorize low cost reactants like CO_2 and CH_4. The production of benzoic acid from CO_2 and benzene is equally interesting. Furthermore, acrylic acid production through the direct carboxylation of ethylene with CO_2 on Ni catalysts (Eq. (29)) is of great interest. This reaction is particularly interesting for valorizing CO_2 generated in the ethylene production units by steam cracking of naphthas [90].

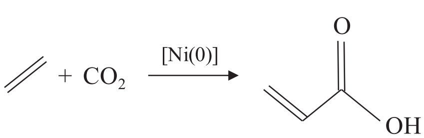

(29)

Here, CO_2 is a raw material for the production of linear and cyclic carbonates. Among the first ones, dimethyl carbonate (DMC) $(CH_3O)_2CO$, with low toxicity, is used as solvent, gasoline additive and reactant in alkylation and acylation reactions. It is produced by reacting with methanol (Eq. (30)). Several catalysts have been reported for this reaction (based on Cu and Cu-Ni, and on CeO_2) [91–96].

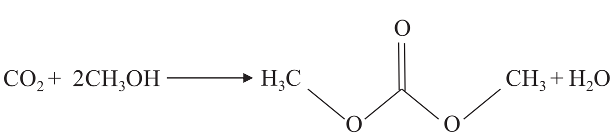

(30)

Cyclic carbonates (of ethylene, propylene, cyclohexane, styrene and others) are produced by the addition of CO_2 to an epoxy (Eq. (31)). They are used as solvents, electrolytes and raw material in the production of poly-carbonates, other polymeric materials and fine chemicals (dialkyl carbonates, glycols, carbamates, pyrimidines, *etc.*). The formation reactions are catalyzed by alkali metal halides, metal oxides, zeolites and organic bases [97].

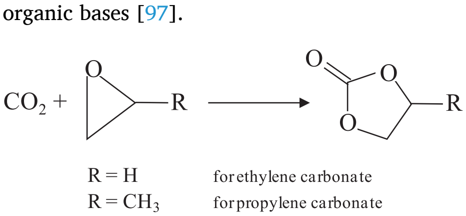

(31)

Acetylsalicylic synthesis ($CH_3COOC_6H_4COOH$) is an example of the insertion capacity of CO_2 in the C-H bonds of alkenes, aromatics or olefins. The products of greatest interest are carbonic acids, esters, lactones, and heterocyclic; in other words, compounds with functional groups potentially applicable as solvents, plasticizers, detergents, antioxidants, sun-protection agents, *etc.* [98].

CO_2 is valorized in the NH_3 production industry itself for the synthesis of urea (carbamide, $(NH_2)_2CO$). This consists of the carbamate (H_2N-$COONH_4$) (Eq. (32)) formation reaction and further dehydration towards urea (Eq. (33)). Xiang et al. [99] reach a CO_2 conversion up to 82.16% at atmospheric pressure and 20 °C. According to the stoichiometry, to obtain 1 t of urea 0.75 t of CO_2 are required. Nevertheless, urea is principally used as fertilizer, with the role of releasing NH_3 (adsorbed by plants) and CO_2. Therefore, this route would not diminish CO_2 emissions. Urea production at room temperature has been studied by means of electrochemical synthesis by coupling CO_2 and N_2 in H_2O using PdCu/TiO_2 electrocatalyst [100].

$$2NH_3 + CO_2 \rightleftharpoons H_2N - COONH_4 \tag{32}$$

$$H_2N - COONH_4 \rightleftharpoons (NH_2)_2CO + H_2O \tag{33}$$

Other polymers, like aliphatic polycarbonates, are produced by the reaction of CO_2 with epoxides or through transesterification of diols with DMC. They are substitutes of polyethers for the fabrication of polyurethane (formed by urethane bonds, $-N-(C=O)-O-$) [101]. In the same way, by the reaction of CO_2 with epoxides, aromatic polycarbonates based on bisphenol can be synthesized. Polyoxymethylene is another polycondensation polymer that can be produced from CO_2 and 1,3,5-trioxane (in this case with formic acid as intermediate). Although polyoxymethylene incurs a higher cost than poly- ethylene and propylene, it provides a higher mechanical resistance. Moreover, using another intermediate (such as methanol) CO_2 can be applied in the large scale production of polymethyl-methacrylate (PMMA).

2.2. CO_2 hydrogenation routes

In different reviews the main advances conducted in these routes are collected [102–106]. The scheme in Fig. 4 (reproduced from [106], adapted from [107,108]) includes the main routes, which according to the products can be classified as: routes with C1 compounds as products (methane, carbon monoxide, methanol, formaldehyde); and those that form compounds with 2 or more carbon atoms (hydrocarbons and oxygenates). The mechanisms for these routes are significantly different, and, consequently, have been studied under different process conditions and with different catalysts.

As aforementioned, the hydrogenation routes in Fig. 4 require external energy supply and the use of catalysts, due to unfavorable thermodynamics. In Table 1 the standard enthalpy and Gibbs free energies values of different CO_2 hydrogenation reactions are listed (values taken from [46,109]). The role of the conditions (pressure, temperature, H_2/CO_2 ratio) on thermodynamics is important to achieve an acceptable extent of the reaction and adequate products distribution, but the use of active, selective and stable catalysts is also necessary.

2.2.1. Methane production

Even if alternative routes for CO_2 methanation are studied, including photosynthesis and photocatalysis [110], electrochemical reduction [111] and biological conversion [112], the main attention is focused on the thermal catalytic process [113,114]. It proceeds with the following stoichiometry:

$$CO_2 + 4H_2 \rightarrow CH_4 + 2H_2O \tag{34}$$

Additionally, the CO formed through the rWGS reaction (Eq. (35)) also leads to CH_4 formation:

$$CO + 3H_2 \rightarrow CH_4 + H_2O \tag{35}$$

In addition, the side reactions of methane dry reforming (MDR), (Eq. (19)), Boudouard (reverse of Eq. (7)), decomposition of CH_4 (Eq. (25)) and gasification of the coke formed by the two previous reactions (Eq. (7)) also take place.

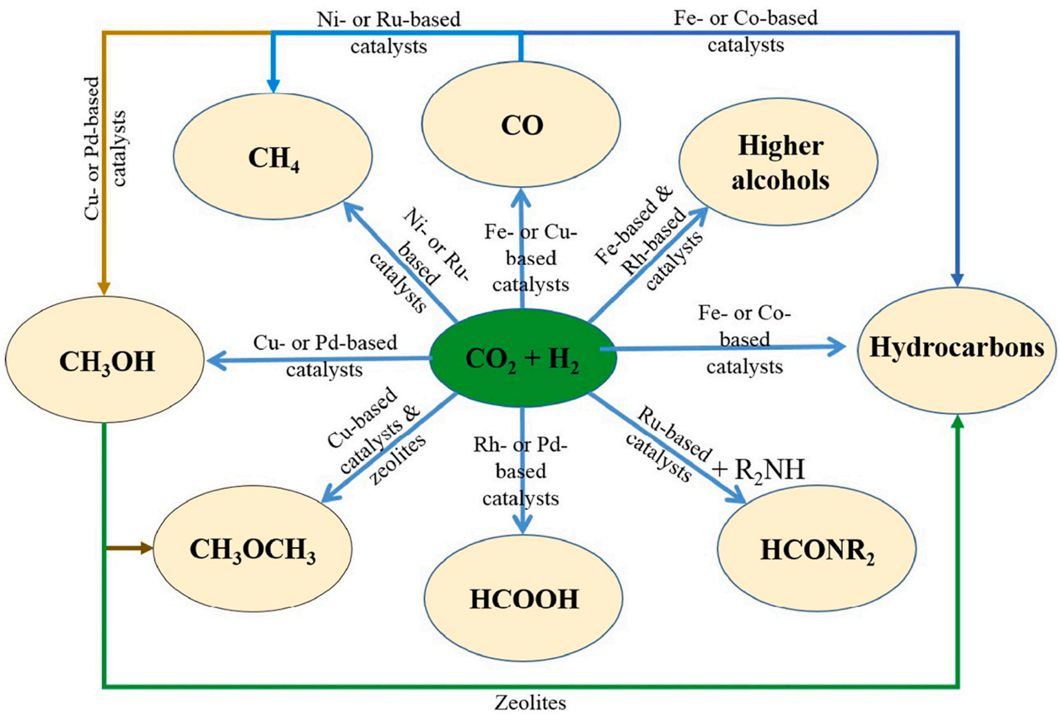

Fig. 4. Catalytic routes for CO_2 hydrogenation (reproduced from the work by Vu et al. [106], copyright 2021, Elsevier).

Table 1
Standard enthalpies (ΔH^0) and Gibbs free energies (ΔG^0) for different CO_2 hydrogenation reactions. Adapted with permission from [46], copyright 2020 American Chemical Society; and from [109], copyright 2016, Elsevier.

Reaction	$\Delta H^0{}_{298\ K}$ ($kJ\ mol^{-1}$)	$\Delta G^0{}_{298\ K}$ ($kJ\ mol^{-1}$)
$CO_2 + H_2 \rightleftharpoons CO + H_2O$	41.2	28.6
$CO_2 + 3H_2 \rightleftharpoons CH_3OH + H_2O$	−49.5	3.5
$CO_2 + 3H_2 \rightleftharpoons \frac{1}{2}C_2H_5OH + \frac{3}{2}H_2O$	−86.7	−32.4
$CO_2 + 3H_2 \rightleftharpoons \frac{1}{3}C_3H_7OH + \frac{5}{3}H_2O$	−94.6	−39.9
$CO_2 + 3H_2 \rightleftharpoons \frac{1}{4}C_4H_9OH + \frac{7}{4}H_2O$	−98.3	−43.2
$CO_2 + 4H_2 \rightleftharpoons CH_4 + 2H_2O$	−165.0	−113.5
$CO_2 + \frac{7}{2}H_2 \rightleftharpoons \frac{1}{2}C_2H_6 + 2H_2O$	−132.1	−78.7
$CO_2 + \frac{10}{3}H_2 \rightleftharpoons \frac{1}{3}C_3H_8 + 2H_2O$	−125.0	−70.9
$CO_2 + \frac{13}{4}H_2 \rightleftharpoons \frac{1}{4}C_4H_{10} + 2H_2O$	−121.6	−66.9
$CO_2 + 3H_2 \rightleftharpoons \frac{1}{2}C_2H_4 + 2H_2O$	−64.0	−28.7
$CO_2 + 3H_2 \rightleftharpoons \frac{1}{3}C_3H_6 + 2H_2O$	−86.6	−42.1
$CO_2 + 3H_2 \rightleftharpoons \frac{1}{4}C_4H_8 + 2H_2O$	−90.3	−45.2
$CO_2 + H_2 \rightleftharpoons HCOOH$	14.9	43.5
$CO_2(g) + H_2(g) + NH_3(aq) \rightleftharpoons HCO_2^-(aq) + NH_4^+(aq)$	−84.3	−9.5
$CO_2(aq) + H_2(aq) + NH_3(aq) \rightleftharpoons HCO_2^-(aq) + NH_4^+(aq)$	−59.8	−35.4
$CO_2 + 2H_2 \rightleftharpoons \frac{1}{2}CH_3COOH + H_2O$	−64.8	−21.6
$CO_2 + \frac{7}{3}H_2 \rightleftharpoons \frac{1}{3}C_2H_5COOH + \frac{4}{3}H_2O$	−80.1	−32.6
$CO_2 + \frac{5}{2}H_2 \rightleftharpoons \frac{1}{4}C_3H_7COOH + \frac{3}{2}H_2O$	−88.2	−38.5
$CO_2 + 2H_2 \rightleftharpoons HCHO + H_2O$	35.8	55.9
$CO_2 + \frac{5}{2}H_2 \rightleftharpoons \frac{1}{2}CH_3CHO + \frac{3}{2}H_2O$	−54.6	−12.9
$CO_2 + \frac{8}{3}H_2 \rightleftharpoons \frac{1}{3}C_2H_5CHO + \frac{5}{3}H_2O$	−71.6	−28.1
$CO_2 + \frac{11}{4}H_2 \rightleftharpoons \frac{1}{4}C_3H_7CHO + \frac{7}{4}H_2O$	−81.4	−34.7

According to thermodynamics, CO_2 conversion and CH_4 selectivity are favored at high pressure and low temperature [115,116], and the results are good (almost complete conversion and selectivity close to 100%) with the appropriate catalyst even at atmospheric pressure if temperature is low enough (< 350 °C). Catalysts based on noble and non-noble metals are used [117], according to activity ordered as: Ru > Fe > Ni > Co > Rh > Pd > Pt > Ir, and according to selectivity: Pd > Pt > Ir > Ni > Rh > Co > Fe > Ru. The general use of Ni catalysts (due to the good compromise between their performance and cost), instead of Ru-based catalysts, requires working at temperatures for which catalyst stability problems arise, especially due to the formation of coke.

The improvements of Ni catalysts are aimed at increasing surface defects, to facilitate the generation of surface-dissociated hydrogen, active for the removal of surface nickel carbonyls [118]. The role of the supports, aside from increasing surface defects, is to improve the dispersion of the metal and facilitate the storage and release of oxygen (redox properties). For these purposes, Al_2O_3, SiO_2, ZrO_2, TiO_2, CeO_2, perovskite, structured metal oxides, carbon materials and zeolites have been used as supports. Among the interesting properties of the supports, the following are to be mentioned, providing: i) Mechanical resistance; ii) metallic sites dispersion capacity (minimizing their aggregation); iii) hydrophilicity (the presence of H_2O favors the sintering of the metallic sites); iv) thermal conductivity (avoiding the generation of "hot spots"), and: v) reduced presence of acidic sites capable for coke formation. Some of these properties are improved incorporating promoters, including ZrO_2, CeO_2, La_2O_3, Mn_2O_3, MgO and alkali metals [113,114].

CO_2 methanation mechanism takes place with three pathways, the relative importance of which depends on the catalyst and reaction conditions [116]: i) Direct CO_2 dissociation and hydrogenation of CO (intermediate) to CH_4; ii) through the reaction of formate ($HCOO^-$) (intermediate formed from the adsorption of CO_2) with chemisorbed hydrogen, and; iii) with formyl species as intermediates. These species result from the reaction of adsorbed CO (product of CO_2 dissociation) with atomic hydrogen. Miguel et al. [116] have compared the LHHW kinetic equations of these mechanisms for a commercial Ni catalyst, proving that the best fit to their experimental results corresponds to the kinetic model for the pathway with formil species as intermediates, developed by Koschany et al. [119], assuming hydroxylic groups as the most abundant species.

From the operational point of view, it is important to highlight the relevance of separating the H_2O from the reaction medium to favor the extent of the reaction. This objective has led to the proposal using reactors with hydrophilic, steam-selective sodalite membranes [120,121] to replace conventional packed or fluidized bed reactors.

2.2.2. *Reverse Water Gas Shift (rWGS)*

CO is more reactive than CO_2 and a key intermediate for the production of methane, methanol, DME and hydrocarbons from CO_2, which explains why synthesis gas is used as feedstock in commercial processes for the production of these compounds. However, these reactions are carried out under unfavorable conditions for CO production. The conversion of CO_2 by the rWGS (Eq. (5)) is an endothermic reaction, and temperatures above 700 °C are required in order to obtain considerable CO_2 conversion. Under these conditions, CO_2 and CO methanation (Eqs. (34) and (35), respectively) and Boudouard (Eq. (7)) side reactions also take place.

The reaction mechanisms for the rWGS reaction is a topic of intensive debate [122], being redox and dissociative mechanisms the most widely accepted. In the redox mechanism, H_2 does not participate as reactant, but reduces the surface of the catalyst. Metallic crystals are the active sites for CO_2 dissociation, and the oxidized metallic sites are reduced releasing H_2O and being therefore the metallic sites regenerated. Thus, the redox stages for Cu catalysts are:

$$CO_{2(g)} + 2Cu^0_{(s)} \rightarrow CO_{(g)} + Cu_2O_{(s)} \tag{36}$$

$$H_{2(g)} + Cu_2O_{(s)} \rightarrow H_2O_{(g)} + Cu^0_{(s)} \tag{37}$$

In the dissociative mechanism H_2 reacts with CO_2, leading to the subsequent formation of formate species (HCO_2-M), which will release CO right away. These formate species are formed by the attack of OH^- groups on M-CO species and MO_2H species, formed through intermediates CO_2-metal protonation. According to this mechanism, the significant effect of the presence of surface hydroxyl groups to facilitate CO_2 adsorption and hydrogenation has been verified [123].

The activity of the catalysts for rWGS is associated with the presence of oxygen vacancies and the capability for adsorbing CO_2 and generating formate active species. These are formed in the vicinity of the H supply (metal-support interface) [124]. However, the selection of the catalyst is conditioned by stability and selectivity requirements, due to the high reaction temperature. A key property for CO selectivity is to achieve a weak binding energy of CO. Cu catalysts (with low CO adsorption energy) are commercially used for the WGS reaction with CuO-ZnO/Al_2O_3 (CZA) configuration, but undergo notable sintering in the rWGS reaction. The stability of the Cu sites improves using different supports (β-Mo_2C, In_2O_3 [125,126]); with Cu-Al spinel [122]; or generating particular configurations as Cu/CeO_2 hollow spheres [127] or an inverse metal-oxide/metal structure of CeO_x/CuO_x [128].

Promising CO selectivity has also been achieved with other non-noble metal catalysts using carbide structures prepared with Ti, V or W [129,130] and with bimetallic catalysts (Ni-Fe, Ni-Co) [131]. Although noble metals have high CO adsorption energy, high CO selectivity is achieved with strategies such as the preparation of bimetallic catalysts (Pd-Ni) [132] and the atomic dispersion of Rh or Ru nanoparticles on the support [133].

2.2.3. *Synthesis of methanol*

Olah [134] reflected the relevance of the "methanol economy" as a complement to the established "oil economy". Fulfilling his forecasts, the production of methanol is a key reaction in the development of the GTL (Gas to Liquid) concept, with synthesis gas (produced from biomass, carbon or natural gas) as feedstock (Fig. 5). Methanol is an energy vector according to its utilization as fuel, whether pure or mixed with gasoline and the production of H_2 by reforming. Additionally, it is an important raw material for the production of other fuels, solvents and base-chemical products, such as light olefins (MTO process), BTX aromatics, formaldehyde, acetic acid, methyl methacrylate, dimethyl terephthalate, methylamines, chloromethane, dimethyl carbonate, methyl tertbutyl ether (MTBE) and others.

Albeit methanol production is carried out from synthesis gas (with a small concentration of CO_2) (Eq. (38)), its potential capacity for valorizing CO_2 on a large scale led Goeppert et al. [136] to highlight the strategic interest of the reaction for this objective. The plant in Reykjavik (Iceland), with an annual capacity of 4000 metric tons and valorization of 5600 tons of CO_2, is the main industrial reference for renewable methanol synthesis from CO_2 and H_2 using geothermal energy [137].

$$CO + 2H_2 \rightleftharpoons CH_3OH \tag{38}$$

The exothermic synthesis of methanol from CO_2 (Eq. (39)) requires 3 H_2 molecules per CO_2 molecule. Thermodynamically, low temperature and high pressure are required to facilitate the extent of the reaction. However, given the low reactivity of CO_2, temperature above 240 °C is necessary to achieve an acceptable reaction rate. Thus, under the reaction conditions, the side reactions of rWGS (Eq. (5)) and synthesis from CO (Eq. (38)) take place. The rWGS generates a high content of H_2O, which limits the equilibrium conversion of CO_2, attenuates the activity of the catalysts and favors deactivation.

$$CO_2 + 3H_2 \rightleftharpoons CH_3OH + H_2O \tag{39}$$

To overcome the limitations of the reaction, the action routes are focused on developing new, active, selective and stable catalysts [138–141], reactors and operating strategies [142]. The knowledge of the mechanism for the conversion of CO_2 into methanol is necessary to

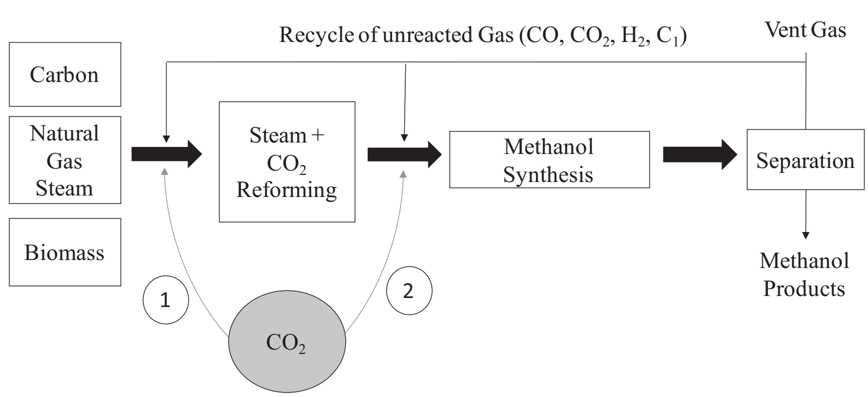

Fig. 5. Steps in methanol production (adapted from the work by Zhang et al. [135], copyright 2017, Elsevier).

progress in the improvement of catalysts, and so, has received great attention due to its relevance in the synthesis of methanol from syngas, where CO_2, of greater apparent reactivity than CO at low conversion conditions [143] is co-fed in a concentration within the 2–8% range. In Fig. 6, the three routes proposed for CO_2 conversion are outlined [142], that is, with formate and hydrocarboxyl species as intermediates or through the rWGS reaction.

$Cu/ZnO/Al_2O_3$ is the most commonly used catalyst for the synthesis of methanol from CO_2, given its commercial use for the same purpose from synthesis gas feedstock, based on the proposal of Imperial Chemical Industries in 1960. In this catalyst, Al_2O_3 acts as structural promoter favoring the distribution of Cu and providing surface area and mechanical resistance to the catalyst. ZnO also acts as a structural promoter, separating the Cu crystals, and modulates the electronic properties owing to the metal/support interactions between Cu and ZnO. The presence of ZnO reduces the sintering of Cu [139]. The use of ZrO_2 in Cu/ZrO_2 or $Cu/ZnO/ZrO_2$ catalysts leads to good results, due to the lower hydrophilicity of ZrO_2 with respect to Al_2O_3. Furthermore, the presence of Lewis acidic sites, non-active for the conversion of methanol into hydrocarbons, contributes to attenuate the formation of coke [144]. The incorporation of metallic oxides (SiO_2, MgO, Ga_2O_3, La_2O_3, TiO_2, Y_2O_3) and noble metals (Pd, Au) as promoters favors Cu dispersion and modifies acid-base and redox properties of the catalyst, improving the selectivity and stability of the catalyst [138]. As an alternative to Cu catalysts, more stable Pd and PdZn alloys on different supports have been proposed, including metal oxides (ZnO, CeO_2, In_2O_3) mesoporous silica (SBA-15, MCM-41) and carbon materials [140].

Alternatively to the direct synthesis of methanol from CO_2, a two-step process (rWGS-syngas hydrogenation) has been adopted. The advantages over the direct methanol synthesis process rely on the ease for removing the H_2O generated in the rWGS. With this approach, its entry to the hydrogenation reactor is avoided and the temperature in each reactor can be optimized. With this technology the Korea Institute of Science and Technology installed the CAMERE (carbon dioxide hydrogenation to methanol *via* reverse water gas shift) process on a pilot plant scale, with a capacity of 100 kg of methanol per day [142].

2.2.4. Synthesis of ethanol

The mechanism for ethanol synthesis from CO_2 (Eq. (40)) is more complex than that for methanol, because comprises more elementary reactions involving C-C coupling and accurate stages of carbon chain growth and termination. The most accepted mechanism is the so-called CO_2-Fischer Tropsch (CO_2-FTS). CO generated through the rWGS reaction inserts into $^*CH_3$ or $^*CH_3$-$(CH_2)_n$ species produced by CO-FTS to form ethanol or superiors alcohols ($C_{3+}OH$) [108].

$$2CO_2 + 6H_2 \rightarrow C_2H_5OH + 3H_2O \quad (40)$$

The selection of the composition of the selective multifunctional catalyst is also complex. So far, good results have been obtained with Rh-based catalysts with SiO_2 and TiO_2 as supports and Fe, Li and Se as promoters [145]. Other catalysts also selective towards ethanol production are prepared with Pt, Au, Mo, Co, and Cu as metallic function [140].

2.2.5. Synthesis of hydrocarbons

The direct production of hydrocarbons from CO_2 is a paradigm of catalytic processes integration, with the attraction of lowering equipment cost. However, this route implies important challenges to select the catalyst and establish the appropriate reaction conditions for a good compliance between the thermodynamic requirements and the mechanism of the involved reaction stages [105]. The reaction is carried out in tandem catalysts in the same reactor, through two alternative routes [104,146]: i) Modified Fischer-Tropsch synthesis (MFTS), incorporating a zeolite together with the FTS catalyst. In this manner, hydrocarbons are formed according to the Anderson-Schulz-Flory mechanism [43] and selectively converted on the zeolite, and; ii) with methanol/DME as intermediates (Eq. (41)), using OX/ZEO (metal oxide/zeolite) catalysts, suitable for the reactions of methanol/DME synthesis and the *in situ* conversion of these oxygenates into hydrocarbons [44].

$$CO + CO_2 + H_2 \Rightarrow CH_3OH/DME + H_2O \Rightarrow Light\ olefins \Rightarrow Light\ paraffins \quad (41)$$

The development of the MFTS route has been carried out mainly using Fe-based catalysts. CO_2 hydrogenation proceeds through a mechanism with two stages. The formation of CO by the rWGS reaction followed by the chain growth in FT reactions. The selection of the zeolite allows the selective formation of light olefins, aromatics or isoparaffinic gasoline (Fig. 7) [147,148]. The addition of other metals (Co, Cu or Ni) to Fe, modifies the adsorption of H_2 and CO, improving conversion and selectivity. Thus, with Fe-Cu the selectivity of C_2-C_7 hydrocarbons is four times that obtained with Fe, decreasing the formation of CH_4 [149]. In this case, as Fe support γ-Al_2O_3 (followed by SiO_2 and TiO_2) shows a better behavior than other supports to avoid sintering, thanks to the good dispersion of Fe obtained, based on the strong metal-support interaction [150].

In the route with methanol/DME as intermediates, the limitations of the Anderson-Schulz-Flory mechanism are avoided, and as a result, achieving higher selectivities of a family of hydrocarbons is feasible.

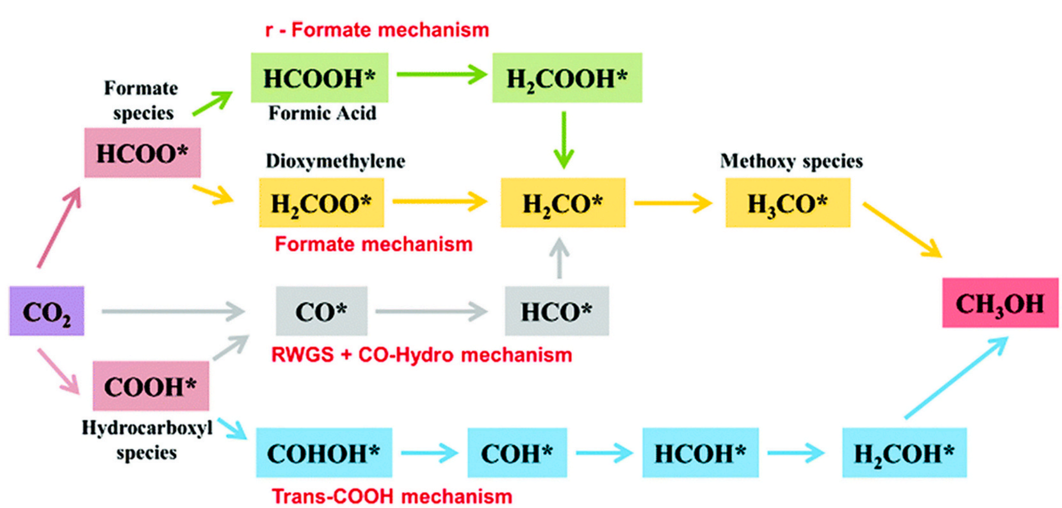

Fig. 6. Proposed mechanisms for methanol synthesis from CO_2 hydrogenation. (Reproduced from the work by Zhong et al. [142] with permission from the Royal Society of Chemistry).

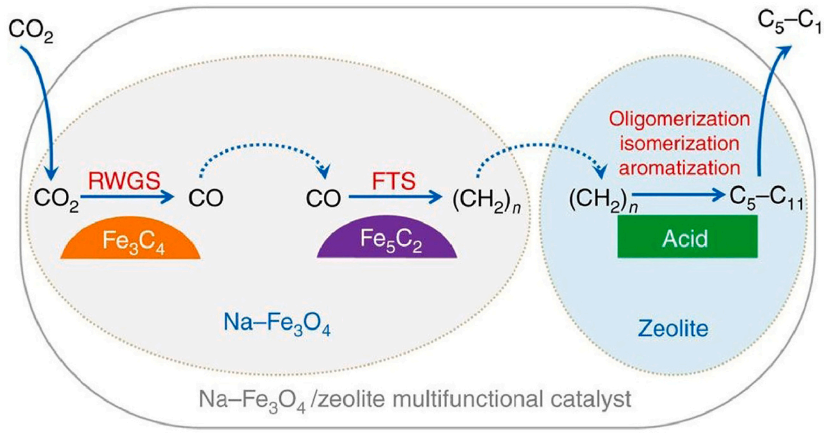

Fig. 7. Stages of hydrocarbons synthesis through the MFTS route. Reproduced from the work by Wei et al. [148].

Carrying out the second reaction (oxygenates conversion) in the same reactor displaces the thermodynamic equilibrium of methanol/DME synthesis, favoring the further conversion of CO_2 and CO. Consequently, the reaction can be performed at lower pressure and lower H_2/CO_2 ratio than for methanol/DME synthesis, easing the supply of H_2 from commercial PEM electrolyzers, which supply hydrogen at 15–30 bar [151]. The reaction conditions must be intermediate to those suitable for the two reaction steps. Thus, the conversion of methanol/DME into hydrocarbons occurs through the dual cycle mechanism (Fig. 8) [152], requiring temperature above 325 °C for a significant extent [153]. However, this temperature is excessive for the synthesis of methanol/DME, which occurs through a mechanism with formate ions as intermediates [154].

The presence of oxygen vacancies in the metallic function is a key feature for the adsorption of CO_2 [139]. In addition, this function must have a limited capacity for over-hydrogenating the double C=C bonds, as to avoid the formation of methane [155]. Besides, the distribution of hydrocarbons depends on the acidic strength and pore size of the zeolite [156]. According to these conditions, In_2O_3-ZrO_2/SAPO-34 tandem catalyst shows good prospects for the selective production of light olefins from CO_2 [157], given the capacity of the superficial oxygen vacancies of the In_2O_3-ZrO_2 system for CO_2 adsorption and the high light-olefin selectivity achieved in the conversion of methanol/DME over SAPO-34 (CHA topology). Similarly, the use of HZSM-5 zeolites (MFI topology) together with the ZnO/ZrO_2 system allows obtaining high aromatics selectivity [152].

Wang et al. [158,159] obtained high gasoline yield with a Fe/Zn/Zr@HZSM-5 core-shell catalyst, with isoalkanes as main components and with low aromatics concentration. However, as a drawback, CO selectivity of 40% resulted from the RWGS reaction. This reaction was later suppressed by treating the Fe/Zn/Zr catalyst with tetrapropylammonium bromide (TPAR) [160]. These authors also determine that the treatment affects the hydrocarbon formation mechanism, which proceeds through the two routes (FT and oxygenates as intermediates) with the Fe/Zn/Zr catalyst and mainly with oxygenates as intermediates with Fe/Zn/Zr-Treated catalyst, due to the enhanced adsorption strength of the HCOO* species and desorption rate of CH_3O* species. The Fe/Zn/Zr-Treated@HZSM-5 core-shell catalyst is stable for 120 h on stream, with 76% hydrocarbons selectivity and C_{5+} isoalkane content of 93% in the gasoline, with a CO selectivity of 24% and a CO_2 conversion of 18%.

3. Interest of dimethyl ether and thermodynamics of the conventional and direct synthesis

The interest in the production of DME is based on its usefulness as fuel and intermediate raw material for the production of hydrocarbon fuels and chemicals, and on the capacity of the process for valorizing synthesis gas derived from renewable sources (biomass) and CO_2. The cost and energy- and exergy- efficiencies of DME production from syngas depend on the syngas source and the reactants used in gasification or reforming. These factors determine the H_2/CO ratio of the resulting

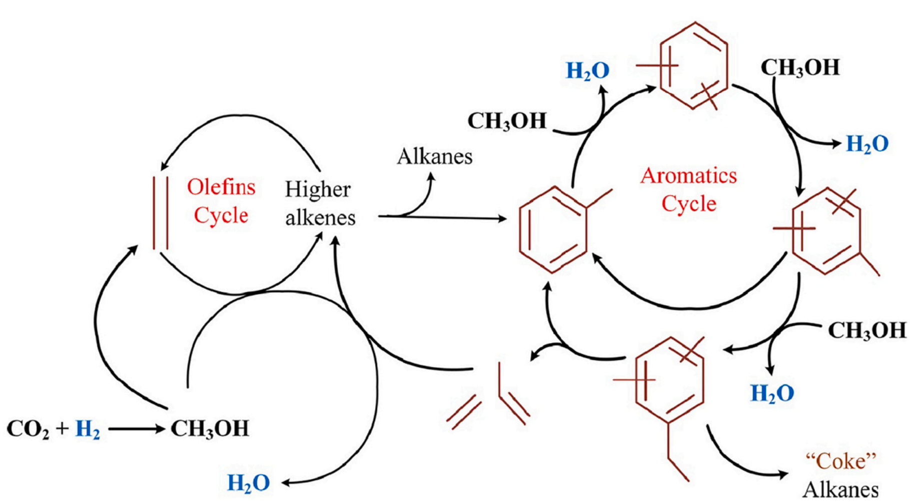

Fig. 8. The role of the dual cycle mechanism in the route with methanol/DME as intermediates. Reproduced from the work by Zhang et al. [152], copyright 2019, Elsevier.

syngas. The interest of valorizing low rank coal to DME *via* gasification has received continued attention [161] and this attention has extended to the valorization of natural gas and biomass [162]. The urgency for mitigating the effects of climate change by reducing CO_2 emission rates has reoriented DME production technologies to make CO_2 co-feeding together with syngas or CO_2 hydrogenation feasible. The joint valorization of CO and CO_2 as carbon sources is an initiative applicable to different industrial emissions and to bio-gas (product of the anaerobic fermentation of biomass composed of CH_4 (50–70%) and CO_2 (30–50%) [163]). In this line, recycling in the synthesis of DME the CO_2 used as biomass gasifying agent reduces up to 20% the environmental impact of the process [164].

Dieterich et al. [165] gather the pathways for transforming renewable energy into sustainable energy vectors (DME, methanol and hydrocarbons) in the diagram in Fig. 9.

3.1. Properties and applications of DME

DME (CH_3-O-CH_3) is an environmentally benign, non-toxic, non-teratogenic, and non-carcinogenic species, with a slight ethereal odour, which has multiple applications due to its properties (Table 2) [166–168]. Among others, it is used as aerosol, propellant (substituting chlorofluorocarbons), pesticide and ecological refrigerant [169]. It is of great interest also as organic solvent, due to the low dielectric constant of liquid DME (5.34 at 30.5 °C and 6.3 MPa), medium polarity, partial miscibility with water, no reactivity, chemical inertness, and affinity for oily compounds (given its capacity for developing one-way hydrogen bonds with hydrogen bonding solutes). These properties along with the easy removal by pressure reduction make it suitable for the extraction of products in food and pharmaceutical industry (lipids, essential oil, flavonoids), of contaminants (as phenols) from mixtures with water [170,171] and in solvent injection processes for heavy oil recovery [172].

The large-scale implementation of DME production is based on its properties as fuel, either for domestic use, in the automotive industry or for electrical energy generation. According to Semelsberger et al. [166] a transition from petroleum to DME to hydrocarbons is more cost-effective than a direct change to hydrogen, considered as the "end-game" fuel, since the existing LPG and NG transport and storage infrastructure can be used. The main advantages as fuel are: [173]: i) High oxygen content, lack of C-C bonds, N, and S compounds, reasons for the soot-, SO_x- and NO_x-free combustion; ii) low boiling point (−24.9 °C) and consequently, small energy requirement for vaporization, which facilitates its use as fuel gas, alone or blended with liquefied petroleum gases (LPG: propane and butane) given its similar vapor pressure and the same storage and transport characteristics [174]. In addition to domestic use, gas DME is used as fuel in homogeneous charge compression ignition (HCCI) engines, in mixtures with natural gas and hydrogen [175]. iii) High cetane number (> 55) that results in very low auto-ignition temperature. In spite of its low heating value (LHV) of 27.6 MJ/kg, inferior to that of diesel fuel (42.5 MJ/kg), the high cetane number and the short delay-time in the injection, make DME suitable for compression ignition (CI) engines. Using the existing technology, the well-to-wheel efficiency is DME > LPG > Gasoline > CNG (compressed natural gas) and the associated greenhouse gas emissions are significantly lower (DME < CNG < LPG < Gasoline) [167]. Tomatis et al. [164] estimate that replacing diesel by pure DME results in a decrease in greenhouse gases (GHG) of 72%, while limiting the emission of particulates (diesel soot). This emissions decrease has an impact on human health and ecosystem of 55% and 68%, respectively. However, due its high vapor pressure, very low boiling point, high compressibility, low density, low viscosity and the capacity of dissolving some elastomers and plastics, different modifications in diesel engines and in the selection of the materials are required for using DME. The main modifications consist of incorporating a pressurized DME tank, and a high-pressure fuel pump.

The evolution towards a DME economy is based not only on its use as fuel, but also on its future as intermediate sustainable raw material. Thus, DTO (dimethyl ether-to-olefins) process may replace or complement MTO (methanol-to-olefins) process, developed by UOP/Mobil and successively improved [32]; and MTP, developed by Lurgi (to selectively obtain propylene) [176]. The implementation of both processes is growing as to satisfy the burgeoning demand of light olefins, which is currently covered through naphtha steam cracking [177] and fluid catalytic cracking (FCC) [178] processes with high energy requirements and high CO_2 emissions. The DTO process offers advantages over MTO: i) DME is more reactive than methanol, which allows carrying out the reaction at lower temperature [179]; ii) the lower reaction heat favors temperature control. The DTO process has been mainly studied using SAPO-34 [180,181] and HZSM-5 zeolites [182] as catalysts. For the selective production of olefins, the use of HZSM-5 zeolites of moderate acidity (SiO_2/Al_2O_3 ratio around 180) is suitable. Indeed, the rate of coke deposition is also reduced. Whereas higher acidity (SiO_2/Al_2O_3 of 30) boosts (C_5-C_{11}) gasoline yield [35]. Using pseudo-boehmite as a binder, HZSM-5 zeolite is embedded in a mesoporous matrix of γ-Al_2O_3, providing mechanical resistance to the catalyst particles and attenuating the blockage of the micropores of the zeolite by coke [183,184].

DME conversion into hydrocarbons proceeds, like methanol conversion, through the dual cycle mechanism [37], with poly-alkylbenzenes as intermediates for the formation of light olefins as

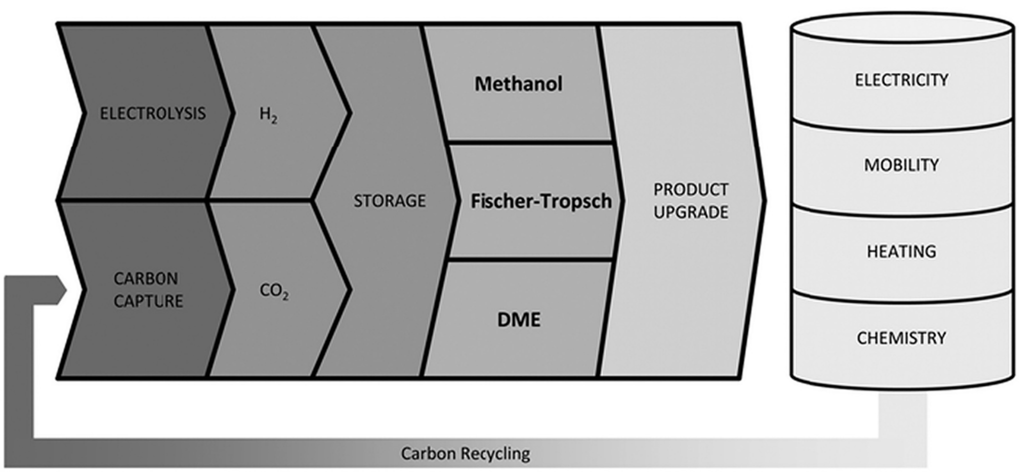

Fig. 9. Pathways for converting renewable electricity into energy vectors. Reproduced from the work by Dieterich et al. [165] with permission from the Royal Society of Chemistry.

Table 2
Properties of DME *vs* other common fuels. Adapted from the works by Semelsberger et al.; and Arcoumanis et al. [166,167], copyright 2006, 2008, Elsevier.

	Methane	Methanol	DME	Ethanol	Gasoline	Diesel
Formula	CH_4	CH_3OH	CH_3OCH_3	CH_3CH_2OH	C_7H_{16}	$C_{14}H_{30}$
Molecular weight (g mol^{-1})	16.04	32.04	46.07	46.07	100.2	198.4
Density (g cm^{-3})	0.00072[a]	0.792	0.661[b]	0.785	0.737	0.856
Normal boiling point (°C)	−162	64	−24.9	78	38–204	125–400
LHV (kJ cm^{-3})	0.0346[a]	15.82	18.92	21.09	32.05	35.66
LHV (kJ g^{-1})	47.79	19.99	28.62	26.87	43.47	41.66
Exergy (MJ L^{-1})	0.037	17.8	20.63	23.1	32.84	33.32
Exergy (MJ/kg)	51.76	22.36	30.75	29.4	47.46	46.94
Carbon Content (wt%)	75	37.5	52.2	52.2	84	84.8
Hydrogen Content (wt%)	25	12.5	13.0	13.0	16	15.2
Oxygen Content (wt%)	–	50	34.8	34.8	–	–
C/H ratio	0.25	0.25	0.33	0.33	0.44	0.47
Critical Temp. (°C)	−82.45	239.6	127	243.25		435
Critical Pressure (MPa)	4.60	8.10	5.37	6.39		3.00
Critical density (kg m^3)	562.2	275.5	259	280		–
Sulfur content (ppm)	~7–25	0	0	0	~200	~250
Cetane number	0	3–5.0[d]	>55	5-8[c]	4–20	40–50
Auto-ignition temperature (°C)	580	464	235	363	246–280	250
Stoichiometric air/fuel mass ratio	17.19	6.47	9	9.0[g]	14.7	14.6

[a] Values per cm^3 of vapor at standard temperature and pressure.
[b] Density at1 atm and − 25 °C.
[c] Data reproduced from: [187].
[d] Data reproduced from: [188,189].

primary products. The mechanism occurs along with different side reactions (isomerization, cyclization and hydrogen transfer) forming together with olefins: light paraffins, BTX aromatics, C_5^+ aliphatics and coke. On the basis of this mechanism, kinetic models for HZSM-5 based catalysts have been established, which allow quantifying the evolution of products distribution with time on stream [185]. With these models, evaluating the effect of various operating strategies on the deactivation and on products distribution is possible, such as the effect of co-feeding H_2O or feedstock dilution. Indeed, the models have been used in the design of alternative reactors (packed bed, captive fluidized and fluidized with catalyst circulation) and of a reactor-regenerator system with circulation of the catalyst between both units, based on the technology implemented for the MTO process [186].

Another application for DME with development potential is as H_2 vector, because its characteristics (high hydrogen content, absence of C-C bonds and low toxicity) facilitates the reforming at low temperature (< 300 °C) and results in high H_2 yield. This can be applied for proton exchange membrane fuel cells (PEMFC) [190] and solid oxide fuel cells (SOFC) [191], as well as to cover, on a large-scale, the growing demand of H_2 in the petrochemical industry. Catizzone et al. [39] propose DME as a good candidate for energy storage through the cycle comprising the synthesis of DME from CO_2 (exothermic) and the reforming of DME to H_2 (endothermic). In this way, the energy demand of the reforming is covered by the energy generated intermittently from renewable sources.

Steam reforming takes place on bifunctional catalysts, through DME hydrolysis in the acidic function (Eq. (42)) followed by methanol reforming in the metallic function (reverse of Eq. (39)). Additionally, the secondary reactions (rWGS (Eq. (5)), DME partial decomposition, methanation (Eqs. (34) and (35)), Boudouard (reverse of Eq. (7)) and hydrocarbons formation) contribute to products distribution,

$$CH_3OCH_3 + H_2O \rightleftharpoons 2CH_3OH \quad (42)$$

The most used catalysts in a lab-scale have been prepared with CuO-ZnO-Al_2O_3 (CZA) metallic function, based on the commercial catalyst for methanol synthesis and methane reforming. The main innovations have mainly consisted of the utilization of CuM_2O_4 spinels (M = Fe, Mn, Cr, Ga, Al, etc). Among these, $CuFe_2O_4$ spinel has received a great attention due to its thermal stability [192,193], which recovers its activity in reaction-regeneration cycles [194,195]. γ-Al_2O_3 has been the most used acid function for DME hydroxylation [196,197], but has been progressively substituted by HZSM-5 (more active). HZSM-5 needs to be adequately treated (as desilicated by alkaline treatment) in order to avoid the formation of hydrocarbons and the consequent formation of coke [198,199]. Oar-Arteta et al. [194,200] have improved the properties of γ-Al_2O_3, obtaining it by calcination of pseudo-boehmite. This treatment provides the catalyst with high mechanical resistance (a deficiency of the $CuFe_2O_4$ spinel) and also with moderate acidity, limiting the formation of hydrocarbons. Therefore, it allows for stably operating in reaction-regeneration cycles at 350 °C achieving a yield of 82%. Filling the gap in the kinetic modeling for oxygenates reforming, Oar-Arteta et al. [195] have proposed a kinetic model based on LHHW expressions for each step, establishing as optimal reforming conditions: 360–380 °C and a steam/DME ratio of around 6. The use of microreactors with ceramic channels eases H_2 generation for portable fuel cell applications [201].

Zhan et al. [202] have conducted a review of the studies of ethanol production from DME through carbonylation. This reaction is a key stage in the valorization of synthesis gas. The reaction, as the formation of methyl acetate (MA), takes place through the Koch-type CO insertion into DME, with zeolites (typically HMOR and HZSM-5) as catalysts. The MA is later converted into ethanol on Cu-based catalysts.

3.2. Conventional synthesis

DME production (10 Million tons per year) is carried out in a two step process, in separate units (indirect synthesis) using syngas feedstocks [203]. Methanol is synthesized in the first unit (under reaction conditions described in Section 2.3.3) and dehydrated towards DME in the second unit (MTD process). Methanol dehydration is a reversible exothermic reaction on acid catalysts, whose thermodynamics is not favored increasing pressure, but rather decreasing temperature. The process has been reoriented towards valorizing CO_2. In Fig. 10 the routes for CO_2 upgrading to DME are plotted [165]. Michailos et al. [204] estimate within the 1.83–2.32 € kg^{-1} range the cost of DME production from captured CO_2. Schemme et al. [205] determine that the production of DME (equaling its technical maturity to that of methanol synthesis) is a cheaper route for valorizing CO_2 than the production of alcohols (methanol, ethanol, butanol, octanol), polyoxy dimethyl ether, and hydrocarbons (synthetic gasoline, paraffinic diesel, and paraffinic kerosene), emphasizing the relevance of H_2 production costs (58–83% of the total manufacturing costs). Uddin et al. [206] make a techno-economic analysis of the two stage DME synthesis *via* the birreforming of landfill

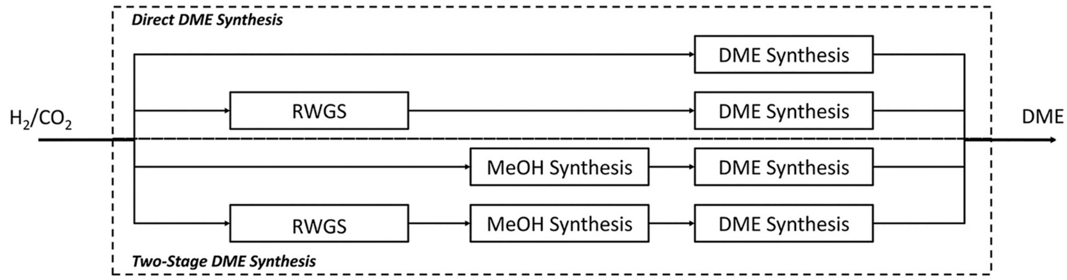

Fig. 10. Routes for DME production from CO_2. Reproduced from the work by Dieterich et al. [165] with permission from the Royal Society of Chemistry.

gas (with steam and CO_2 from an ammonia plant). These authors estimate a price of 0.87–0.91 \$ gal^{-1}, competitive with the price of diesel fuel. Furthermore, using landfill gas sourced CO_2, the process achieved negative emissions.

The industrial process has different licenses and an extensive implementation in asiatic countries since the beginning of the 21st century with carbon as raw material [174]. It is performed under moderate pressure (below 20 bar) and within 150–300 °C temperature range. γ-Al_2O_3, of low manufacturing cost, is generally used as catalyst [207–209]. The weakly acidic nature of the Lewis sites of γ-Al_2O_3 is appropriate to achieve a high DME selectivity, inhibiting the formation of hydrocarbons as by-products. Nonetheless, its activity is moderate and temperatures above 250 °C are required, besides the activity may be improved by modifying γ-Al_2O_3 with P, Ti, Nb, B, *etc.* [210]. In addition, due to its hydrophilic character, it has a great capacity for adsorbing H_2O (product of dehydration), reducing thereby its activity and causing dealumination, particularly when aqueous methanol is fed [211]. Catalysts with higher acidity than γ-Al_2O_3 have also been studied, which allows the reaction to take place at lower temperature, avoiding the formation of hydrocarbons. For this purpose, the optimal performance of heteropolyacids (HPAs) (more active than HZSM-5 catalyst) has been proven, and enhanced by incorporating W and P [212] and supporting HPAs on TiO_2 [213].

The greatest research effort in the design of catalysts for methanol dehydration has focused on zeolites, whose performance (activity, DME selectivity and stability) is influenced by the configuration of the channels of their crystalline structures and the quantity and strength of the acidic sites [214]. HZSM-5 zeolite (MFI topology), which is less hydrophilic than γ-Al_2O_3 has received a special attention. In particular, for the valorization of CO_2 together with syngas, in order to avoid the separation of the high content of H_2O in the aqueous methanol produced in the first stage. This zeolite contains pores with moderate severity of shape selectivity and the acidity is dependent on the SiO_2/Al_2O_3 ratio, with sites of moderate acidic strength mainly. Besides, the behavior of hybrid catalysts composed of HZSM-5 zeolite impregnated with γ-Al_2O_3 is also of interest, being it more active and selective than each separate catalyst, due to the dilution of the strong sites of the zeolite [215,216]. The desilication of HZSM-5 by means of an aqueous solution of NaOH is effective to attenuate the deactivation by coke, because the treatment decreases the acidic strength of the sites. In addition, the coke is deposited in the generated mesopores, reducing the blockage of the micropores of the zeolite [217].

Catizzone et al. [218] have proposed ferrierite (FE) as ideal catalyst, since its crystalline structure with two dimension channels make it highly selective and, additionally, coke deposition is reduced. This zeolite, prepared with a high Al content, allows achieving DME selectivity close to 100% at 200 °C and high methanol conversion (up to 82%), in contrast to γ-Al_2O_3 (conversion of 25%). Moreover, methanol conversion and DME selectivity of FE can be improved by increasing the density of Lewis sites and reducing the crystal size [219]. Comparing the features of FMI and FE zeolites, Catizzone et al. [220] achieve similar DME selectivity with nano-sized MFI and FER, whereas for the former higher reaction rate and lower coke deposition are reported.

Methanol dehydration to DME (reverse of Eq. (42)) proceeds through two competitive reaction pathways: Associative (or direct) and dissociative (or sequential) (Fig. 11). In the first, two methanol molecules are adsorbed on an acidic site and react to form DME and H_2O. The reaction can occur by splitting of protonated methanol dimer into the methyl carboxonium ion and carbenium ion at the same time, or into two methyl carboxonium ions, which are further combined to form DME molecule [221]. In the second, one adsorbed methanol molecule reacts to form H_2O and a CH_3 species bound to the deprotonated zeolite, and then, a second methanol molecule adsorbs to react with the CH_3 group to form DME. Park et al. [222] highlight the discrepancies in the literature on the predominant mechanism, which depends on the catalyst and the operating conditions. These authors, using computational chemistry and microkinetic modeling, determine that the dissociative pathway is the dominant for the reaction with an H-zeolite, being DME formation reaction the rate-controlling step. However, these theoretical results differ from those obtained by Trypolskyi et al. [223]. Adjusting the experimental results of methanol dehydration on a HZSM-5 zeolite these authors propose methanol adsorption as the rate-limiting stage; being equally valid the kinetic expressions of LHHW deduced for the associative and dissociative pathways to adjust the experimental results.

3.3. Thermodynamics of the direct synthesis

The reactions involved in the process are:

Methanol synthesis (Eqs. (38) and (39)); Reverse Water Gas Shift (rWGS) (Eq. (5)); Methanol dehydration towards DME (Eq. (43)):

$$2CH_3OH \rightleftharpoons CH_3OCH_3 + H_2O \quad \begin{matrix} \Delta H^0 = -23.4 \text{ kJ mol}^{-1} \\ \Delta G^0 = -16.8 \text{ kJ mol}^{-1} \end{matrix} \tag{43}$$

and paraffins formation secondary reaction (mainly methane):

$$nCO + (2n+1)H_2 \rightleftharpoons C_nH_{2n+2} + nH_2O \ (n = 1-3) \tag{44}$$

The interest in the direct route for DME synthesis is based on different factors: i) Thermodynamic advantages. Conducting methanol dehydration (Eq. (43)) *in situ* in the same reactor displaces the equilibrium of methanol formation reactions (Eqs. (38) and (39)). ii) lower cost of production in comparison to the synthesis of DME in two steps and to the synthesis of methanol [224]. Thus, the energy efficiency is around 64–68% for a 2500 equivalent t/day, higher than methanol synthesis, with an energy requirement 5% lower and a lower capital cost (8% lower) [225,226]; iii) possibility of using synthesis gas generated from various hydrocarbonated raw materials as carbon, natural gas, biomass or residues of the consumer society (Fig. 12), and from a steel-making plant (mixture of coke oven gas and tail gas) [227]; iv) boost of gasification and anaerobic digestion of biomass [228] in order to contribute to neutral carbon balance. A comparative exergo-economic analysis of the indirect and direct routes for DME synthesis, based on air-steam biomass gasification with CO_2, has evidenced the lower cost of DME production through the direct route (1.66 \$ kg^{-1}, whilst 2.26 \$ Kg^{-1} for the indirect route), and also, the lower energy consumption and net CO_2 emission [229]. In addition, given the higher price of the product, the

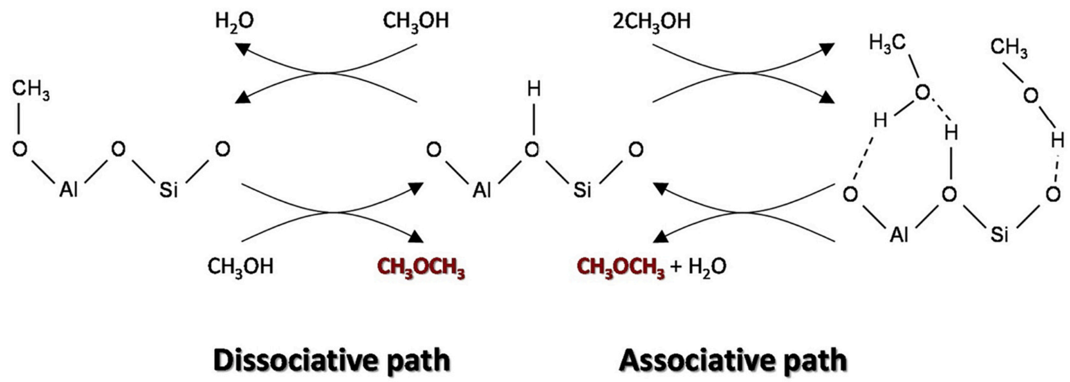

Fig. 11. Reaction pathways for methanol dehydration to DME. Reproduced from the work by Park et al. [222], copyright 2021, Elsevier.

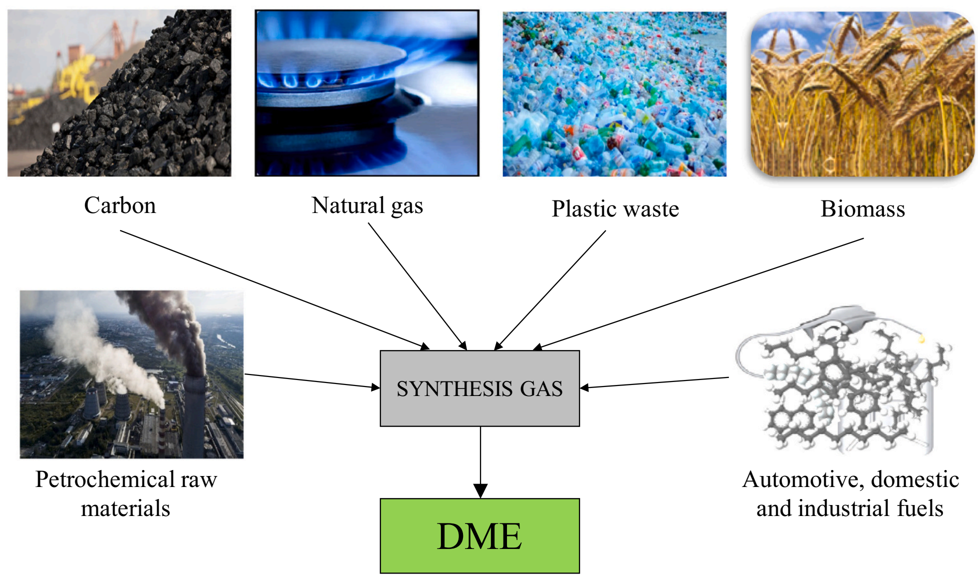

Fig. 12. DME production from fossil sources, biomass and waste.

gasification-DME process from biomass was approximately 7% more economically feasible than the gasification-MeOH process [230]; v) opportunity to maximize the natural gas operating profit, integrating its valorization with DME synthesis.

Taking into account these advantages, Olah et al. [231] considered the one step synthesis of DME (Fig. 13) a key route for the catalytic valorization of CO_2 on a large-scale. Furthermore, these authors have placed great emphasis on the sustainability of the process when CO_2 is co-fed with synthesis gas produced from lignocellulosic biomass.

In the literature regarding methanol synthesis thermodynamics [232–234] and one step DME synthesis [235–237], synthesis gas has been studied as feestock, whereas little attention has been given to CO_2 conversion capacity, whose role has been restricted to secondary product of the reaction. The interest in CO_2 conversion processes on a large-scale requires new studies regarding the thermodynamics and kinetics, aimed at establishing the appropriate conditions and the reactor design. Chen et al. [238] have compared the DME synthesis thermodynamics in two steps and in a single step, co-feeding CO_2 with synthesis gas. The results support that with both strategies CO_2 co-feeding decreases DME yield, and also that the direct synthesis of DME has lower thermodynamic limitations and allows achieving higher CO_2 conversion.

Ateka et al. [153] have compared in depth the thermodynamics of

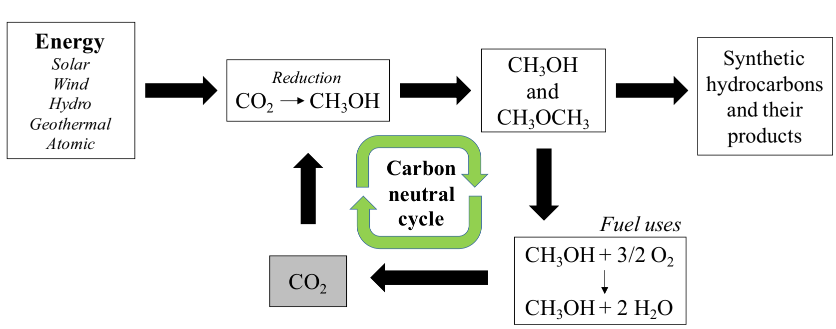

Fig. 13. Methanol and DME production valorizing CO_2. Adapted with permission from the work by Olah et al. [231]. Copyright 2021, American Chemical Society.

both methanol synthesis (MS) and the direct synthesis of DME (DS), from the perspective of the capacity of these processes for valorizing CO_2. The effect of the reaction conditions (temperature, pressure and feed composition) in regard to CO_2 conversion, oxygenates yield and selectivity (MeOH and DME) and heat generated in each process were determined. Being CO and CO_2 hydrogenation exothermic reactions with reduction of mole number, oxygenates production is favored with increasing reaction pressure, while penalized upon increasing temperature. The study ascertained that valorizing CO_2 is feasible in MS and DS processes for CO_2 rich feedstocks (CO_2/CO_x > 50%) at 250–300 °C (suitable range to obtain good catalytic performance [239] and avoid sintering [240]) (Fig. 14). Nonetheless, higher CO_2 conversion values can be achieved in DS than in MS (for CO_2/CO_x > 75%), greater upon further increasing CO_2 concentration in the feedstock (Fig. 15).

The study of Ateka et al. [153] highlighted the relevance of the CO_2 content in the feedstock, and that the DS is more thermodynamically favorable than MS for oxygenates production under suitable operating conditions. For its interest for simplifying reactor design, the possibility for operating at thermo-neutral conditions was tested, combining the aforementioned exothermic nature of CO and CO_2 hydrogenation reactions and the endothermic nature of the involved rWGS reaction (of special relevance for CO_2 containing feedstocks). Clearly, CO_2 co-feeding positively contributes to reduce the heat released in the reaction and helps avoiding hot spot formation (Fig. 15). Heat production diminishes from 80 to 45 kJ mol^{-1} for MS and from 90 to 60 kJ mol^{-1} for DS for CO_2/CO_X = 0.5 feedstocks. Anyhow, the study reveals the impossibility of working with Cu based traditional catalysts at thermo neutral conditions, since temperatures above 340 °C are required for this purpose in any case and Cu catalysts undergo sintering at temperatures above ~300 °C.

Furthermore, it should be noted that the effect of the reaction conditions on DME yield is opposite to the effect on CO_2 conversion and so, that optimizing of each of these objectives requires different reaction conditions. Thus, CO_2/CO_x ratios below 0.25 are suitable for enhancing DME production, whereas ratios above 0.5 improve the conversion of CO_2. Consequently, to combine the economic objective associated with the production of DME and the economic/environmental target of reducing CO_2 emission rates, intermediate conditions are necessary.

4. Advances in the catalyst design for the direct synthesis of DME

For this process, bifunctional catalysts comprising metallic catalysts for methanol synthesis (as introduced in Section 2.2.3) and acidic catalysts for methanol dehydration into DME are required. In addition, by feeding CO_2 various differences from the syngas-to-DME process arouse. One the one hand, as introduced in Section 3.3, according to thermodynamics, lower DME yield is obtained. On the other, the role of the rWGS (Eq. (5)) reaction is more relevant, giving way to higher H_2O content in the medium. H_2O inhibits the production of methanol (reduces the reaction rates of methanol formation by CO and CO_2 hydrogenation and of WGS reactions) since H_2O molecules tend to strongly adsorb on the surface active sites of the catalyst [241–243]. Moreover, deactivation problem assumes greater relevance [244]. Thus, the higher CO_2 and H_2O concentrations in the reaction medium favor CuO oxidation and its sintering, which is an important feature due to its irreversibility. However, these unfavorable effects should not fade the main advantage, that is, the attenuation of coke deposition due to the aforementioned role of H_2O in the reaction medium for controlling the concentration of superficial methoxy species, as well as the ability of H_2O to

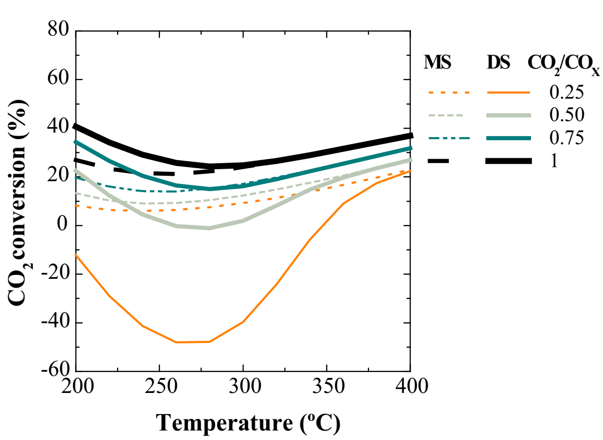

Fig. 14. Evolution of CO_2 conversion with temperature in the methanol synthesis (MS) and the direct DME synthesis (DS) processes for feedstocks of different CO_2 concentration. Adapted from the work by Ateka et al. [153], copyright 2017, Elsevier.

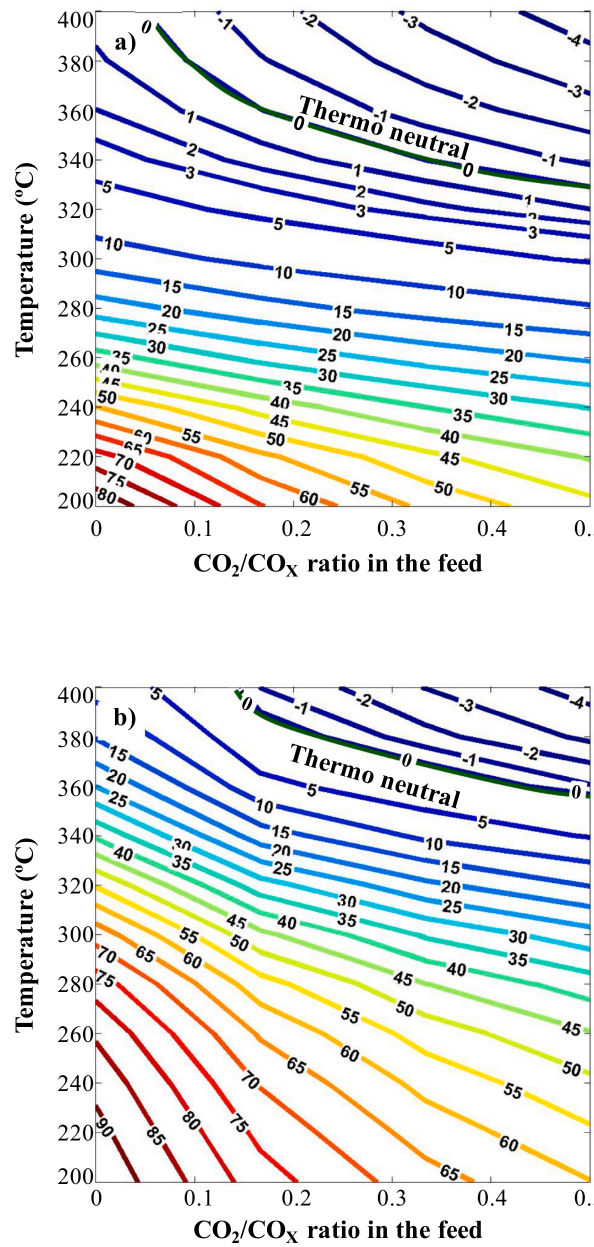

Fig. 15. Temperature *vs* fed CO_2 concentration (CO_2/CO_X ratio) diagram for heat generated (in kJ mol^{-1}) in methanol synthesis (a) and direct DME synthesis (b). Reproduced from [153], copyright 2017, Elsevier.

diffuse coke precursors [245]. This said, within the research works to improve the catalyst, two pathways can be distinguished: 1) focused on improving each function of the catalyst, and; 2) oriented towards optimizing the contact between both functions of the catalyst by changing the structure of the bifunctional catalyst particle. Besides, given its importance in the viability of the process, the deactivation of the catalyst is also worth of study. These features of the bifunctional catalysts for the direct synthesis of DME from CO_2 are studied separately in the following sections.

4.1. Methanol synthesis catalyst

4.1.1. Based on Cu

In the 1960s Imperial Chemical Industries proposed $CuO\text{-}ZnO\text{-}Al_2O_3$ (CZA) metallic function a suitable option for methanol synthesis under mild conditions and has been widely used since [246]. Cu (Cu^0 and Cu^+) is the active species for CO and CO_2 hydrogenation, whereas ZnO is used as geometric spacer for enhancing its dispersion and for stabilizing it [247,248], helping to hider sintering and poisoning. Nevertheless, it has been substituted by La_2O_3 [249], MgO [250], Fe_2O_3 and CeO_2 [251,252] for promoting CuO dispersion, catalyst stability and CO_x conversion.

Al_2O_3 in the CZA catalyst has also been replaced, partially or totally, by other metal and non-metal materials. Among others, MnO has been reported to enhance CuO and ZnO dispersion and reduce the temperature required for CuO reduction, giving way to a larger specific surface area of active Cu^0 [253,254], and so, boosting DME yield. Moreover, the Cu-Mn spinel formed resulted very active in the WGS reaction [253,254]. Likewise, the addition of ZrO_2 is widely reported [255,256] to improve the performance of the catalysts as a result of the stabilization of the $Cu^{\delta+}$ sites under reducing and oxidizing conditions [257] and higher H_2O tolerance [258–264]. On the one hand, the weak hydrophilicity of ZrO_2 hinders the adsorption of H_2O (competing with the adsorption of the reactants), and on the other, its basicity favors CO_2 adsorption, improving therefore methanol production. Given the promising results of Cu/Zn/Zr catalysts, various authors have deepened in broadening the knowledge on their activity. As to tailoring the catalyst, Sánchez-Contador et al. [144] have further studied the effect of ZrO_2 loading into the CuO-ZnO metallic function, synthesizing MeOH from $CO_2/CO/H_2$ mixtures under the reaction conditions required for the direct synthesis of DME. Cu/Zn/Zr = 2:1:1 was determined to be the most suitable ratio for achieving an optimal agreement between CO_x conversion (8.14%), methanol yield and selectivity (over 98%) and catalyst stability. Singh et al. [265] attribute the high activity of the Cu/Zn/Zr catalysts to the interactions between Cu and ZnO and ZrO_2 oxides, generating oxygen vacancies and stabilizing the methoxy species intermediates in the formation of methanol. Moreover, ZrO_2 tunes the acidity of the bifunctional $Cu/ZnO/ZrO_2$, adapting it to the selective production of DME. Through steam-treatment of Cu/Zn/Zr catalysts using tetrapropylammonium bromide (TPABr) Chen et al. [266] manage to suppress the formation of CO *via* the RWGS reaction, in addition to increasing the activity, selectivity and stability of the catalysts, due to the increase in the concentration of oxygen vacancies. The same goal is achieved by ultrasonic-assisted impregnation of TPABr to stabilize the CuBr phase on the catalyst surface [267].

As to the reaction mechanism regards, Frusteri et al. [268] hypothesize that ZrO_2 could also have the capability for activating the adsorbed CO_2 giving way to CO_2* species. These CO_2* species are assumed to react with H_2* species to give intermediate species (formate, dioxomethylene, methoxy), which will further evolve to methanol. According to Witoon et al. [269,270] bicarbonate species formed from CO_2* are considered to be the ones reacting with H_2* to give way to methanol. Both CuO-ZnO-MnO and $CuO\text{-}ZnO\text{-}ZrO_2$ catalysts outperform the results obtained with $CuO\text{-}ZnO\text{-}Al_2O_3$ in a similar manner for $H_2 + CO + CO_2$ feedstocks. The cost of the former is lower, and so its use for CO/CO_2 mixtures hydrogenation is suitable, while for pure CO_2 hydrogenation the latter outstands [255]. Li and Chen [271] studied in detail the synergyes induced by ZrO_2 (Fig. 16) and summarized the approaches to improve the catalytic performance of ZrO_2-containing catalysts for CO_2 hydrogenation to methanol.

Ga_2O_3 promoter (with lower capability for adsorbing H_2O than ZrO_2) [272] has been reported to facilitate the reducibility of the catalyst [273–275], improve Cu stability [276,277] and dispersion [278]. Moreover, enhances ZnO conductivity and favors the creation of redox-active defect sites as structural promoters [273]. Also, high methanol yields have been achieved by the addition of Ga_2O_3 to $Cu\text{-}ZrO_2$ catalysts [279,280]. Furthermore, in this line, quaternary catalysts have also been proposed, like $Cu\text{-}ZnO\text{-}ZrO_2\text{-}TiO_2$ [259] given the addition of TiO_2 leads to the creation of oxygen vacancies for the adsorption of CO_2 [281], and $Cu\text{-}ZnO\text{-}Al_2O_3\text{-}CeO_2$ [282,283].

Pursuing the increase of methanol formation reaction rate by favoring the adsorption of the reactants (H_2 and CO_2), the addition of small amounts of noble metals to Cu-ZnO based catalysts has been suggested [284]. The promoting effects of this addition have been mainly attributed to the hydrogen spill-over mechanism [285]. Among these metals: Au [286–288], Pd [289–291], Pt, Rh [292].

As an alternative approach, the use of SBA as support for the confinement of Cu-ZnO actives sites within its mesoporous structure has been studied by Prieto et al. [293]. This configuration enhanced the contact of the active sites with the reactants, resulting in higher activity and thus, methanol production. Carbon nanotubes [294], graphene oxides [281], and carbonaceous coordination polymers have also been reported as supports to boost the activity and stability of Cu-ZnO catalysts. These supports reduce the size of the active sites and favor distribution, facilitating the reduction, and hampering the strong adsorption of H_2O, giving way to more stable and active catalysts for methanol production.

4.1.2. Based on Cu alternative metals

Nevertheless, as to overcome the limitations of Cu based catalysts (sintering, low CO_2 activation capacity) non Cu-based oxide catalysts are being tested for methanol production, especially seeking for stable catalysts for CO_2 hydrogenation. In this regard, Wang et al. [295] studied binary $ZnO\text{-}ZrO_2$ catalyst obtaining high per-pass CO_2 conversion and resistance to poisoning by SO_2 and H_2S. The -Zn-O region for dissociating H_2 is also the active site for the direct hydrogenation of CO_2 to methanol with HCOO, H_2COO and H_2CO as intermediates. These authors reported outstanding stability during 500 h TOS, and Wang et al. [296] doubled (1000 h TOS) the stability with In_2O_3 catalyst. In these catalysts, defective oxygen vacancies are considered the active sites for the direct hydrogenation of CO_2 to methanol with HCOO, H_2COO and H_2CO as intermediates [297–299]. With this catalyst the rWGS reaction is inhibited [300], thus, the CO_2-CO-methanol pathway of Cu based catalysts is avoided. The addition of ZrO_2 as structural promoter prevents In_2O_3 sintering and, considering that In and Zr metals have different valence number, within the In_2O_3 structure additional surface oxygen vacancies are created due to the replacement of In by Zr atoms [301], helping CO_2 adsorption [299,302] and so, the selective formation of methanol [299,303]. Similar effect has been demonstrated for Ga insertion into the In_2O_3 lattice [304], and in both cases, controlling the ratio between the metals is a key feature to be optimized for maximizing the performance of the catalyst.

Co containing catalysts have also exhibited high activity for selectively producing methanol from CO_2, inhibiting the rWGS reaction [305]. With Mn-Co catalysts a synergy between the metals results in increasing surface basicity and improving methanol selectivity [305,306]. According to Wang et al. [307], for Co based catalysts, the addition of SiO_2 leads to the formation of Co-O-Si species, favoring the formation of methanol by increasing $*CH_3O$ species reactivity and hydrogenation over methane production by C-O dissociation.

For their excellent stability and resistance to poisoning, noble-metal based catalysts such as Pd/ZnO [308], Pd/In_2O_3 [309] and Au/ZrO_2 [310], with different supports (*i.e.* Ga_2O_3 [311], CeO_2 [312] or In_2O_3

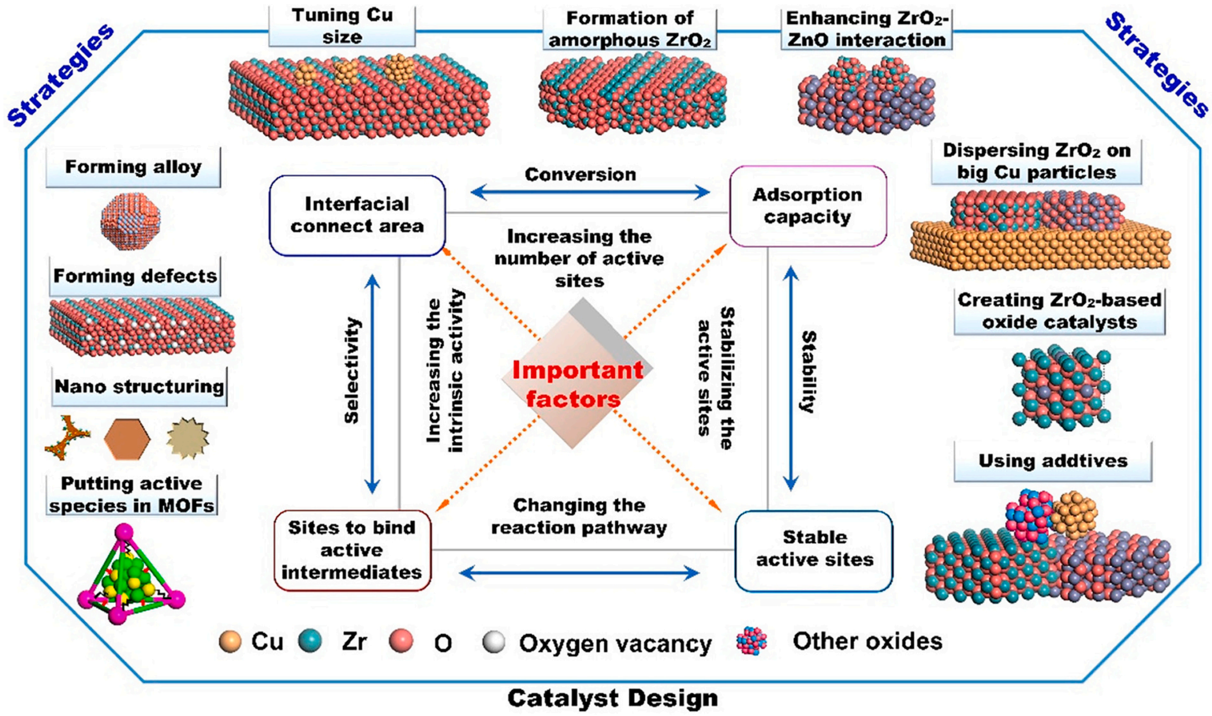

Fig. 16. Relevant factors affecting the activity of ZrO_2 containing catalysts for CO_2 hydrogenation to methanol. Reprinted with the permission from the work by Li and Chen [271]. Copyright 2019, American Chemical Society.

[309], MOF, SBA-15, CNT, *SiC*…), promoters (*e.g.* K_2O, MgO, CaO) and preparation methods are also being tested with good results despite its higher cost. Ca-promoted Pd nanoparticles (2–6 nm) over mesoporous CeO_2 are active for metanol synthesis and dehydration to DME [313]. To be highlighted, the stability of Pd^0 nanoparticles, the induction of structural defects by Ca in CeO_2 that favor the absorption of CO_2 and the balance between the amount of basic and acidic sites. It is claimed that Pd-Zn alloys stabilize the formate intermediates and ease the direct formation of methanol from CO_2, inhibiting the CO formation by the rWGS reaction [314,315].

For Au-based catalysts, the relevance of the support on the overall activity and product selectivity is highlighted [142]. For these catalysts, Hartadi et al. [316] explain the selectivity order: Au/ZnO > Au/ZrO_2 > Au/TiO_2 > Au/Al_2O_3 by the larger size of Au particles, although it is accompanied by a decrease in activity. These authors determine for the Au/ZnO catalyst that CO_2 is directly hydrogenated to methanol and that this reaction proceeds *via* an independent reaction pathway (presumably with adsorbed formate and methoxy species as intermediates) [317]. This independence of the mechanisms explains the shift in the main carbon source for methanol from CO_2 to CO as the temperature increases from 240 to 300 °C [318]. Wu et al. [310] confirmed the higher activity and selectivity of Au/ZrO_2 catalysts prepared with sub-nanometric particles (1.6 nm) was due to the appropriate coupling between the Au and the support.

4.2. Methanol dehydration catalyst

For methanol dehydration to DME solid-acid catalysts are required. Desirably hydrophobic, stable, active and selective under the required reaction conditions. In the vast majority of studies, γ-Al_2O_3 is used, given its reported high selectivity within the temperature range required in the process (200–300 °C) and relatively low manufacturing cost [208,319]. Ghorbanpour et al. [320] made a computational assessment of the reaction mechanism and determined that depending on the reaction conditions (temperature and pressure) methanol dehydration could proceed through: i) A dissociative route, that is, methanol adsorbed in an acidic site would lose a water molecule and transfer into a surface methoxy group to react to with another methanol molecule leading to the formation of DME; or ii) an associative route, where two methanol molecules co-adsorb on an acidic site to give DME. Nonetheless, given the hydrophilic nature of γ-Al_2O_3, its activity decays significantly due to the ability for adsorbing the H_2O formed in the process leading to dealumination. Moreover, H_2O has multiple roles in the conversion of methanol to DME: i) shifts the thermodynamic equilibrium of methanol dehydration to DME; ii) decreases the acidity of the catalyst by adsorbing on the acid sites (competing with methanol [321,322]), and iii) inhibits the formation of methoxy ions by shifting the equilibrium [245]:

$$Al-OH+CH_3OH \rightleftharpoons Al-O-CH_3+H_2O \quad (45)$$

This feature is way more relevant for the direct CO_2-to-DME process, where hydrothermal conditions are more severe than with syngas as reactant. Therefore, the research on the acid catalysts has focused on mitigating the activity decay due to H_2O adsorption by progressively diminishing hydrophilicity and facilitating its desorption from the acid sites, bearing in mind the acid catalyst for the process requires limited acid strength, as to avoid the formation of hydrocarbons [323]. MCM-41 supported tungstophosphoric acid (TPA) has also been used, based on the high turnover frequencies for methanol dehydration to DME [324]. On the basis of the above premises, besides modifications of γ-Al_2O_3 [210,325], various alternatives have aroused among which zeolites (framework types as BEA, EUO, FER, MOR, MTW, TON [326,327]) and in a wider extent MFI type (HZSM-5 [328,329] and silicoaluminophosphates (SAPO-11, −18, −34)) outstand [330]. Catizzone et al. conducted a screening among different framework type zeolites for methanol to DME dehydration and studied the effect of crystal size, Si/Al ratio and acidity. These authors claimed the better performance of FER- and MFI-type zeolites among others, especially in terms of selectivity, stability and limited formation of carbon species [326,327]. In the literature HZSM-5 is the most studied zeolite since it exhibits good hydrothermal stability and activity due to its topology and acidic properties. Anyhow, the strong Brönsted nature of the sites makes it prone to coke deposition [331]. To overcome this a great deal of effort has been placed on tailoring HZSM-5 [332] and numerous modifications have been widely studied [333–335], most of them oriented towards the passivation of the acid strength, to attenuate coke deposition [218,336]. Zeng et al. [216] determined that with the partial desilication and dealumination of ZSM-5 the strength of the surface acidic sites diminishes and the mesoporous presence increases. As a consequence, not only the catalytic performance, but also the hydrothermal stability and deactivation resistance improved. According to Ordomsky et al. [337] silication also resulted effective for stabilizing the HZSM-5 based catalyst, minimizing the progress of the hydrocarbon pool mechanism, while Wei et al. [338] used alkaline treatment passivation and partial activation for the same purpose. Aboul-Fotouh et al. [339] tuned the acidity (more active catalysts achieved) by chlorination or fluorination methods. Aloise et al. [217] reported that the increase of mesopore diameter, obtained by desilication, allows the formation of larger amount of accessible acidic sites, minimizing therefore the formation of coke deposits and upgrading DME production. Krim et al. [340] attained a DME selectivity of 74% with hollow nano-HZSM-5 with mesoporous shell synthesized by alkaline treatment.

Sanchez-Contador et al. [330] compared the performance of HZSM-5 zeolite with SiO_2/Al_2O_3 ratios of 80 and 280, subjected to thermal and dry steaming treatments for acidity passivation, and SAPO-18 and -11 [330]. This study claims that under the conditions required for the CO_2-to-DME process (250–325 °C, ~20 bar), the performance of SAPO-11 is slightly better than that of the thermally treated HZSM-5(280) zeolite, and this, better than for SAPO-18 [255]. The better behavior of SAPO-11 molecular sieve is attributed to the properties of the acidic sites (high density of weak strength acidic sites) and the AEL topology of its porous structure) [341,342]. These properties minimize the adsorption and retention of hydrocarbon molecules, as well as their condensation to form polyaromatic components of coke [330]. Chen et al. [342] demonstrated that the acidity of SAPO-11 could be diminished and specific surface and mesoporosity increased by synthesizing nano-sized particles (~200 nm), resulting in a better activity for methanol dehydration. On the other hand, even if high methanol conversion and DME selectivity is accomplished with SAPO-34, given the large channels and narrow openings of its structure, suffers severe deactivation since large hydrocarbon molecules are retained blocking the pores [343,344].

To a lesser extent, other materials have also been tested. For example, HY zeolites or HMCM-22, Witoon et al. studied the use of sulfated zirconia, Frusteri et al. [345] and Catizzone et al. [214,326] justified the optimal performance of ferrierite by its porous structure and moderate acidic strength.

4.3. Configuration of the bifunctional catalyst and catalytic bed

For the preparation of the catalyst, the metallic functions presented in Section 4.1 and the acid functions presented in Section 4.2 have to be combined. The typical strategy is to provide an excess of acid function. In this way, the displacement of methanol synthesis equilibrium is ensured (see Section 3.3) and the overall reaction is controlled by methanol formation, which is the slowest step. Given the relevance of the intimacy of the contact between the metallic and the acidic functions on the overall performance of the catalyst, the configuration of the catalytic bed has been largely addressed. Yao et al. [346] ascertain that with a close contact between the functions DME could be generated through a shortcut methoxy-DME pathway, with no need for methanol formation as intermediate (typical methoxy-methanol-DME route), resulting in a more efficient production of DME. In the literature the following arrangements are studied: 1) Dual bed configuration, placing first the metallic function for CO_2 hydrogenation to methanol, and subsequently the acidic function for its dehydration to DME; 2) physical mixture of metallic function and acidic function particles; 3) hybrid configuration, the most common configuration where both functions are mixed conforming bifunctional catalyst particles; 4) core-shell configuration, where one function is encapsulated by the other, and; 5) structured catalyst. Regarding thermodynamic basis, in the first strategy a two-set process would be taking place, at the same reaction conditions. Therefore, the lower activity of this system over other configurations reported by several authors is to be expected [258,346–349].

Ateka et al. [347] conducted the comparison of the strategies 1–3 for the combination of CuO-ZnO-MnO (CZMn) metallic and SAPO-18 acidic functions, for valorizing CO_2 co-fed with synthesis gas, emphasizing the low cost of CZMn metallic catalyst among other options [153,255]. In all cases, both functions where mixed at the optimal 2/1 mass ratio (metallic function/acid function). In the dual bed strategy (strategy 1), DME selectivity did not surpass 85%, evidencing the suitability of combining the proposed functions. The conversion of the CO_2 + CO mixture fed (50% each) with the dual bed strategy resulted 50% lower than when particles of both functions where mixed conforming a single catalytic bed (strategy 2). Moreover, combining CZMn and SAPO-18 in a single hybrid catalyst particle (strategy 3), the closer contact between the functions led to improve DME selectivity (~95%) and boost CO_2 + CO conversion, doubling that obtained in the dual bed strategy (22% *vs* 10%). Yao et al. [346] performed a similar study for the combination of Cu-In-Zr-O (CIZO) and SAPO-34. They reported that the adjacency of both functions facilitates the migration of intermediate methoxy ions from CIZO to SAPO-34, so that DME could form directly. That is, CO_2 conversion improved from <3% to ~4.5% when changing from the dual bed strategy to hybrid catalyst, whereas DME selectivity remained around 60% in all cases. In other cases, like for Bonura et al. [348], the performance of the catalyst is lower for the hybrid catalyst configuration than for the catalytic bed composed of pre-pelletized individual functions (strategy 2) of Cu-ZnO-ZrO_2 (CZZr) and HZSM-5 zeolite in a 1/1 mass ratio [348]. This decay is related to the blockage of the zeolite pores inlet by the metallic function on the mortar treatment and pelletizing steps. Later, these authors studied the influence of the precipitating agent on the generation of the metallic function directly in a solution containing the zeolite (HZSM-5 [350], MOR or FER [349]) as to "englobe" the latter. The procedure improved the activity of the system, presumably by the enhanced hydrogenation functionality related to the "multisite" reaction path; primary adsorption of H_2 on the metallic sites reacting with the CO_2 adsorbed on the strong basic sites to form methanol, and the subsequent dehydration on the acidic sites of the zeolite.

The core-shell structure (strategy 4) is being explored as an alternative to hybrid catalysts [342,351]. Unlike the hybrid catalysts prepared by extrusion of the metallic and acidic functions configuring each catalyst particle, the core-shell structure consists of depositing the one function on a previously prepared nucleus of the other. Typically, the acid function covering the metallic nucleus (Fig. 17). This structure can be prepared by either hydrothermal synthesis, single-crystal crystallization, dual-layer method or physically adhesive method. The general objective of the core-shell structure in catalytic processes is to preserve the catalyst from poisons adsorption, attenuating the sintering of the metallic particles and controlling DME selectivity by space confining the reactions. Thus, in multiple step reactions (cascade reactions), a more

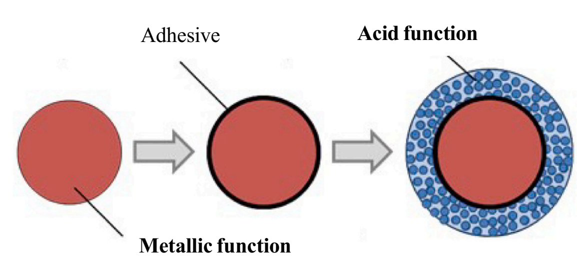

Fig. 17. Configuration of a bifunctional catalyst particle with core-shell structure. Reproduced from the work by Sánchez-Contador et al. [359], copyright 2019, Elsevier.

favorable reaction medium is achieved for each step. There are contributions in the literature for this initiative in the direct synthesis of DME, with core-shell catalysts prepared with the conventional CuO-ZnO-Al_2O_3 metallic function and using as acidic function HZSM-5 zeolite [352], γ-Al_2O_3 [353,354], SiO_2-Al_2O_3 [355] or SAPO-11 [356]. Guffanti et al. have conducted model analyses for evaluating the effect of the active phase distribution [357] and of the kinetics, adsorption capacity and mass and heat transfer [354] in the performance of hybrid, mechanically mixed and acidic-function@metallic-function and metallic-function@acidic-function structured core-shell catalysts. These works highlight the influence of the internal diffusion on productivity, pointing out metallic-function@acidic-function as the most suitable configuration, and that the small particle diameters and limited contact between phases avoids hot spots generation, favoring DME formation.

Sánchez-Contador et al. [144,330,351] have prepared a CuO-ZnO-ZrO_2@SAPO-11 core-shell catalyst by physical adhesive methodology (in a mass ratio of 1/2) with SiO_2 solution as adhesive [356,358]. With this configuration, methanol synthesis occurs in the CuO-ZnO-ZrO_2 core and diffuses for later being dehydrated in the surrounding SAPO-11 acidic shell. These authors have corroborated that the preparation method of core-shell particles prevents the partial blockage of SAPO-11 mesopores by CuO-ZnO-ZrO_2 particles in the pelletizing step used for preparing hybrid catalysts. For CO_2 + CO mixture hydrogenation (50% each) a DME yield of 8.7% and selectivity of 81% are achieved with this core-shell catalyst, whereas 7% and 77%, respectively, for the hybrid system (325 °C, 30 bar, 7.6 g_{cat} h mol_C^{-1}). Fig. 18 compares the CO_X conversion and products yields obtained with the core-shell configuration with those obtained with the conventional hybrid configuration. Moreover, the core-shell configuration prevents catalysts deactivation. After 24 h TOS, ~ 37% of DME yield decrease has been reported for conventional hybrid catalysts (from 7.4 to 4.7%), whereas the lessening is contained (to 21%) for the core-shell configuration (from 8.67 to 6.8%) [351].

Among the causes for the better performance of the core-shell over hybrid catalysts, the above mentioned works emphasize the creation of a favorable reaction medium by separating the methanol synthesis and its dehydration reactions in different regions, providing a higher availability of acidic sites on the catalyst particle surroundings for the conversion of the methanol formed in the nucleus. On this manner, limiting the presence of H_2O in the metallic nucleus leads to a greater resistance towards sintering of the Cu species in the nucleus [359]. Moreover, with a core-shell structure the adverse effects derived from the interaction between phases can be minimized. Thus, Nie et al. [360] have highlighted the advantage of the confinement of Cu species in the nucleus, avoiding their migration towards the acidic function. García-Trenco and Martínez [361] have proven through XPS analysis and 27 Al MAS-NMR spectra the migration of Al^{3+} species from HZSM-5 zeolite towards the CuO-ZnO-Al_2O_3 metallic function, resulting in catalyst deactivation by Cu sintering.

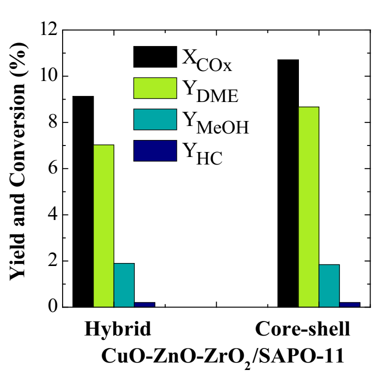

Fig. 18. Comparison of CO_x conversion and products yield at zero time on stream for bifunctional catalysts composed of CuO-ZnO-ZrO_2 metallic function and SAPO-11 acidic function in hybrid and core-shell configuration. Reaction conditions: 275 °C; 30 bar; feedstock, H_2/CO_X of 3 and $CO_2/(CO_2 + CO)$ of 0.5; 7.6 g_{cat} h mol_C^{-1}. Adapted from the work by Sánchez-Contador et al. [351], copyright 2018, Elsevier.

An important challenge for the scale-up of the CO_2-derived DME synthesis is to prepare catalysts with appropriate particle size and mechanical strength for industrial fixed-bed reactors. This requires addressing the agglomeration (using binders) of the catalysts configured with optimal structure according to laboratory scale results (as shown in this section) to build catalysts of several mm of particle size, high mechanical resistance and minimal performance loss (activity and selectivity) due to limitations of mass and heat transport. An overall view of the stages to progress towards the scale-up in the preparation of catalysts has been described in the literature [362,363].

To overcome the heat transfer limitations of the commonly used packed bed reactors with catalyst particles, the use of monolithic reactors (strategy 5) has been proposed and experimentally studied for syngas feedstocks [364,365]. For such configuration, the conductivity of the materials, cell density of corrugated monoliths and tortuosity of open cell foams are relevant parameters. Magzob et al. [364] compared the performance of HZSM-5 powder and monolith-structured (HZSM-5 and HZSM-5@SAPO-34) catalysts within 180–320 °C temperature range. With the HZSM-5 monolith configuration, a reduction on Brönsted acidic sites (and increase of Lewis acidic site density) and improvement of mesoporosity was reported. With this characteristics, better catalytic performance than for the powder zeolite was achieved, thus, methanol conversion ~70%, with high DME selectivity (96%) yet at 180 °C. Pérez-Miqueo et al. [365] investigated the use of metallic structured reactors for the direct DME synthesis process. These authors prepared the monoliths by wash coating the substrates with CZA and HZSM-5, and concluded that working at almost isothermal conditions is feasible with a volumetric productivity up to 0.20 L_{DME} h^{-1} m^{-3} at 300 °C and 4 MPa, with a catalyst hold-up of 0.33 g_{cat} cm^{-3} in a brass monolith (for syngas feedstocks).

4.4. Catalyst deactivation and regeneration

Given its importance in the viability of the process, the attenuation of catalyst deactivation is a priority challenge. Understanding the problem is hampered by the coexistence of different causes and by the synergy between the deactivation mechanisms of the metallic and acid functions. The main causes of deactivation are [366]: i) partial blockage of the metallic sites by coke (being considered as the fastest step in the deactivation); ii) coke deposition on the micro and mesopores of the acid function; iii) sintering of the metallic function; and iv) the detrimental interactions between the metallic and the acidic sites.

Coke characterization studies through Temperature Programmed Oxidation (TPO) have determined its presence both on the metallic and acidic sites, as well as on the interphase between them (corresponding to the inert Al_2O_3 in the CuO-ZnO-Al_2O_3/γ-Al_2O_3 catalyst [254,367–369]). However, coke is present on the metallic function since the initial stages of the reaction, achieving a limit value in a short period of time. This dynamic can be explained because the hydrogenation of coke precursors slows down its evolution [370,371]. The amount of coke deposited on the acidic function increases with time on stream, tending to a maximum value, resulting from the equilibrium between its formation and its diffusion to the exterior of the catalyst particles. Consequently, the properties of the acidic function are also important both for attenuating coke formation and for favoring the circulation of the intermediates towards the exterior of the catalyst particles.

It is worth mentioning the contribution of promoters like MgO [250,372], CeO_2 [252], and ZrO_2 [373] for preventing the sintering of CuO-ZnO metallic functions. The incorporation of these promoters pursues enhancing CuO crystallites dispersion and stabilizing its interaction with the support.

The presence of H_2O in the reaction medium (higher in the conversion of CO_2 than of syngas) has different effects on the activity of the catalyst. In first place, decreases the initial activity of the catalyst due to the competitive adsorption with the reactants in the metallic and acidic sites of the catalyst. The effect is very important for γ-Al_2O_3, due to the affinity for H_2O of its Lewis sites [211,370]. Furthermore, it favors the sintering of the metallic function, which has been proven for Cu catalysts as their oxidation is favored [337,374,375] and generates the disruption of the Cu-Zn synergy [240]. Fan et al. [376] have verified the increased stability of a Cu-ZnO-ZrO_2-Al_2O_3 catalyst used together with HZSM-5 catalyst, when modified with Fe, which is attributed to oxygen spillover between deficient iron oxide and Cu, mitigating oxidation (by CO_2 and H_2O) and Cu sintering.

On the other hand, it is well established that the presence of H_2O decreases the rate of coke formation [328]. This effect has been explained by the key role of methoxy ions as coke precursors on the metallic and acidic sites, whose formation is thermodynamically limited with the increase of H_2O concentration [245]. In addition, H_2O is competitively adsorbed with coke-forming intermediates, which are identified as monocyclic arenes, and whose formation takes place from hydrocarbons formed from methanol and DME [35]. Besides, the acidity and porous structure of the acid function have a great effect on the rate of coke deposition and on its nature and deactivating effect. Thus, Brønsted sites with high acidic strength are active in the reactions of coke precursors condensation towards polyaromatic structures and, their confinement is favored in acid functions with cavities in the porous structure [366].

Fan et al. [377] compare the individual deactivation of the two catalysts, CuO-ZnO-ZrO_2-Al_2O_3 (CZZA) and HZSM-5 zeolite, when mixed or separated in cascade (first CZZA and zeolite in line). Among the conclusions, the convenience of the proximity of both catalysts stands out, but avoiding an excessive concentration of H_2O on the surface of the CZZA catalyst (to attenuate the sintering of Cu) and also the excessive concentration of methanol (precursor of coke deposition in the HZSM-5 zeolite).

The configuration of the catalyst particle receives great attention for avoiding deactivation due to the close contact between the metallic and acid functions. García-Trenco and Martínez [361] have verified the migration of extra-framework Al^{3+}species of the HZSM-5 zeolite to the metallic function (CuO-ZnO-Al_2O_3) through a mechanism assisted by H_2O, causing the disruption of the Cu-Zn synergy, and facilitating the sintering of Cu. Likewise, the migration of Cu^{2+} ions is facilitated by the presence of H_2O and hydroxyls (Brønsted) sites [337,378,379]. These problems advise avoiding intimate contact between the metallic and acid functions in the preparation of the catalyst, being the pre-pelletization of each function separately more suitable than the joint pelletization of a fine powder of both functions in this case [380].

Ateka et al. [254] have studied the regeneration of a CuO-ZnO-MnO/SAPO-18 hybrid catalyst, on which coke deposition is reported to be the main responsible for deactivation. Working at reaction-regeneration cycles, these authors have determined that it is possible to regenerate the bifunctional catalyst by coke combustion with air at 300 °C for 48 h. Even if at these conditions the catalyst undergoes a slight sintering of Cu in the first cycle, in the succeeding cycles it demonstrated to reach a pseudo-steady state, completely recovering the activity. Being therefore coke deactivation reversible, this study pointed out sintering as the limiting factor for using these type of catalysts. The small activity loss observed in the first reaction-regeneration cycle was attributed to the sintering of a certain fraction of unstable metallic sites either due to the high water content in the reaction medium or by the generation of hot spots in the regeneration step [254]. Consequently, enhancing the stability of the metallic function also favors the regeneration of the catalyst by allowing to perform coke combustion at higher temperature. In addition, the porous structure and acidity of the catalyst, besides being important for the attenuation of coke condensation [366], are also relevant factors to facilitate its combustion.

5. Conclusions and prospects

The interest of the direct synthesis of DME for valorizing CO_2 on a large scale is based on the capacity for the conversion of CO_2 and syngas and on the good prospects of the applications of DME as "green" fuel and as raw material for the sustainable production of chemicals and H_2.

Carrying out the methanol dehydration reaction *in situ*, in the same reactor as methanol synthesis, shifts the thermodynamic equilibrium, upgrading oxygenates formation. Moreover, with this strategy co-feeding of CO_2 together with syngas is more favorable than in the synthesis of methanol, which is interesting to valorize (*via* gasification) lignocellulosic biomass and wastes from the consumer society (as plastics and used tires). The conversion of CO_2 attained in the direct synthesis of DME is higher than that in the synthesis of methanol and in the conventional production of DME in two stages.

The reaction conditions (pressure and temperature) in the direct synthesis of DME are different to the optimal conditions for each of the individual reactions. Furthermore, CO_2 is less reactive than CO and its hydrogenation generates a higher concentration of H_2O. These differences in the operating conditions and concentration have required studying the suitable composition and properties of the metallic and acid functions of the catalyst. As consequence, a reasonable understanding of the performance of some suitable compositions has been reached, in particular for conventional configurations (hybrid catalysts prepared by mixing and pelletizing/extrusion of both functions). As in most catalytic processes, the main challenges correspond to the attenuation of the deactivation of the catalyst, being the sintering of the metallic function and coke deposition on both functions the main causes.

It is well established that the contact of the metallic and acid functions favors deactivation, due to the development of species (as Cu^{2+} and Al^{3+}) transport mechanisms, and also that favors the synergy of coke formation mechanisms in both functions. This knowledge has opened a wide research field pursuing to establish the ideal core-shell configuration to minimize the negative effects derived from the contact between the two functions of the catalyst, and in particular, to achieve the stability of the catalyst.

The level of knowledge achieved in the fundamental aspects (collected in this review) allows considering that the CO_2 to DME synthesis process can effectively contribute to the mitigation of climate change. Achieving the necessary challenges for this objective requires a multidisciplinary work at different scales (catalyst, kinetic modeling, reactor design and scaling).

The scaling-up of the CO_2-derived DME synthesis process requires catalysts prepared based on the important advances carried out in the design of catalysts for the reactions of CO_2-to-methanol and methanol dehydration to DME. To meet this objective, the advances must be adapted to the different conditions and the different composition of the reaction medium of the integrated process. In this sense, the co-feeding of CO_2 together with syngas has good perspectives to favor the viability of the process, but requires adequate catalysts, and the resolution of the unknowns regarding the different mechanism for the formation of methanol from CO and CO_2 and the synergy between both mechanisms. Likewise, the stability of the catalyst is a challenge requiring more attention.

The adaptation of catalysts optimized at nanometric scale to the needs of the industrial reactors is an important challenge. This requires studying composites with the appropriate size and with high mechanical resistance, without deterioration of the performance of the catalyst particles.

The viability of the process on an industrial scale also requires adapting the design of the catalysts to the innovations in the design of the reactors, which, like for the hydrophilic membrane reactor, require increasing the per pass conversion. With a different composition in the reaction medium, a different thermodynamic situation is created in these reactors. Accordingly, an adaptation of the catalysts to the optimal conditions and composition in these reactors will also be required.

Furthermore, the important development of CO_2 valorization initiatives to mitigate climate change, advise expanding the field of study of the CO_2-derived DME synthesis process, also considering it as preceding stage to the subsequent synthesis (online stage, or in an integrated process) of fuels and chemicals (olefins or aromatics). In the latter case, the direct DME synthesis catalyst will be used in a tandem catalyst together with an acid catalyst for the selective conversion of DME.

Declaration of Competing Interest

The authors declare that they have no known competing financial interests or personal relationships that could have appeared to influence the work reported in this paper.

Acknowledgements

This work has been carried out with the financial support of the Ministry of Science, Innovation and Universities of the Spanish Government (PID2019-108448RB-100); the Basque Government (Project IT1645-22); the European Regional Development Funds (ERDF); and the European Commission (HORIZON H2020-MSCA RISE-2018. Contract No. 823745).

References

[1] B. TM, Considering environmental costs of greenhouse gas emissions for setting a CO_2 tax: a review, Sci. Total Environ. 720 (2020), 137524, https://doi.org/10.1016/J.SCITOTENV.2020.137524.

[2] Marsh and McLennan companies, Climate Resilience Handbook, (2020). https://www.marshmclennan.com/insights/publications/2020/september/climate-resilience-handbook.html, 2020 (accessed November 2, 2021).

[3] C. Cao, H. Liu, Z. Hou, F. Mehmood, J. Liao, W. Feng, A review of CO_2 storage in view of safety and cost-effectiveness, Energies. 13 (2020) 600, https://doi.org/10.3390/EN13030600.

[4] S. Hafeez, T. Safdar, E. Pallari, G. Manos, E. Aristodemou, Z. Zhang, S.M. Al-Salem, A. Constantinou, CO_2 capture using membrane contactors: a systematic literature review, Front. Chem. Sci. Eng. 15 (2020) 720–754, https://doi.org/10.1007/S11705-020-1992-Z.

[5] U. Kamran, S.J. Park, Chemically modified carbonaceous adsorbents for enhanced CO_2 capture: a review, J. Clean. Prod. 290 (2021), 125776, https://doi.org/10.1016/J.JCLEPRO.2020.125776.

[6] A.M. Varghese, G.N. Karanikolos, CO_2 capture adsorbents functionalized by amine – bearing polymers: a review, Int. J. Greenh. Gas Control. 96 (2020), 103005, https://doi.org/10.1016/J.IJGGC.2020.103005.

[7] R. Sharifian, R.M. Wagterveld, I.A. Digdaya, C. Xiang, D.A. Vermaas, Electrochemical carbon dioxide capture to close the carbon cycle, Energy Environ. Sci. 14 (2021) 781–814, https://doi.org/10.1039/D0EE03382K.

[8] X. Shi, H. Xiao, H. Azarabadi, J. Song, X. Wu, X. Chen, K.S. Lackner, Sorbents for the direct capture of CO_2 from ambient air, Angew. Chemie Int. Ed. 59 (2020) 6984–7006, https://doi.org/10.1002/ANIE.201906756.

[9] A. Dutta, S. Farooq, I.A. Karimi, S.A. Khan, Assessing the potential of CO_2 utilization with an integrated framework for producing power and chemicals, J. CO2 Util. 19 (2017) 49–57, https://doi.org/10.1016/J.JCOU.2017.03.005.

[10] A. Rafiee, K. Rajab Khalilpour, D. Milani, M. Panahi, Trends in CO_2 conversion and utilization: a review from process systems perspective, J. Environ. Chem. Eng. 6 (2018) 5771–5794, https://doi.org/10.1016/j.jece.2018.08.065.

[11] A.D.N. Kamkeng, M. Wang, J. Hu, W. Du, F. Qian, Transformation technologies for CO_2 utilisation: current status, challenges and future prospects, Chem. Eng. J. 409 (2021), 128138, https://doi.org/10.1016/j.cej.2020.128138.

[12] H. Naims, Economics of carbon dioxide capture and utilization—a supply and demand perspective, Environ. Sci. Pollut. Res. 23 (2016) 22226–22241, https://doi.org/10.1007/S11356-016-6810-2.

[13] E. Alper, O. Yuksel Orhan, CO_2 utilization: developments in conversion processes, Petroleum. 3 (2017) 109–126, https://doi.org/10.1016/j.petlm.2016.11.003.

[14] Y. Zheng, W. Zhang, Y. Li, J. Chen, B. Yu, J. Wang, L. Zhang, J. Zhang, Energy related CO_2 conversion and utilization: advanced materials/nanomaterials, reaction mechanisms and technologies, Nano Energy 40 (2017) 512–539, https://doi.org/10.1016/J.NANOEN.2017.08.049.

[15] S.M. Jarvis, S. Samsatli, Technologies and infrastructures underpinning future CO_2 value chains: a comprehensive review and comparative analysis, Renew. Sust. Energ. Rev. 85 (2018) 46–68, https://doi.org/10.1016/J.RSER.2018.01.007.

[16] R.S. Norhasyima, T.M.I. Mahlia, Advances in CO_2 utilization technology: a patent landscape review, J. CO2 Util. 26 (2018) 323–335, https://doi.org/10.1016/J.JCOU.2018.05.022.

[17] G. Chen, G.I.N. Waterhouse, R. Shi, J. Zhao, Z. Li, L.Z. Wu, C.H. Tung, T. Zhang, From solar energy to fuels: recent advances in light-driven C1 chemistry, Angew. Chemie - Int. Ed. 58 (2019) 17528–17551, https://doi.org/10.1002/anie.201814313.

[18] G. Centi, E.A. Quadrelli, S. Perathoner, Catalysis for CO_2 conversion: a key technology for rapid introduction of renewable energy in the value chain of chemical industries, Energy Environ. Sci. 6 (2013) 1711–1731, https://doi.org/10.1039/C3EE00056G.

[19] M. Aresta, A. Dibenedetto, E. Quaranta, State of the art and perspectives in catalytic processes for CO_2 conversion into chemicals and fuels: the distinctive contribution of chemical catalysis and biotechnology, J. Catal. 343 (2016) 2–45, https://doi.org/10.1016/J.JCAT.2016.04.003.

[20] R.G. Grim, Z. Huang, M.T. Guarnieri, J.R. Ferrell, L. Tao, J.A. Schaidle, Transforming the carbon economy: challenges and opportunities in the convergence of low-cost electricity and reductive CO_2 utilization, Energy Environ. Sci. 13 (2020) 472–494, https://doi.org/10.1039/C9EE02410G.

[21] Z. Zhang, S.Y. Pan, H. Li, J. Cai, A.G. Olabi, E.J. Anthony, V. Manovic, Recent advances in carbon dioxide utilization, Renew. Sust. Energ. Rev. 125 (2020), 109799, https://doi.org/10.1016/J.RSER.2020.109799.

[22] H. Salehizadeh, N. Yan, R. Farnood, Recent advances in microbial CO_2 fixation and conversion to value-added products, Chem. Eng. J. 390 (2020), 124584, https://doi.org/10.1016/J.CEJ.2020.124584.

[23] A. Mustafa, B.G. Lougou, Y. Shuai, Z. Wang, H. Tan, Current technology development for CO_2 utilization into solar fuels and chemicals: a review, J. Energy Chem. 49 (2020) 96–123, https://doi.org/10.1016/J.JECHEM.2020.01.023.

[24] J. Godin, W. Liu, S. Ren, C.C. Xu, Advances in recovery and utilization of carbon dioxide: a brief review, J. Environ. Chem. Eng. 9 (2021), 105644, https://doi.org/10.1016/J.JECE.2021.105644.

[25] J. Wu, Y. Huang, W. Ye, Y. Li, CO_2 Reduction: from the Electrochemical to Photochemical Approach, Adv. Sci. 4 (2017) 1700194, https://doi.org/10.1002/ADVS.201700194.

[26] Y. Jiang, F. Chen, C. Xia, A review on cathode processes and materials for electro-reduction of carbon dioxide in solid oxide electrolysis cells, J. Power Sources 493 (2021), 229713, https://doi.org/10.1016/J.JPOWSOUR.2021.229713.

[27] J. Low, B. Cheng, J. Yu, Surface modification and enhanced photocatalytic CO_2 reduction performance of TiO_2: a review, Appl. Surf. Sci. 392 (2017) 658–686, https://doi.org/10.1016/J.APSUSC.2016.09.093.

[28] N. Homs, J. Toyir, P.R. De La Piscina, Catalytic processes for activation of CO_2, in: S.L. Suib (Ed.), New Futur. Dev. Catal, Elsevier, 2013, pp. 1–26, https://doi.org/10.1016/B978-0-444-53882-6.00001-2.

[29] A. Rafiee, M. Panahi, K.R. Khalilpour, CO_2 utilization through integration of post-combustion carbon capture process with Fischer-Tropsch gas-to-liquid (GTL) processes, J. CO2 Util. 18 (2017) 98–106, https://doi.org/10.1016/J.JCOU.2017.01.016.

[30] G. Leonzio, State of art and perspectives about the production of methanol, dimethyl ether and syngas by carbon dioxide hydrogenation, J. CO2 Util. 27 (2018) 326–354, https://doi.org/10.1016/j.jcou.2018.08.005.

[31] M.D. Garba, M. Usman, S. Khan, F. Shehzad, A. Galadima, M.F. Ehsan, A. S. Ghanem, M. Humayun, CO_2 towards fuels: a review of catalytic conversion of carbon dioxide to hydrocarbons, J. Environ. Chem. Eng. 9 (2021), 104756, https://doi.org/10.1016/J.JECE.2020.104756.

[32] P. Tian, Y. Wei, M. Ye, Z. Liu, Methanol to olefins (MTO): from fundamentals to commercialization, ACS Catal. 5 (2015) 1922–1938, https://doi.org/10.1021/acscatal.5b00007.

[33] P. Pérez-Uriarte, A. Ateka, M. Gamero, A.T. Aguayo, J. Bilbao, Effect of the operating conditions in the transformation of DME to olefins over a HZSM-5 zeolite catalyst, Ind. Eng. Chem. Res. 55 (2016) 6569–6578, https://doi.org/10.1021/acs.iecr.6b00627.

[34] A.T. Aguayo, D. Mier, A.G. Gayubo, M. Gamero, J. Bilbao, Kinetics of methanol transformation into hydrocarbons on a HZSM-5 zeolite catalyst at high temperature (400−550 °C), Ind. Eng. Chem. Res. 49 (2010) 12371–12378, https://doi.org/10.1021/IE101047F.

[35] T. Cordero-Lanzac, A. Ateka, P. Pérez-Uriarte, P. Castaño, A.T. Aguayo, J. Bilbao, Insight into the deactivation and regeneration of HZSM-5 zeolite catalysts in the conversion of dimethyl ether to olefins, Ind. Eng. Chem. Res. 57 (2018) 13689–13702, https://doi.org/10.1021/acs.iecr.8b03308.

[36] T. Shoinkhorova, T. Cordero-Lanzac, A. Ramirez, S.H. Chung, A. Dokania, J. Ruiz-Martinez, J. Gascon, Highly selective and stable production of aromatics via high-pressure methanol conversion, ACS Catal. 11 (2021) 3602–3613, https://doi.org/10.1021/acscatal.0c05133.

[37] M. Bjørgen, S. Svelle, F. Joensen, J. Nerlov, S. Kolboe, F. Bonino, L. Palumbo, S. Bordiga, U. Olsbye, Conversion of methanol to hydrocarbons over zeolite H-ZSM-5: on the origin of the olefinic species, J. Catal. 249 (2007) 195–207, https://doi.org/10.1016/j.jcat.2007.04.006.

[38] G. Garcia, E. Arriola, W.H. Chen, M.D. De Luna, A comprehensive review of hydrogen production from methanol thermochemical conversion for sustainability, Energy 217 (2021), 119384, https://doi.org/10.1016/J.ENERGY.2020.119384.

[39] E. Catizzone, C. Freda, G. Braccio, F. Frusteri, G. Bonura, Dimethyl ether as circular hydrogen carrier: catalytic aspects of hydrogenation/dehydrogenation steps, J. Energy Chem. 58 (2021) 55–77, https://doi.org/10.1016/j.jechem.2020.09.040.

[40] C. Brookes, M. Bowker, P.P. Wells, Catalysts for the selective oxidation of methanol, Catalysts 6 (2016) 92, https://doi.org/10.3390/CATAL6070092.

[41] A.M. Bahmanpour, F. Héroguel, M. Kılıç, C.J. Baranowski, L. Artiglia, U. Röthlisberger, J.S. Luterbacher, O. Kröcher, Cu–Al spinel as a highly active and

stable catalyst for the reverse water gas shift reaction, ACS Catal. 9 (2019) 6243–6251, https://doi.org/10.1021/ACSCATAL.9B01822.

[42] A. Abdulrasheed, A.A. Jalil, Y. Gambo, M. Ibrahim, H.U. Hambali, M.Y. Shahul Hamid, A review on catalyst development for dry reforming of methane to syngas: recent advances, Renew. Sust. Energ. Rev. 108 (2019) 175–193, https://doi.org/10.1016/J.RSER.2019.03.054.

[43] H. Yang, C. Zhang, P. Gao, H. Wang, X. Li, L. Zhong, W. Wei, Y. Sun, A review of the catalytic hydrogenation of carbon dioxide into value-added hydrocarbons, Catal. Sci. Technol. 7 (2017) 4580–4598, https://doi.org/10.1039/C7CY01403A.

[44] L. Tan, P. Zhang, Y. Cui, Y. Suzuki, H. Li, L. Guo, G. Yang, N. Tsubaki, Direct CO_2 hydrogenation to light olefins by suppressing CO by-product formation, Fuel Process. Technol. 196 (2019), 106174, https://doi.org/10.1016/j.fuproc.2019.106174.

[45] A. Portillo, A. Ateka, J. Ereña, A.T. Aguayo, J. Bilbao, Conditions for the joint conversion of CO_2 and syngas in the direct synthesis of light olefins using In_2O_3-ZrO_2/SAPO-34 catalyst, Ind. Eng. Chem. Res. (2022), https://doi.org/10.1021/acs.iecr.1c03556 (n.d.).

[46] S. De, A. Dokania, A. Ramirez, J. Gascon, Advances in the design of heterogeneous catalysts and thermocatalytic processes for CO_2 utilization, ACS Catal. 10 (2020) 14147–14185, https://doi.org/10.1021/acscatal.0c04273.

[47] J. Carlos Colmenares, Novel trends in the utilization of CO_2 as a reagent and mild oxidant in the C-C coupling reactions, Curr. Org. Synth. 7 (2011) 533–542, https://doi.org/10.2174/157017910794328600.

[48] A.M. Arinaga, M.C. Ziegelski, T.J. Marks, Alternative oxidants for the catalytic oxidative coupling of methane, Angew. Chemie Int. Ed. 60 (2021) 10502–10515, https://doi.org/10.1002/ANIE.202012862.

[49] E.N. Al-Shafei, D. Robert Brown, S.P. Katikaneni, H. Aljama, H.H. Al-Badairy, Direct conversion of CO_2 with methane into chemicals over ZrO_2/TiO_2 catalysts, Chem. Eng. J. 419 (2021), 129416, https://doi.org/10.1016/J.CEJ.2021.129416.

[50] Y.-M. Liu, Y. Cao, N. Yi, W.-L. Feng, W.-L. Dai, S.-R. Yan, H.-Y. He, K.-N. Fan, Vanadium oxide supported on mesoporous SBA-15 as highly selective catalysts in the oxidative dehydrogenation of propane, J. Catal. 224 (2004) 417–428, https://doi.org/10.1016/j.jcat.2004.03.010.

[51] B. Zheng, W. Hua, Y. Yue, Z. Gao, Dehydrogenation of propane to propene over different polymorphs of gallium oxide, J. Catal. 232 (2005) 143–151, https://doi.org/10.1016/J.JCAT.2005.03.001.

[52] S. Najari, S. Saeidi, P. Concepcion, D.D. Dionysiou, S.K. Bhargava, A.F. Lee, K. Wilson, Oxidative dehydrogenation of ethane: catalytic and mechanistic aspects and future trends, Chem. Soc. Rev. 50 (2021) 4564–4605, https://doi.org/10.1039/D0CS01518K.

[53] X. Jiang, L. Sharma, V. Fung, S.J. Park, C.W. Jones, B.G. Sumpter, J. Baltrusaitis, Z. Wu, Oxidative dehydrogenation of propane to propylene with soft oxidants via heterogeneous catalysis, ACS Catal. 11 (2021) 2182–2234, https://doi.org/10.1021/ACSCATAL.0C03999.

[54] P. Michorczyk, P. Pietrzyk, J. Ogonowski, Preparation and characterization of SBA-1–supported chromium oxide catalysts for CO_2, Microporous Mesoporous Mater. 161 (2012) 56–66, https://doi.org/10.1016/J.MICROMESO.2012.05.011.

[55] K. Song, S. Wang, Q. Sun, D. Xu, Study of oxidative dehydrogenation of ethylbenzene with CO_2 on supported CeO_2-Fe_2O_3 binary oxides, Arab. J. Chem. 13 (2020) 7357–7369, https://doi.org/10.1016/J.ARABJC.2020.08.013.

[56] D.R. Burri, K.M. Choi, J.H. Lee, D.S. Han, S.E. Park, Influence of SBA-15 support on CeO_2–ZrO_2 catalyst for the dehydrogenation of ethylbenzene to styrene with CO_2, Catal. Commun. 8 (2007) 43–48, https://doi.org/10.1016/J.CATCOM.2006.05.024.

[57] L. Wang, Y. Wang, R. Zhang, R. Ding, X. Chen, B. Lv, Edge-activating CO_2-mediated ethylbenzene dehydrogenation by a hierarchical porous BN catalyst, ACS Catal. 10 (2020) 6697–6706, https://doi.org/10.1021/ACSCATAL.0C00070.

[58] Y. Sakurai, T. Suzaki, N.O. Ikenaga, T. Suzuki, Dehydrogenation of ethylbenzene with an activated carbon-supported vanadium catalyst, Appl. Catal. A Gen. 192 (2000) 281–288, https://doi.org/10.1016/S0926-860X(99)00398-1.

[59] Z.-W. Liu, C. Wang, W.-B. Fan, Z.-T. Liu, Q.-Q. Hao, X. Long, J. Lu, J.-G. Wang, Z.-F. Qin, D.S. Su, $V_2O_5/Ce_{0.6}Zr_{0.4}O_2$-$Al_2O_3$ as an efficient catalyst for the oxidative dehydrogenation of ethylbenzene with carbon dioxide, ChemSusChem. 4 (2011) 341–345, https://doi.org/10.1002/CSSC.201000351.

[60] S. Jung, J. Lee, D.H. Moon, K.H. Kim, E.E. Kwon, Upgrading biogas into syngas through dry reforming, Renew. Sust. Energ. Rev. 143 (2021), 110949, https://doi.org/10.1016/J.RSER.2021.110949.

[61] C. Song, W. Pan, Tri-reforming of methane: a novel concept for catalytic production of industrially useful synthesis gas with desired H_2/CO ratios, Catal. Today 98 (2004) 463–484, https://doi.org/10.1016/J.CATTOD.2004.09.054.

[62] Z. Li, Q. Lin, M. Li, J. Cao, F. Liu, H. Pan, Z. Wang, S. Kawi, Recent advances in process and catalyst for CO_2 reforming of methane, Renew. Sust. Energ. Rev. 134 (2020), 110312, https://doi.org/10.1016/J.RSER.2020.110312.

[63] B. Abdullah, N.A. Abd Ghani, D.V.N. Vo, Recent advances in dry reforming of methane over Ni-based catalysts, J. Clean. Prod. 162 (2017) 170–185, https://doi.org/10.1016/J.JCLEPRO.2017.05.176.

[64] R. Singh, A. Dhir, S.K. Mohapatra, S.K. Mahla, Dry reforming of methane using various catalysts in the process: review, Biomass Convers. Biorefinery. 10 (2019) 567–587, https://doi.org/10.1007/S13399-019-00417-1.

[65] A. Erdőhelyi, Catalytic reaction of carbon dioxide with methane on supported noble metal catalysts, Catalysts 11 (2021) 159, https://doi.org/10.3390/CATAL11020159.

[66] A.H.K. Owgi, A.A. Jalil, I. Hussain, N.S. Hassan, H.U. Hambali, T.J. Siang, D.V. N. Vo, Catalytic systems for enhanced carbon dioxide reforming of methane: a review, Environ. Chem. Lett. 193 (19) (2021) 2157–2183, https://doi.org/10.1007/S10311-020-01164-W.

[67] C. Wang, Y. Wang, M. Chen, D. Liang, Z. Yang, W. Cheng, Z. Tang, J. Wang, H. Zhang, Recent advances during CH_4 dry reforming for syngas production: a mini review, Int. J. Hydrog. Energy 46 (2021) 5852–5874, https://doi.org/10.1016/J.IJHYDENE.2020.10.240.

[68] Y. Ruan, Y. Zhao, Y. Lu, D. Guo, Y. Zhao, S. Wang, X. Ma, Mesoporous $LaAl_{0.25}Ni_{0.75}O_3$ perovskite catalyst using SBA-15 as templating agent for methane dry reforming, Microporous Mesoporous Mater. 303 (2020), 110278, https://doi.org/10.1016/J.MICROMESO.2020.110278.

[69] A. Corma, V. Fornés, J.M. Guil, S. Pergher, T.L.M. Maesen, J.G. Buglass, Preparation, characterisation and catalytic activity of ITQ-2, a delaminated zeolite, Microporous Mesoporous Mater. 38 (2000) 301–309, https://doi.org/10.1016/S1387-1811(00)00149-9.

[70] M.A. Goula, N.D. Charisiou, G. Siakavelas, L. Tzounis, I. Tsiaoussis, P. Panagiotopoulou, G. Goula, I.V. Yentekakis, Syngas production via the biogas dry reforming reaction over Ni supported on zirconia modified with CeO_2 or La_2O_3 catalysts, Int. J. Hydrog. Energy 42 (2017) 13724–13740, https://doi.org/10.1016/J.IJHYDENE.2016.11.196.

[71] L. Dehimi, M. Gaillard, M. Virginie, A. Erto, Y. Benguerba, Investigation of dry reforming of methane over Mo-based catalysts, Int. J. Hydrog. Energy 45 (2020) 24657–24669, https://doi.org/10.1016/J.IJHYDENE.2020.06.203.

[72] Y. Wang, Q. Zhao, Y. Wang, C. Hu, P. Da Costa, One-step synthesis of highly active and stable Ni–ZrO_x for dry reforming of methane, Ind. Eng. Chem. Res. 59 (2020) 11441–11452, https://doi.org/10.1021/ACS.IECR.0C01416.

[73] V.I. Savchenko, Y.S. Zimin, A.V. Nikitin, I.V. Sedov, V.S. Arutyunov, Utilization of CO_2 in non-catalytic dry reforming of C_1–C_4 hydrocarbons, J. CO2 Util. 47 (2021), 101490, https://doi.org/10.1016/J.JCOU.2021.101490.

[74] S. Bac, S. Keskin, A.K. Avci, Recent advances in sustainable syngas production by catalytic CO_2 reforming of ethanol and glycerol, Sustain, Energy Fuel 4 (2020) 1029–1047, https://doi.org/10.1039/C9SE00967A.

[75] A.M. da Silva, K.R. de Souza, G. Jacobs, U.M. Graham, B.H. Davis, L.V. Mattos, F. B. Noronha, Steam and CO_2 reforming of ethanol over Rh/CeO_2 catalyst, Appl. Catal. B Environ. 102 (2011) 94–109, https://doi.org/10.1016/J.APCATB.2010.11.030.

[76] S. Zhao, W. Cai, Y. Li, H. Yu, S. Zhang, L. Cui, Syngas production from ethanol dry reforming over Rh/CeO_2 catalyst, J. Saudi Chem. Soc. 22 (2018) 58–65, https://doi.org/10.1016/J.JSCS.2017.07.003.

[77] X. Wu, S. Kawi, Rh/Ce-SBA-15: active and stable catalyst for CO_2 reforming of ethanol to hydrogen, Catal. Today 148 (2009) 251–259, https://doi.org/10.1016/J.CATTOD.2009.08.006.

[78] A. Drif, N. Bion, R. Brahmi, S. Ojala, L. Pirault-Roy, E. Turpeinen, P.K. Seelam, R. L. Keiski, F. Epron, Study of the dry reforming of methane and ethanol using Rh catalysts supported on doped alumina, Appl. Catal. A Gen. 504 (2015) 576–584, https://doi.org/10.1016/J.APCATA.2015.02.019.

[79] T. Hou, Y. Lei, S. Zhang, J. Zhang, W. Cai, Ethanol dry reforming for syngas production over Ir/CeO_2 catalyst, J. Rare Earths 33 (2015) 42–45, https://doi.org/10.1016/S1002-0721(14)60381-1.

[80] M.B. Bahari, B.C. Goo, T.L.M. Pham, T.J. Siang, H.T. Danh, N. Ainirazali, D.V. N. Vo, Hydrogen-rich syngas production from ethanol dry reforming on La-doped Ni/Al_2O_3 catalysts: effect of promoter loading, Procedia Eng. 148 (2016) 654–661, https://doi.org/10.1016/J.PROENG.2016.06.531.

[81] M.B. Bahari, N.H.H. Phuc, F. Alenazey, K.B. Vu, N. Ainirazali, D.V.N. Vo, Catalytic performance of La-Ni/Al_2O_3 catalyst for CO_2 reforming of ethanol, Catal. Today 291 (2017) 67–75, https://doi.org/10.1016/J.CATTOD.2017.02.019.

[82] F. Fayaz, H.T. Danh, C. Nguyen-Huy, K.B. Vu, B. Abdullah, D.V.N. Vo, Promotional effect of Ce-dopant on Al_2O_3-supported Co catalysts for syngas production via CO_2 reforming of ethanol, Procedia Eng. 148 (2016) 646–653, https://doi.org/10.1016/J.PROENG.2016.06.530.

[83] M.N.N. Shafiqah, H.N. Tran, T.D. Nguyen, P.T.T. Phuong, B. Abdullah, S.S. Lam, P. Nguyen-Tri, R. Kumar, S. Nanda, D.V.N. Vo, Ethanol CO_2 reforming on La_2O_3 and CeO_2-promoted Cu/Al_2O_3 catalysts for enhanced hydrogen production, Int. J. Hydrog. Energy 45 (2020) 18398–18410, https://doi.org/10.1016/J.IJHYDENE.2019.10.024.

[84] M. Tavanarad, F. Meshkani, M. Rezaei, Production of syngas via glycerol dry reforming on Ni catalysts supported on mesoporous nanocrystalline Al_2O_3, J. CO2 Util. 24 (2018) 298–305, https://doi.org/10.1016/J.JCOU.2018.01.009.

[85] K.W. Siew, H.C. Lee, M.R. Khan, J. Gimbun, C.K. Cheng, CO_2 reforming of glycerol over La-Ni/Al_2O_3 catalyst: a longevity evaluative study, J. Energy Chem. 24 (2015) 366–373, https://doi.org/10.1016/S2095-4956(15)60324-2.

[86] N.N.M. Arif, N. Harun, N.M. Yunus, D.-V.N. Vo, M.T. Azizan, S.Z. Abidin, Reforming of glycerol for hydrogen production over Ni based catalysts: effect of support type, Energy Sources, Part A Recover. Util. Environ. Eff. 39 (2017) 657–663, https://doi.org/10.1080/15567036.2016.1244580.

[87] N. Harun, J. Gimbun, M.T. Azizan, S.Z. Abidin, Characterization of Ag-promoted Ni/SiO_2 catalysts for syngas production via carbon dioxide (CO_2) Dry reforming of glycerol, Bull. Chem. React. Eng. Catal. 11 (2016) 220–229, https://doi.org/10.9767/BCREC.11.2.553.220-229.

[88] N.N. Mohd Arif, S.Z. Abidin, O.U. Osazuwa, D.V.N. Vo, M.T. Azizan, Y.H. Taufiq-Yap, Hydrogen production via CO_2 dry reforming of glycerol over ReNi/CaO catalysts, Int. J. Hydrog. Energy 44 (2019) 20857–20871, https://doi.org/10.1016/J.IJHYDENE.2018.06.084.

[89] M. Tavanarad, F. Meshkani, M. Rezaei, Synthesis and application of noble metal nanocatalysts supported on $MgAl_2O_4$ in glycerol dry reforming reaction, Catal. Letters. 148 (2017) 164–172, https://doi.org/10.1007/S10562-017-2221-3.

[90] B. Yu, Z.F. Diao, C.X. Guo, L.N. He, Carboxylation of olefins/alkynes with CO_2 to industrially relevant acrylic acid derivatives, J. CO2 Util. 1 (2013) 60–68, https://doi.org/10.1016/J.JCOU.2013.01.001.
[91] D. Ballivet-Tkatchenko, J.H.Z. Dos Santos, K. Philippot, S. Vasireddy, Carbon dioxide conversion to dimethyl carbonate: the effect of silica as support for SnO_2 and ZrO_2 catalysts, Comptes Rendus Chim. 14 (2011) 780–785, https://doi.org/10.1016/J.CRCI.2010.08.003.
[92] M. Honda, M. Tamura, Y. Nakagawa, S. Sonehara, K. Suzuki, K. Fujimoto, K. Tomishige, Ceria-catalyzed conversion of carbon dioxide into dimethyl carbonate with 2-cyanopyridine, ChemSusChem. 6 (2013) 1341–1344, https://doi.org/10.1002/CSSC.201300229.
[93] S. Verma, R.B.N. Baig, M.N. Nadagouda, R.S. Varma, Fixation of carbon dioxide into dimethyl carbonate over titanium-based zeolitic thiophene-benzimidazolate framework, Sci. Rep. 7 (2017) 1–5, https://doi.org/10.1038/s41598-017-00736-1.
[94] J. Bian, M. Xiao, S.J. Wang, Y.X. Lu, Y.Z. Meng, Carbon nanotubes supported Cu–Ni bimetallic catalysts and their properties for the direct synthesis of dimethyl carbonate from methanol and carbon dioxide, Appl. Surf. Sci. 255 (2009) 7188–7196, https://doi.org/10.1016/J.APSUSC.2009.03.057.
[95] Y. Chen, Y. Yang, S. Tian, Z. Ye, Q. Tang, L. Ye, G. Li, Highly effective synthesis of dimethyl carbonate over CuNi alloy nanoparticles @Porous organic polymers composite, Appl. Catal. A Gen. 587 (2019), 117275, https://doi.org/10.1016/J.APCATA.2019.117275.
[96] C.L. Chiang, K.S. Lin, S.H. Yu, Improvement of dimethyl carbonate formation via methanol carbonation over vanadium-doped Cu–Ni/AC catalyst, J. Taiwan Inst. Chem. Eng. 98 (2019) 132–149, https://doi.org/10.1016/J.JTICE.2018.08.001.
[97] F. Jutz, J.D. Grunwaldt, A. Baiker, In situ XAS study of the Mn(III)(salen)Br catalyzed synthesis of cyclic organic carbonates from epoxides and CO_2, J. Mol. Catal. A Chem. 297 (2009) 63–72, https://doi.org/10.1016/J.MOLCATA.2008.10.009.
[98] M. Gu, Z. Cheng, M. Gu, Z. Cheng, Carboxylation of aromatics by CO_2 under "Si/Al based frustrated lewis pairs" catalytic system, J. Mater. Sci. Chem. Eng. 3 (2015) 103–108, https://doi.org/10.4236/MSCE.2015.31015.
[99] X. Xiang, L. Guo, X. Wu, X. Ma, Y. Xia, Urea formation from carbon dioxide and ammonia at atmospheric pressure, Environ. Chem. Lett. 10 (2012) 295–300, https://doi.org/10.1007/S10311-012-0366-2.
[100] C. Chen, X. Zhu, X. Wen, Y. Zhou, L. Zhou, H. Li, L. Tao, Q. Li, S. Du, T. Liu, D. Yan, C. Xie, Y. Zou, Y. Wang, R. Chen, J. Huo, Y. Li, J. Cheng, H. Su, X. Zhao, W. Cheng, Q. Liu, H. Lin, J. Luo, J. Chen, M. Dong, K. Cheng, C. Li, S. Wang, Coupling N_2 and CO_2 in H_2O to synthesize urea under ambient conditions, Nat. Chem. 12 (2020) 717–724, https://doi.org/10.1038/s41557-020-0481-9.
[101] N. von der Assen, A. Sternberg, A. Kätelhön, A. Bardow, Environmental potential of carbon dioxide utilization in the polyurethane supply chain, Faraday Discuss. 183 (2015) 291–307, https://doi.org/10.1039/C5FD00067J.
[102] R.-P. Ye, J. Ding, W. Gong, M.D. Argyle, Q. Zhong, Y. Wang, C.K. Russell, Z. Xu, A. G. Russell, Q. Li, M. Fan, Y.-G. Yao, CO_2 hydrogenation to high-value products via heterogeneous catalysis, Nat. Commun. 10 (2019) 1–15, https://doi.org/10.1038/s41467-019-13638-9.
[103] A. Modak, P. Bhanja, S. Dutta, B. Chowdhury, A. Bhaumik, Catalytic reduction of CO_2 into fuels and fine chemicals, Green Chem. 22 (2020) 4002–4033, https://doi.org/10.1039/D0GC01092H.
[104] T.A. Atsbha, T. Yoon, P. Seongho, C.J. Lee, A review on the catalytic conversion of CO_2 using H_2 for synthesis of CO, methanol, and hydrocarbons, J. CO2 Util. 44 (2021), 101413, https://doi.org/10.1016/J.JCOU.2020.101413.
[105] S. Saeidi, S. Najari, V. Hessel, K. Wilson, F.J. Keil, P. Concepción, S.L. Suib, A. E. Rodrigues, Recent advances in CO_2 hydrogenation to value-added products — current challenges and future directions, Prog. Energy Combust. Sci. 85 (2021), 100905, https://doi.org/10.1016/j.pecs.2021.100905.
[106] T.T.N. Vu, A. Desgagnés, M.C. Iliuta, Efficient approaches to overcome challenges in material development for conventional and intensified CO_2 catalytic hydrogenation to CO, methanol, and DME, Appl. Catal. A Gen. 617 (2021), 118119, https://doi.org/10.1016/j.apcata.2021.118119.
[107] W. Wang, S. Wang, X. Ma, J. Gong, Recent advances in catalytic hydrogenation of carbon dioxide, Chem. Soc. Rev. 40 (2011) 3703–3727, https://doi.org/10.1039/c1cs15008a.
[108] J. Li, L. Wang, Y. Cao, C. Zhang, P. He, H. Li, Recent advances on the reduction of CO_2 to important C_{2+} oxygenated chemicals and fuels, Chinese, J. Chem. Eng. 26 (2018) 2266–2279, https://doi.org/10.1016/J.CJCHE.2018.07.008.
[109] C. Jia, J. Gao, Y. Dai, J. Zhang, Y. Yang, The thermodynamics analysis and experimental validation for complicated systems in CO_2 hydrogenation process, J. Energy Chem. 25 (2016) 1027–1037, https://doi.org/10.1016/J.JECHEM.2016.10.003.
[110] M. Bailera, P. Lisbona, L.M. Romeo, S. Espatolero, Power to gas projects review: lab, pilot and demo plants for storing renewable energy and CO_2, Renew. Sust. Energ. Rev. 69 (2017) 292–312, https://doi.org/10.1016/J.RSER.2016.11.130.
[111] M. Thema, F. Bauer, M. Sterner, Power-to-gas: electrolysis and methanation status review, Renew. Sust. Energ. Rev. 112 (2019) 775–787, https://doi.org/10.1016/J.RSER.2019.06.030.
[112] N. Aryal, T. Kvist, F. Ammam, D. Pant, L.D.M. Ottosen, An overview of microbial biogas enrichment, Bioresour. Technol. 264 (2018) 359–369, https://doi.org/10.1016/J.BIORTECH.2018.06.013.
[113] I. Hussain, A.A. Jalil, N.S. Hassan, M.Y.S. Hamid, Recent advances in catalytic systems for CO_2 conversion to substitute natural gas (SNG): perspective and challenges, J. Energy Chem. 62 (2021) 377–407, https://doi.org/10.1016/J.JECHEM.2021.03.040.
[114] W.J. Lee, C. Li, H. Prajitno, J. Yoo, J. Patel, Y. Yang, S. Lim, Recent trend in thermal catalytic low temperature CO_2 methanation: a critical review, Catal. Today 368 (2021) 2–19, https://doi.org/10.1016/J.CATTOD.2020.02.017.
[115] P. Gao, F. Li, H. Zhan, N. Zhao, F. Xiao, W. Wei, L. Zhong, H. Wang, Y. Sun, Influence of Zr on the performance of Cu/Zn/Al/Zr catalysts via hydrotalcite-like precursors for CO_2 hydrogenation to methanol, J. Catal. 298 (2013) 51–60, https://doi.org/10.1016/j.jcat.2012.10.030.
[116] C.V. Miguel, M.A. Soria, A. Mendes, L.M. Madeira, Direct CO_2 hydrogenation to methane or methanol from post-combustion exhaust streams – a thermodynamic study, J. Nat. Gas Sci. Eng. 22 (2015) 1–8, https://doi.org/10.1016/J.JNGSE.2014.11.010.
[117] P. Frontera, A. Macario, M. Ferraro, P. Antonucci, Supported catalysts for CO_2 methanation: a review, Catalysts 7 (2017) 59, https://doi.org/10.3390/CATAL7020059.
[118] M.H. Weng, H.-T. Chen, Y.-C. Wang, S.-P. Ju, J.-G. Chang, M.C. Lin, Kinetics and mechanisms for the adsorption, dissociation, and diffusion of hydrogen in Ni and Ni/YSZ slabs: a DFT study, Langmuir 28 (2012) 5596–5605, https://doi.org/10.1021/LA300305M.
[119] F. Koschany, D. Schlereth, O. Hinrichsen, On the kinetics of the methanation of carbon dioxide on coprecipitated $NiAl(O)_x$, Appl. Catal. B Environ. 181 (2016) 504–516, https://doi.org/10.1016/J.APCATB.2015.07.026.
[120] A.C. Faria, C.V. Miguel, A.E. Rodrigues, L.M. Madeira, Modeling and simulation of a steam-selective membrane reactor for enhanced CO_2 methanation, Ind. Eng. Chem. Res. 59 (2020) 16170–16184, https://doi.org/10.1021/ACS.IECR.0C02860.
[121] I.G.I. Iwakiri, A.C. Faria, C.V. Miguel, L.M. Madeira, Split feed strategy for low-permselective membrane reactors: a simulation study for enhancing CO_2 methanation, Chem. Eng. Process. - Process Intensif. 163 (2021), 108360, https://doi.org/10.1016/J.CEP.2021.108360.
[122] A.M. Bahmanpour, M. Signorile, O. Kröcher, Recent progress in syngas production via catalytic CO_2 hydrogenation reaction, Appl. Catal. B Environ. 295 (2021), 120319, https://doi.org/10.1016/J.APCATB.2021.120319.
[123] P. Hongmanorom, J. Ashok, G. Zhang, Z. Bian, M.H. Wai, Y. Zeng, S. Xi, A. Borgna, S. Kawi, Enhanced performance and selectivity of CO_2 methanation over phyllosilicate structure derived Ni-Mg/SBA-15 catalysts, Appl. Catal. B Environ. 282 (2021), 119564, https://doi.org/10.1016/J.APCATB.2020.119564.
[124] D. Ferri, T. Bürgi, A. Baiker, Probing boundary sites on a Pt/Al_2O_3 model catalyst by CO_2 hydrogenation and in situ ATR-IR spectroscopy of catalytic solid–liquid interfaces, Phys. Chem. Chem. Phys. 4 (2002) 2667–2672, https://doi.org/10.1039/B111498K.
[125] X. Zhang, X. Zhu, L. Lin, S. Yao, M. Zhang, X. Liu, X. Wang, Y.-W. Li, C. Shi, D. Ma, Highly dispersed copper over β-Mo_2C as an efficient and stable catalyst for the reverse water gas shift (RWGS) reaction, ACS Catal. 7 (2016) 912–918, https://doi.org/10.1021/ACSCATAL.6B02991.
[126] P. Devi, K. Malik, E. Arora, S. Bhattacharya, V. Kalendra, K.V. Lakshmi, A. Verma, J.P. Singh, Selective electrochemical reduction of CO_2 to CO on CuO/In_2O_3 nanocomposites: role of oxygen vacancies, Catal, Sci. Technol. 9 (2019) 5339–5349, https://doi.org/10.1039/C9CY01396B.
[127] Y. Zhang, L. Liang, Z. Chen, J. Wen, W. Zhong, S. Zou, M. Fu, L. Chen, D. Ye, Highly efficient Cu/CeO_2-hollow nanospheres catalyst for the reverse water-gas shift reaction: investigation on the role of oxygen vacancies through in situ UV-Raman and DRIFTS, Appl. Surf. Sci. 516 (2020), 146035, https://doi.org/10.1016/J.APSUSC.2020.146035.
[128] M. Konsolakis, M. Lykaki, Facet-dependent reactivity of ceria nanoparticles exemplified by CeO_2-based transition metal catalysts: a critical review, Catalysts 11 (2021) 452, https://doi.org/10.3390/catal11040452.
[129] J.R. Morse, M. Juneau, J.W. Baldwin, M.D. Porosoff, H.D. Willauer, Alkali promoted tungsten carbide as a selective catalyst for the reverse water gas shift reaction, J. CO2 Util. 35 (2020) 38–46, https://doi.org/10.1016/j.jcou.2019.08.024.
[130] A. Pajares, H. Prats, A. Romero, F. Viñes, P.R. de la Piscina, R. Sayós, N. Homs, F. Illas, Critical effect of carbon vacancies on the reverse water gas shift reaction over vanadium carbide catalysts, Appl. Catal. B Environ. 267 (2020), 118719, https://doi.org/10.1016/J.APCATB.2020.118719.
[131] B. Yan, B. Zhao, S. Kattel, Q. Wu, S. Yao, D. Su, J.G. Chen, Tuning CO_2 hydrogenation selectivity via metal-oxide interfacial sites, J. Catal. 374 (2019) 60–71, https://doi.org/10.1016/J.JCAT.2019.04.036.
[132] A.H. Braga, N.J.S. Costa, K. Philippot, R.V. Gonçalves, J. Szanyi, L.M. Rossi, Structure and activity of supported bimetallic NiPd nanoparticles: influence of preparation method on CO_2 reduction, ChemCatChem. 12 (2020) 2967–2976, https://doi.org/10.1002/CCTC.201902329.
[133] J.C. Matsubu, V.N. Yang, P. Christopher, Isolated metal active site concentration and stability control catalytic CO_2 reduction selectivity, J. Am. Chem. Soc. 137 (2015) 3076–3084, https://doi.org/10.1021/JA5128133.
[134] G.A. Olah, Beyond oil and gas: the methanol economy, Angew. Chemie - Int. Ed. 44 (2005) 2636–2639, https://doi.org/10.1002/anie.200462121.
[135] C. Zhang, K.W. Jun, R. Gao, G. Kwak, H.G. Park, Carbon dioxide utilization in a gas-to-methanol process combined with CO_2/Steam-mixed reforming: techno-economic analysis, Fuel 190 (2017) 303–311, https://doi.org/10.1016/J.FUEL.2016.11.008.
[136] A. Goeppert, G.A. Olah, G.K. Surya Prakash, Toward a sustainable carbon cycle: The methanol economy, in: Green Chem. An Incl. Approach, Elsevier, Los Angeles, 2018, pp. 919–962, https://doi.org/10.1016/B978-0-12-809270-5.00031-5.
[137] A.A. Tountas, X. Peng, A.V. Tavasoli, P.N. Duchesne, T.L. Dingle, Y. Dong, L. Hurtado, A. Mohan, W. Sun, U. Ulmer, L. Wang, T.E. Wood, C.T. Maravelias, M.

M. Sain, G.A. Ozin, Towards solar methanol: past, present, and future, Adv. Sci. 6 (2019) 1801903, https://doi.org/10.1002/advs.201801903.

[138] R. Guil-López, N. Mota, J. Llorente, E. Millán, B. Pawelec, J.L.G. Fierro, R. M. Navarro, Methanol synthesis from CO_2: a review of the latest developments in heterogeneous catalysis, Materials (Basel). 12 (2019) 3902, https://doi.org/10.3390/MA12233902.

[139] X. Jiang, X. Nie, X. Guo, C. Song, J.G. Chen, Recent advances in carbon dioxide hydrogenation to methanol via heterogeneous catalysis, Chem. Rev. 120 (2020) 7984–8034, https://doi.org/10.1021/acs.chemrev.9b00723.

[140] S. Zhang, Z. Wu, X. Liu, K. Hua, Z. Shao, B. Wei, C. Huang, H. Wang, Y. Sun, A short review of recent advances in direct CO_2 hydrogenation to alcohols, Top. Catal. 64 (2021) 371–394, https://doi.org/10.1007/S11244-020-01405-W.

[141] X. Zhang, G. Zhang, C. Song, X. Guo, Catalytic conversion of carbon dioxide to methanol: current status and future perspective, Front. Energy Res. 8 (2021), 621119, https://doi.org/10.3389/FENRG.2020.621119.

[142] J. Zhong, X. Yang, Z. Wu, B. Liang, Y. Huang, T. Zhang, State of the art and perspectives in heterogeneous catalysis of CO_2 hydrogenation to methanol, Chem. Soc. Rev. 49 (2020) 1385–1413, https://doi.org/10.1039/c9cs00614a.

[143] O. Martin, J. Pérez-Ramírez, New and revisited insights into the promotion of methanol synthesis catalysts by CO_2, Catal. Sci. Technol. 3 (2013) 3343–3352, https://doi.org/10.1039/C3CY00573A.

[144] M. Sánchez-Contador, A. Ateka, P. Rodriguez-Vega, J. Bilbao, A.T. Aguayo, Optimization of the Zr content in the CuO-ZnO-ZrO_2/SAPO-11 catalyst for the selective hydrogenation of CO+CO_2 mixtures in the direct synthesis of dimethyl ether, Ind. Eng. Chem. Res. 57 (2018) 1169–1178, https://doi.org/10.1021/acs.iecr.7b04345.

[145] C. Yang, R. Mu, G. Wang, J. Song, H. Tian, Z.-J. Zhao, J. Gong, Hydroxyl-mediated ethanol selectivity of CO_2 hydrogenation, Chem. Sci. 10 (2019) 3161–3167, https://doi.org/10.1039/C8SC05608K.

[146] S. Saeidi, S. Najari, F. Fazlollahi, M.K. Nikoo, F. Sefidkon, J.J. Klemeš, L.L. Baxter, Mechanisms and kinetics of CO_2 hydrogenation to value-added products: a detailed review on current status and future trends, Renew. Sust. Energ. Rev. 80 (2017) 1292–1311, https://doi.org/10.1016/j.rser.2017.05.204.

[147] A. Ramirez, A.D. Chowdhury, A. Dokania, P. Cnudde, M. Caglayan, I. Yarulina, E. Abou-Hamad, L. Gevers, S. Ould-Chikh, K. De Wispelaere, V. Van Speybroeck, J. Gascon, Effect of zeolite topology and reactor configuration on the direct conversion of CO_2 to light olefins and aromatics, ACS Catal. 9 (2019) 6320–6334, https://doi.org/10.1021/acscatal.9b01466.

[148] J. Wei, Q. Ge, R. Yao, Z. Wen, C. Fang, L. Guo, H. Xu, J. Sun, Directly converting CO_2 into a gasoline fuel, Nat. Commun. 8 (2017) 1–9, https://doi.org/10.1038/ncomms15174.

[149] W. Wang, X. Jiang, X. Wang, C. Song, Fe–Cu bimetallic catalysts for selective CO_2 hydrogenation to olefin-rich C_{2+} hydrocarbons, Ind. Eng. Chem. Res. 57 (2018) 4535–4542, https://doi.org/10.1021/ACS.IECR.8B00016.

[150] P.S. Sai Prasad, J.W. Bae, K.-W. Jun, K.-W. Lee, Fischer–Tropsch synthesis by carbon dioxide hydrogenation on Fe-based catalysts, Catal. Surv. from Asia. 12 (2008) 170–183, https://doi.org/10.1007/S10563-008-9049-1.

[151] M.R. Shaner, H.A. Atwater, N.S. Lewis, E.W. Mcfarland, A comparative technoeconomic analysis of renewable hydrogen production using solar energy, Energy Environ. Sci. 9 (2016) 2354, https://doi.org/10.1039/c5ee02573g.

[152] X. Zhang, A. Zhang, X. Jiang, J. Zhu, J. Liu, J. Li, G. Zhang, C. Song, X. Guo, Utilization of CO_2 for aromatics production over ZnO/ZrO_2-ZSM-5 tandem catalyst, J. CO2 Util. 29 (2019) 140–145, https://doi.org/10.1016/j.jcou.2018.12.002.

[153] A. Ateka, P. Pérez-Uriarte, M. Gamero, J. Ereña, A.T. Aguayo, J. Bilbao, A comparative thermodynamic study on the CO_2 conversion in the synthesis of methanol and of DME, Energy 120 (2017) 796–804, https://doi.org/10.1016/j.energy.2016.11.129.

[154] L.C. Grabow, M. Mavrikakis, Mechanism of methanol synthesis on cu through CO_2 and CO hydrogenation, ACS Catal. 1 (2011) 365–384, https://doi.org/10.1021/cs200055d.

[155] P. Gao, S. Dang, S. Li, X. Bu, Z. Liu, M. Qiu, C. Yang, H. Wang, L. Zhong, Y. Han, Q. Liu, W. Wei, Y. Sun, Direct production of lower olefins from CO_2 conversion via bifunctional catalysis, ACS Catal. 8 (2018) 571–578, https://doi.org/10.1021/acscatal.7b02649.

[156] U. Olsbye, S. Svelle, M. Bjrgen, P. Beato, T.V.W. Janssens, F. Joensen, S. Bordiga, K.P. Lillerud, Conversion of methanol to hydrocarbons: how zeolite cavity and pore size controls product selectivity, Angew. Chemie - Int. Ed. 51 (2012) 5810–5831, https://doi.org/10.1002/anie.201103657.

[157] S. Dang, S. Li, C. Yang, X. Chen, X. Li, L. Zhong, P. Gao, Y. Sun, Selective transformation of CO_2 and H_2 into lower olefins over In_2O_3-$ZnZrO_x$/SAPO-34 bifunctional catalysts, ChemSusChem. 12 (2019) 3582–3591, https://doi.org/10.1002/cssc.201900958.

[158] X. Wang, G. Yang, J. Zhang, S. Chen, Y. Wu, Q. Zhang, J. Wang, Y. Han, Y. Tan, Synthesis of isoalkanes over a core (Fe–Zn–Zr)–shell (zeolite) catalyst by CO_2 hydrogenation, Chem. Commun. 52 (2016) 7352–7355, https://doi.org/10.1039/C6CC01965J.

[159] X. Wang, G. Yang, J. Zhang, F. Song, Y. Wu, T. Zhang, Q. Zhang, N. Tsubaki, Y. Tan, Macroscopic assembly style of catalysts significantly determining their efficiency for converting CO_2 to gasoline, Catal. Sci. Technol. 9 (2019) 5401–5412, https://doi.org/10.1039/C9CY01470E.

[160] X. Wang, C. Zeng, N. Gong, T. Zhang, Y. Wu, J. Zhang, F. Song, G. Yang, Y. Tan, Effective suppression of CO selectivity for CO_2 hydrogenation to high-quality gasoline, ACS Catal. 11 (2021) 1528–1547, https://doi.org/10.1021/acscatal.0c04155.

[161] A. Masudi, N.W. Che Jusoh, O. Muraza, Recent progress on low rank coal conversion to dimethyl ether as clean fuel: a critical review, J. Clean. Prod. 277 (2020), 124024, https://doi.org/10.1016/J.JCLEPRO.2020.124024.

[162] T. Nakyai, D. Saebea, Exergoeconomic comparison of syngas production from biomass, coal, and natural gas for dimethyl ether synthesis in single-step and two-step processes, J. Clean. Prod. 241 (2019), 118334, https://doi.org/10.1016/J.JCLEPRO.2019.118334.

[163] F.M. Baena-Moreno, M. Gonzalez-Castaño, H. Arellano-García, T.R. Reina, Exploring profitability of bioeconomy paths: dimethyl ether from biogas as case study, Energy 225 (2021), 120230, https://doi.org/10.1016/J.ENERGY.2021.120230.

[164] M. Tomatis, A. Mahmud Parvez, M.T. Afzal, S. Mareta, T. Wu, J. He, T. He, Utilization of CO_2 in renewable DME fuel production: a life cycle analysis (LCA)-based case study in China, Fuel 254 (2019), 115627, https://doi.org/10.1016/J.FUEL.2019.115627.

[165] V. Dieterich, A. Buttler, A. Hanel, H. Spliethoff, S. Fendt, Power-to-liquid via synthesis of methanol, DME or Fischer–Tropsch-fuels: a review, Energy Environ. Sci. 13 (2020) 3207–3252, https://doi.org/10.1039/D0EE01187H.

[166] T.A. Semelsberger, R.L. Borup, H.L. Greene, Dimethyl ether (DME) as an alternative fuel, J. Power Sources 156 (2006) 497–511, https://doi.org/10.1016/j.jpowsour.2005.05.082.

[167] C. Arcoumanis, C. Bae, R. Crookes, E. Kinoshita, The potential of di-methyl ether (DME) as an alternative fuel for compression-ignition engines: a review, Fuel 87 (2008) 1014–1030, https://doi.org/10.1016/j.fuel.2007.06.007.

[168] Z. Azizi, M. Rezaeimanesh, T. Tohidian, M.R. Rahimpour, Dimethyl ether: a review of technologies and production challenges, Chem. Eng. Process. Process Intensif. 82 (2014) 150–172, https://doi.org/10.1016/j.cep.2014.06.007.

[169] G. Tarlea, M. Vinceriuc, A. Tarlea, A natural refrigerant DME and HC eco-efficient mixture alternative, in: 14th IIR-Gustav Lorentzen Conf. Nat. Refrig. Proceedings. Kyoto, Jpn. December 7-9th 2020, International Institute of Refrigeration, 2020, pp. 453–457, https://doi.org/10.18462/IIR.GL.2020.1181.

[170] M.C. Bauer, A. Kruse, The use of dimethyl ether as an organic extraction solvent for biomass applications in future biorefineries: a user-oriented review, Fuel 254 (2019) 115703–115716, https://doi.org/10.1016/j.fuel.2019.115703.

[171] Q. Wang, K. Oshita, M. Takaoka, Effective lipid extraction from undewatered microalgae liquid using subcritical dimethyl ether, Biotechnol. Biofuels. 14 (2021) 1–13, https://doi.org/10.1186/S13068-020-01871-0.

[172] M. Khalifi, M. Zirrahi, H. Hassanzadeh, J. Abedi, Concentration-dependent molecular diffusion coefficient of dimethyl ether in bitumen, Fuel 274 (2020), 117809, https://doi.org/10.1016/J.FUEL.2020.117809.

[173] V. Kumar, A.K. Agarwal, Material compatibility, technical challenges and modifications required for DME adaptation in compression ignition engines, in: Altern. Fuels Adv. Combust. Tech. as Sustain. Solut. Intern. Combust. Engines, Springer Nature, 2021, pp. 37–57, https://doi.org/10.1007/978-981-16-1513-9_3.

[174] T.H. Fleisch, A. Basu, R.A. Sills, Introduction and advancement of a new clean global fuel: the status of DME developments in China and beyond, J. Nat. Gas Sci. Eng. 9 (2012) 94–107, https://doi.org/10.1016/j.jngse.2012.05.012.

[175] H.A.E.D. Bastawissi, M. Elkelawy, H. Panchal, K. Kumar Sadasivuni, Optimization of the multi-carburant dose as an energy source for the application of the HCCI engine, Fuel 253 (2019) 15–24, https://doi.org/10.1016/J.FUEL.2019.04.167.

[176] S.N. Khadzhiev, N.V. Kolesnichenko, N.N. Ezhova, Manufacturing of lower olefins from natural gas through methanol and its derivatives (review), Pet. Chem. 48 (2008) 325–334, https://doi.org/10.1134/S0965544108050010.

[177] S.M. Sadrameli, Thermal/catalytic cracking of hydrocarbons for the production of olefins: a state-of-the-art review I: thermal cracking review, Fuel 140 (2015) 102–115, https://doi.org/10.1016/J.FUEL.2014.09.034.

[178] O. Awayssa, N. Al-Yassir, A. Aitani, S. Al-Khattaf, Modified HZSM-5 as FCC additive for enhancing light olefins yield from catalytic cracking of VGO, Appl. Catal. A Gen. 477 (2014) 172–183, https://doi.org/10.1016/J.APCATA.2014.03.021.

[179] T. Cordero-Lanzac, C. Martínez, A.T. Aguayo, P. Castaño, J. Bilbao, A. Corma, Activation of n-pentane while prolonging HZSM-5 catalyst lifetime during its combined reaction with methanol or dimethyl ether, Catal. Today 383 (2020) 320–329, https://doi.org/10.1016/j.cattod.2020.09.015.

[180] Y. Gao, S.L. Chen, Y. Wei, Y. Wang, W. Sun, Y. Cao, P. Zeng, Kinetics of coke formation in the dimethyl ether-to-olefins process over SAPO-34 catalyst, Chem. Eng. J. 326 (2017) 528–539, https://doi.org/10.1016/J.CEJ.2017.05.158.

[181] F. Wang, Z. Wen, Z. Qin, Q. Fang, Q. Ge, Z. Li, J. Sun, G. Li, Manganese cluster induce the control synthesis of RHO- and CHA-type silicoaluminaphosphates for dimethylether to light olefin conversion, Fuel 244 (2019) 104–109, https://doi.org/10.1016/J.FUEL.2019.02.013.

[182] P. Pérez-Uriarte, A. Ateka, A.G. Gayubo, T. Cordero-Lanzac, A.T. Aguayo, J. Bilbao, Deactivation kinetics for the conversion of dimethyl ether to olefins over a HZSM-5 zeolite catalyst, Chem. Eng. J. 311 (2017) 367–377, https://doi.org/10.1016/j.cej.2016.11.104.

[183] P. Pérez-Uriarte, A. Ateka, A.T. Aguayo, A.G. Gayubo, J. Bilbao, Kinetic model for the reaction of DME to olefins over a HZSM-5 zeolite catalyst, Chem. Eng. J. 302 (2016) 801–810, https://doi.org/10.1016/j.cej.2016.05.096.

[184] M. Ibáñez, P. Pérez-Uriarte, M. Sánchez-Contador, T. Cordero-Lanzac, A. T. Aguayo, J. Bilbao, P. Castaño, Nature and location of carbonaceous species in a composite HZSM-5 zeolite catalyst during the conversion of dimethyl ether into light olefins, Catalysts 7 (2017) 254–266, https://doi.org/10.3390/catal7090254.

[185] T. Cordero-Lanzac, A.T. Aguayo, J. Bilbao, Reactor–regenerator system for the dimethyl ether-to-olefins process over HZSM-5 catalysts: conceptual development

and analysis of the process variables, Ind. Eng. Chem. Res. 59 (2020) 14689–14702, https://doi.org/10.1021/acs.iecr.0c02276.
[186] T. Cordero-Lanzac, A.T. Aguayo, A.G. Gayubo, J. Bilbao, Consideration of the activity distribution using the population balance theory for designing a dual fluidized bed reactor-regenerator system. Application to the MTO process, Chem. Eng. J. 405 (2021), 126448, https://doi.org/10.1016/J.CEJ.2020.126448.
[187] M. Elamen Babiker, A. Rashid, A. Aziz, M.R. Heikal, S. Yusup, A. Adam, Effects of enhancing cetane number of ethanol fumigation on diesel engine performance and emissions, ARPN J. Eng. Appl. Sci. 11 (2016) 12994–12999. www.arpnjournals.com.
[188] R. Li, Z. Wang, P. Ni, Y. Zhao, M. Li, L. Li, Effects of cetane number improvers on the performance of diesel engine fuelled with methanol/biodiesel blend, Fuel 128 (2014) 180–187, https://doi.org/10.1016/j.fuel.2014.03.011.
[189] L. Mei, R.N. Li, S. Liu, P.H. Chen, Effect of high cetane fuel blended with methanol on combustion characteristics, in: IWEMSE 2018 - Int. Work. Environ. Manag. Sci. Eng. Aromat, 2018, pp. 313–318.
[190] T.Q. Zhang, B. Choi, Y.B. Kim, Numerical and experimental study on hydrogen production via dimethyl ether steam reforming, Int. J. Hydrog. Energy 45 (2020) 11438–11448, https://doi.org/10.1016/J.IJHYDENE.2020.02.091.
[191] X. Su, F. Zhang, Y. Yin, B. Tu, M. Cheng, Thermodynamic analysis of fuel composition and effects of different dimethyl ether processing technologies on cell efficiency, Fuel Process. Technol. 203 (2020), 106391, https://doi.org/10.1016/J.FUPROC.2020.106391.
[192] N. Shimoda, H. Muroyama, T. Matsui, K. Faungnawakij, R. Kikuchi, K. Eguchi, Dimethyl ether steam reforming under daily start-up and shut-down (DSS)-like operation over $CuFe_2O_4$ spinel and alumina composite catalysts, Appl. Catal. A Gen. 409–410 (2011) 91–98, https://doi.org/10.1016/j.apcata.2011.09.031.
[193] L. Oar-Arteta, A. Remiro, J. Vicente, A.T. Aguayo, J. Bilbao, A.G. Gayubo, Stability of $CuZnOAl_2O_3$/HZSM-5 and $CuFe_2O_4$/HZSM-5 catalysts in dimethyl ether steam reforming operating in reaction–regeneration cycles, Fuel Process. Technol. 126 (2014) 145–154, https://doi.org/10.1016/j.fuproc.2014.04.028.
[194] L. Oar-Arteta, A.T. Aguayo, A. Remiro, J. Bilbao, A.G. Gayubo, Behavior of a $CuFe_2O_4/\gamma$-Al_2O_3 catalyst for the steam reforming of dimethyl ether in reaction-regeneration cycles, Ind. Eng. Chem. Res. 54 (2015) 11285–11294, https://doi.org/10.1021/acs.iecr.5b02901.
[195] L. Oar-Arteta, A. Remiro, F. Epron, N. Bion, A.T. Aguayo, J. Bilbao, A.G. Gayubo, Comparison of noble metal- and copper-based catalysts for the step of methanol steam reforming in the dimethyl ether steam reforming process, Ind. Eng. Chem. Res. 55 (2016) 3546–3555, https://doi.org/10.1021/acs.iecr.6b00126.
[196] K. Faungnawakij, N. Shimoda, N. Viriya-empikul, R. Kikuchi, K. Eguchi, Limiting mechanisms in catalytic steam reforming of dimethyl ether, Appl. Catal. B Environ. 97 (2010) 21–27, https://doi.org/10.1016/j.apcatb.2010.03.010.
[197] D. Kim, B. Choi, G. Park, K. Lee, D.W. Lee, S. Jung, Effect of γ-Al_2O_3 characteristics on hydrogen production of Cu/γ-Al_2O_3 catalyst for steam reforming of dimethyl ether, Chem. Eng. Sci. 216 (2020), 115535, https://doi.org/10.1016/j.ces.2020.115535.
[198] J. Vicente, A.G. Gayubo, J. Ereña, A.T. Aguayo, M. Olazar, J. Bilbao, Improving the DME steam reforming catalyst by alkaline treatment of the HZSM-5 zeolite, Appl. Catal. B Environ. 130–131 (2013) 73–83, https://doi.org/10.1016/j.apcatb.2012.10.019.
[199] A.G. Gayubo, J. Vicente, J. Ereña, L. Oar-Arteta, M.J. Azkoiti, M. Olazar, J. Bilbao, Causes of deactivation of bifunctional catalysts made up of CuO-ZnO-Al_2O_3 and desilicated HZSM-5 zeolite in DME steam reforming, Appl. Catal. A Gen. 483 (2014) 76–84, https://doi.org/10.1016/j.apcata.2014.06.031.
[200] L. Oar-Arteta, A. Remiro, A.T. Aguayo, J. Bilbao, A.G. Gayubo, Effect of operating conditions on dimethyl ether steam reforming over a $CuFe_2O_4/\gamma$-Al_2O_3 bifunctional catalyst, Ind. Eng. Chem. Res. 54 (2015) 9722–9732, https://doi.org/10.1021/acs.iecr.5b02368.
[201] C. Ledesma, E. López, T. Trifonov, Á. Rodríguez, J. Llorca, Catalytic reforming of dimethyl ether in microchannels, Catal. Today 323 (2019) 209–215, https://doi.org/10.1016/J.CATTOD.2018.03.011.
[202] E. Zhan, Z. Xiong, W. Shen, Dimethyl ether carbonylation over zeolites, J. Energy Chem. 36 (2019) 51–63, https://doi.org/10.1016/J.JECHEM.2019.04.015.
[203] E. Catizzone, G. Bonura, M. Migliori, F. Frusteri, G. Giordano, CO_2 recycling to dimethyl ether: state-of-the-art and perspectives, Molecules 23 (2017) 31, https://doi.org/10.3390/MOLECULES23010031.
[204] S. Michailos, S. McCord, V. Sick, G. Stokes, P. Styring, Dimethyl ether synthesis via captured CO_2 hydrogenation within the power to liquids concept: a techno-economic assessment, Energy Convers. Manag. 184 (2019) 262–276, https://doi.org/10.1016/j.enconman.2019.01.046.
[205] S. Schemme, J.L. Breuer, M. Köller, S. Meschede, F. Walman, R.C. Samsun, R. Peters, D. Stolten, H_2-based synthetic fuels: a techno-economic comparison of alcohol, ether and hydrocarbon production, Int. J. Hydrog. Energy 45 (2020) 5395–5414, https://doi.org/10.1016/J.IJHYDENE.2019.05.028.
[206] M.M. Uddin, A. Simson, M.M. Wright, Techno-economic and greenhouse gas emission analysis of dimethyl ether production via the bi-reforming pathway for transportation fuel, Energy 211 (2020), 119031, https://doi.org/10.1016/J.ENERGY.2020.119031.
[207] S.M. Kim, Y.J. Lee, J.W. Bae, H.S. Potdar, K.W. Jun, Synthesis and characterization of a highly active alumina catalyst for methanol dehydration to dimethyl ether, Appl. Catal. A Gen. 348 (2008) 113–120, https://doi.org/10.1016/J.APCATA.2008.06.032.
[208] Z. Hosseini, M. Taghizadeh, F. Yaripour, Synthesis of nanocrystalline γ-Al_2O_3 by sol-gel and precipitation methods for methanol dehydration to dimethyl ether, J. Energy Chem. 20 (2011) 128–134, https://doi.org/10.1016/S1003-9953(10)60172-7.
[209] Z. Zuo, W. Huang, P. Han, Z. Gao, Z. Li, Theoretical studies on the reaction mechanisms of AlOOH- and γ-Al_2O_3-catalysed methanol dehydration in the gas and liquid phases, Appl. Catal. A Gen. 408 (2011) 130–136, https://doi.org/10.1016/J.APCATA.2011.09.011.
[210] F. Yaripour, Z. Shariatinia, S. Sahebdelfar, A. Irandoukht, The effects of synthesis operation conditions on the properties of modified γ-alumina nanocatalysts in methanol dehydration to dimethyl ether using factorial experimental design, Fuel 139 (2015) 40–50, https://doi.org/10.1016/J.FUEL.2014.08.029.
[211] F. Raoof, M. Taghizadeh, A. Eliassi, F. Yaripour, Effects of temperature and feed composition on catalytic dehydration of methanol to dimethyl ether over γ-alumina, Fuel 87 (2008) 2967–2971, https://doi.org/10.1016/J.FUEL.2008.03.025.
[212] W. Alharbi, E.F. Kozhevnikova, I.V. Kozhevnikov, Dehydration of methanol to dimethyl ether over heteropoly acid catalysts: the relationship between reaction rate and catalyst acid strength, ACS Catal. 5 (2015) 7186–7193, https://doi.org/10.1021/acscatal.5b01911.
[213] R.M. Ladera, M. Ojeda, J.L.G. Fierro, S. Rojas, TiO_2-supported heteropoly acid catalysts for dehydration of methanol to dimethyl ether: relevance of dispersion and support interaction, Catal. Sci. Technol. 5 (2014) 484–491, https://doi.org/10.1039/C4CY00998C.
[214] E. Catizzone, A. Aloise, M. Migliori, G. Giordano, From 1-D to 3-D zeolite structures: performance assessment in catalysis of vapour-phase methanol dehydration to DME, Microporous Mesoporous Mater. 243 (2017) 102–111, https://doi.org/10.1016/j.micromeso.2017.02.022.
[215] S.D. Kim, S.C. Baek, Y.J. Lee, K.W. Jun, M.J. Kim, I.S. Yoo, Effect of γ-alumina content on catalytic performance of modified ZSM-5 for dehydration of crude methanol to dimethyl ether, Appl. Catal. A Gen. 309 (2006) 139–143, https://doi.org/10.1016/J.APCATA.2006.05.008.
[216] L. Zeng, Y. Wang, J. Mou, F. Liu, C. Yang, T. Zhao, X. Wang, J. Cao, Promoted catalytic behavior over γ-Al_2O_3 composited with ZSM-5 for crude methanol conversion to dimethyl ether, Int. J. Hydrog. Energy 45 (2020) 16500–16508, https://doi.org/10.1016/J.IJHYDENE.2020.04.115.
[217] A. Aloise, A. Marino, F. Dalena, G. Giorgianni, M. Migliori, L. Frusteri, C. Cannilla, G. Bonura, F. Frusteri, G. Giordano, Desilicated ZSM-5 zeolite: catalytic performances assessment in methanol to DME dehydration, Microporous Mesoporous Mater. 302 (2020), 110198, https://doi.org/10.1016/J.MICROMESO.2020.110198.
[218] E. Catizzone, A. Aloise, M. Migliori, G. Giordano, The effect of FER zeolite acid sites in methanol-to-dimethyl-ether catalytic dehydration, J. Energy Chem. 26 (2017) 406–415, https://doi.org/10.1016/j.jechem.2016.12.005.
[219] E. Catizzone, S. Van Daele, M. Bianco, A. Di Michele, A. Aloise, M. Migliori, V. Valtchev, G. Giordano, Catalytic application of ferrierite nanocrystals in vapour-phase dehydration of methanol to dimethyl ether, Appl. Catal. B Environ. 243 (2019) 273–282, https://doi.org/10.1016/J.APCATB.2018.10.060.
[220] E. Catizzone, A. Aloise, E. Giglio, G. Ferrarelli, M. Bianco, M. Migliori, G. Giordano, MFI vs., FER zeolite during methanol dehydration to dimethyl ether: the crystal size plays a key role, Catal. Commun. 149 (2021), 106214, https://doi.org/10.1016/J.CATCOM.2020.106214.
[221] K.S. Ha, Y.J. Lee, J.W. Bae, Y.W. Kim, M.H. Woo, H.S. Kim, M.J. Park, K.W. Jun, New reaction pathways and kinetic parameter estimation for methanol dehydration over modified ZSM-5 catalysts, Appl. Catal. A Gen. 395 (2011) 95–106, https://doi.org/10.1016/j.apcata.2011.01.025.
[222] J. Park, J. Cho, M.J. Park, W.B. Lee, Microkinetic modeling of DME synthesis from methanol over H-zeolite catalyst: associative vs. dissociative pathways, Catal. Today 375 (2021) 314–323, https://doi.org/10.1016/J.CATTOD.2020.02.011.
[223] A. Trypolskyi, A. Zhokh, V. Gritsenko, M. Chen, J. Tang, P. Strizhak, A kinetic study on the methanol conversion to dimethyl ether over H-ZSM-5 zeolite, Chem. Pap. 75 (2021) 3429–3442, https://doi.org/10.1007/S11696-021-01586-Y.
[224] F. Trippe, M. Fröhling, F. Schultmann, R. Stahl, E. Henrich, A. Dalai, Comprehensive techno-economic assessment of dimethyl ether (DME) synthesis and Fischer–Tropsch synthesis as alternative process steps within biomass-to-liquid production, Fuel Process. Technol. 106 (2013) 577–586, https://doi.org/10.1016/j.fuproc.2012.09.029.
[225] F. Pontzen, W. Liebner, V. Gronemann, M. Rothaemel, B. Ahlers, CO_2-based methanol and DME – Efficient technologies for industrial scale production, Catal. Today 171 (2011) 242–250, https://doi.org/10.1016/j.cattod.2011.04.049.
[226] K.B. Kabir, K. Hein, S. Bhattacharya, Process modelling of dimethyl ether production from Victorian brown coal—Integrating coal drying, gasification and synthesis processes, Comput. Chem. Eng. 48 (2013) 96–104, https://doi.org/10.1016/j.compchemeng.2012.08.008.
[227] H. Park, Y. Woo, H.S. Jung, G. Kim, J.W. Bae, M.J. Park, Development of dimethyl ether synthesis processes using by-product gas from a steel-making plant: single- vs. two-step processes, J. Clean. Prod. 326 (2021), 129367, https://doi.org/10.1016/J.JCLEPRO.2021.129367.
[228] L.P. Merkouri, H. Ahmet, T. Ramirez Reina, M.S. Duyar, The direct synthesis of dimethyl ether (DME) from landfill gas: a techno-economic investigation, Fuel 319 (2022), 123741, https://doi.org/10.1016/J.FUEL.2022.123741.
[229] T. Nakyai, Y. Patcharavorachot, A. Arpornwichanop, D. Saebea, Comparative exergoeconomic analysis of indirect and direct bio-dimethyl ether syntheses based on air-steam biomass gasification with CO_2 utilization, Energy 209 (2020), 118332, https://doi.org/10.1016/J.ENERGY.2020.118332.
[230] K. Im-orb, A. Arpornwichanop, Comparative techno-economic assessment of bio-methanol and bio-DME production from oil palm residue, Energy Convers. Manag. 258 (2022), 115511, https://doi.org/10.1016/J.ENCONMAN.2022.115511.

[231] G.A. Olah, A. Goeppert, G.K.S. Prakash, Chemical recycling of carbon dioxide to methanol and dimethyl ether: from greenhouse gas to renewable, environmentally carbon neutral fuels and synthetic hydrocarbons, J. Org. Chem. 74 (2009) 487–498, https://doi.org/10.1021/jo801260f.

[232] T. Chang, R.W. Rousseau, P.K. Kilpatrick, Methanol synthesis reactions: calculations of equilibrium conversions using equations of state, Ind. Eng. Chem. Process. Des. Dev. 25 (2002) 477–481, https://doi.org/10.1021/I200033A021.

[233] J.G. van Bennekom, R.H. Venderbosch, J.G.M. Winkelman, E. Wilbers, D. Assink, K.P.J. Lemmens, H.J. Heeres, Methanol synthesis beyond chemical equilibrium, Chem. Eng. Sci. 87 (2013) 204–208, https://doi.org/10.1016/j.ces.2012.10.013.

[234] S.S. Iyer, T. Renganathan, S. Pushpavanam, M. Vasudeva Kumar, N. Kaisare, Generalized thermodynamic analysis of methanol synthesis: effect of feed composition, J. CO2 Util. 10 (2015) 95–104, https://doi.org/10.1016/j.jcou.2015.01.006.

[235] G. Jia, Y. Tan, Y. Han, A comparative study on the thermodynamics of dimethyl ether synthesis from CO hydrogenation and CO_2 hydrogenation, Ind. Eng. Chem. Res. 45 (2006) 1152–1159, https://doi.org/10.1021/ie050499b.

[236] G.R. Moradi, J. Ahmadpour, F. Yaripour, J. Wang, Equilibrium calculations for direct synthesis of dimethyl ether from syngas, Can. J. Chem. Eng. 89 (2011) 108–115, https://doi.org/10.1002/cjce.20373.

[237] H.-J. Chen, C.-W. Fan, C.-S. Yu, Analysis, synthesis, and design of a one-step dimethyl ether production via a thermodynamic approach, Appl. Energy 101 (2013) 449–456, https://doi.org/10.1016/j.apenergy.2012.08.025.

[238] W.-H. Chen, C.-L. Hsu, X.-D. Wang, Thermodynamic approach and comparison of two-step and single step DME (dimethyl ether) syntheses with carbon dioxide utilization, Energy 109 (2016) 326–340, https://doi.org/10.1016/j.energy.2016.04.097.

[239] K.L. Ng, D. Chadwick, B.A. Toseland, Kinetics and modelling of dimethyl ether synthesis from synthesis gas, Chem. Eng. Sci. 54 (1999) 3587–3592, https://doi.org/10.1016/S0009-2509(98)00514-4.

[240] I. Sierra, J. Ereña, A.T. Aguayo, J.M. Arandes, J. Bilbao, Regeneration of CuO-ZnO-Al_2O_3/γ-Al_2O_3 catalyst in the direct synthesis of dimethyl ether, Appl. Catal. B Environ. 94 (2010) 108–116, https://doi.org/10.1016/j.apcatb.2009.10.026.

[241] A. Ateka, J. Ereña, J. Bilbao, A.T. Aguayo, Kinetic modeling of the direct synthesis of dimethyl ether over a CuO-ZnO-MnO/SAPO-18 catalyst and assessment of the CO_2 conversion, Fuel Process. Technol. 181 (2018) 233–243, https://doi.org/10.1016/j.fuproc.2018.09.024.

[242] A. Ateka, M. Sánchez-Contador, A. Portillo, J. Bilbao, A.T. Aguayo, Kinetic modeling of CO_2+CO hydrogenation to DME over a CuO-ZnO-ZrO_2@SAPO-11 core-shell catalyst, Fuel Process. Technol. 206 (2020) 106434–106444, https://doi.org/10.1016/j.fuproc.2020.106434.

[243] A. Ateka, A. Portillo, M. Sánchez-Contador, J. Bilbao, A.T. Aguayo, Macro-kinetic model for CuO–ZnO–ZrO_2@SAPO-11 core-shell catalyst in the direct synthesis of DME from CO/CO_2, Renew. Energy 169 (2021) 1242–1251, https://doi.org/10.1016/j.renene.2021.01.062.

[244] J. Ereña, I. Sierra, A.T. Aguayo, A. Ateka, M. Olazar, J. Bilbao, Kinetic modelling of dimethyl ether synthesis from (H_2+CO_2) by considering catalyst deactivation, Chem. Eng. J. 174 (2011) 660–667, https://doi.org/10.1016/j.cej.2011.09.067.

[245] I. Sierra, J. Ereña, A.T. Aguayo, J.M. Arandes, M. Olazar, J. Bilbao, Co-feeding water to attenuate deactivation of the catalyst metallic function (CuO–ZnO–Al_2O_3) by coke in the direct synthesis of dimethyl ether, Appl. Catal. B Environ. 106 (2011) 167–173, https://doi.org/10.1016/j.apcatb.2011.05.021.

[246] G.R. Moradi, S. Nosrati, F. Yaripor, Effect of the hybrid catalysts preparation method upon direct synthesis of dimethyl ether from synthesis gas, Catal. Commun. 8 (2007) 598–606, https://doi.org/10.1016/j.catcom.2006.08.023.

[247] D. Mao, W. Yang, J. Xia, B. Zhang, Q. Song, Q. Chen, Highly effective hybrid catalyst for the direct synthesis of dimethyl ether from syngas with magnesium oxide-modified HZSM-5 as a dehydration component, J. Catal. 230 (2005) 140–149, https://doi.org/10.1016/j.jcat.2004.12.007.

[248] M. Behrens, Meso- and nano-structuring of industrial Cu/ZnO/(Al_2O_3) catalysts, J. Catal. 267 (2009) 24–29, https://doi.org/10.1016/j.jcat.2009.07.009.

[249] Z. Li, J. Li, M. Dai, Y. Liu, D. Han, J. Wu, The effect of preparation method of the Cu–La_2O_3–ZrO_2/γ-Al_2O_3 hybrid catalysts on one-step synthesis of dimethyl ether from syngas, Fuel 121 (2014) 173–177, https://doi.org/10.1016/j.fuel.2013.12.050.

[250] O. Oyola-Rivera, M.A. Baltanás, N. Cardona-Martínez, CO_2 hydrogenation to methanol and dimethyl ether by Pd–Pd_2Ga catalysts supported over Ga_2O_3 polymorphs, J. CO2 Util. 9 (2015) 8–15, https://doi.org/10.1016/j.jcou.2014.11.003.

[251] Z. Qin, X. Zhou, T. Su, Y. Jiang, H. Ji, Hydrogenation of CO_2 to dimethyl ether on La-, Ce-modified Cu-Fe/HZSM-5 catalysts, Catal. Commun. 75 (2016) 78–82, https://doi.org/10.1016/j.catcom.2015.12.010.

[252] X. Zhou, T. Su, Y. Jiang, Z. Qin, H. Ji, Z. Guo, CuO-Fe_2O_3-CeO_2/HZSM-5 bifunctional catalyst hydrogenated CO_2 for enhanced dimethyl ether synthesis, Chem. Eng. Sci. 153 (2016) 10–20, https://doi.org/10.1016/j.ces.2016.07.007.

[253] F. Arena, G. Italiano, K. Barbera, G. Bonura, L. Spadaro, F. Frusteri, Basic evidences for methanol-synthesis catalyst design, Catal. Today 143 (2009) 80–85, https://doi.org/10.1016/j.cattod.2008.11.022.

[254] A. Ateka, P. Pérez-Uriarte, M. Sánchez-Contador, J. Ereña, A.T. Aguayo, J. Bilbao, Direct synthesis of dimethyl ether from syngas on CuO-ZnO-MnO/SAPO-18 bifunctional catalyst, Int. J. Hydrog. Energy 41 (2016), https://doi.org/10.1016/j.ijhydene.2016.07.195.

[255] A. Ateka, I. Sierra, J. Ereña, J. Bilbao, A.T. Aguayo, Performance of CuO–ZnO–ZrO_2 and CuO–ZnO–MnO as metallic functions and SAPO-18 as acid function of the catalyst for the synthesis of DME co-feeding CO_2, Fuel Process. Technol. 152 (2016) 34–45, https://doi.org/10.1016/j.fuproc.2016.05.041.

[256] R. Raudaskoski, M.V. Niemelä, R.L. Keiski, The effect of ageing time on co-precipitated Cu/ZnO/ZrO_2 catalysts used in methanol synthesis from CO_2 and H_2, Top. Catal. 45 (2007) 57–60, https://doi.org/10.1007/S11244-007-0240-9.

[257] S. Natesakhawat, J.W. Lekse, J.P. Baltrus, P.R. Ohodnicki, B.H. Howard, X. Deng, C. Matranga, Active sites and structure-activity relationships of copper-based catalysts for carbon dioxide hydrogenation to methanol, ACS Catal. 2 (2012) 1667–1676, https://doi.org/10.1021/cs300008g.

[258] F. Frusteri, M. Cordaro, C. Cannilla, G. Bonura, Multifunctionality of Cu–ZnO–ZrO_2/H-ZSM5 catalysts for the one-step CO_2-to-DME hydrogenation reaction, Appl. Catal. B Environ. 162 (2015) 57–65, https://doi.org/10.1016/j.apcatb.2014.06.035.

[259] X. Jiang, N. Koizumi, X. Guo, C. Song, Bimetallic Pd–Cu catalysts for selective CO_2 hydrogenation to methanol, Appl. Catal. B Environ. 170–171 (2015) 173–185, https://doi.org/10.1016/J.APCATB.2015.01.010.

[260] F. Arena, K. Barbera, G. Italiano, G. Bonura, L. Spadaro, F. Frusteri, Synthesis, characterization and activity pattern of Cu–ZnO/ZrO_2 catalysts in the hydrogenation of carbon dioxide to methanol, J. Catal. 249 (2007) 185–194, https://doi.org/10.1016/J.JCAT.2007.04.003.

[261] H.J. Wernicke, L. Plass, F. Schmidt, Methanol generation, in: Methanol Basic Chem. Energy Feed. Futur. Asinger's Vis. Today, Springer Berlin Heidelberg, 2014, pp. 51–301, https://doi.org/10.1007/978-3-642-39709-7_4.

[262] D.S.A. Simakov, Thermocatalytic conversion of CO_2, in: Renew. Synth. Fuels Chem. from Carbon Dioxide, Springer, Cham, 2017, pp. 1–25, https://doi.org/10.1007/978-3-319-61112-9_1.

[263] E. Kunkes, M. Behrens, Methanol chemistry, in: Chem. Energy Storage, De Gruyter, Boston, 2013, pp. 413–442, https://doi.org/10.1515/9783110266320.413.

[264] I. Chorkendorff, J.W. Niemantsverdriet, Heterogeneous catalysis in practice: Hydrogen, in: Concepts Mod. Catal. Kinet, Wiley, 2003, pp. 301–348, https://doi.org/10.1002/3527602658.CH8.

[265] R. Singh, K. Tripathi, K.K. Pant, J.K. Parikh, Unravelling synergetic interaction over tandem Cu-ZnO-ZrO_2/hierarchical ZSM5 catalyst for CO_2 hydrogenation to methanol and DME, Fuel 318 (2022), 123641, https://doi.org/10.1016/J.FUEL.2022.123641.

[266] S. Chen, J. Zhang, P. Wang, X. Wang, F. Song, Y. Bai, M. Zhang, Y. Wu, H. Xie, Y. Tan, Effect of vapor-phase-treatment to CuZnZr catalyst on the reaction behaviors in CO_2 hydrogenation into methanol, ChemCatChem. 11 (2019) 1448–1457, https://doi.org/10.1002/CCTC.201801988.

[267] S. Chen, J. Zhang, F. Song, Q. Zhang, G. Yang, M. Zhang, X. Wang, H. Xie, Y. Tan, Induced high selectivity methanol formation during CO_2 hydrogenation over a $CuBr_2$-modified CuZnZr catalyst, J. Catal. 389 (2020) 47–59, https://doi.org/10.1016/J.JCAT.2020.05.023.

[268] F. Frusteri, G. Bonura, C. Cannilla, G. Drago Ferrante, A. Aloise, E. Catizzone, M. Migliori, G. Giordano, Stepwise tuning of metal-oxide and acid sites of CuZnZr-MFI hybrid catalysts for the direct DME synthesis by CO_2 hydrogenation, Appl. Catal. B Environ. 176–177 (2015) 522–531, https://doi.org/10.1016/j.apcatb.2015.04.032.

[269] T. Witoon, J. Chalorngtham, P. Dumrongbunditkul, M. Chareonpanich, J. Limtrakul, CO_2 hydrogenation to methanol over Cu/ZrO_2 catalysts: effects of zirconia phases, Chem. Eng. J. 293 (2016) 327–336, https://doi.org/10.1016/j.cej.2016.02.069.

[270] T. Witoon, N. Kachaban, W. Donphai, P. Kidkhunthod, K. Faungnawakij, M. Chareonpanich, J. Limtrakul, Tuning of catalytic CO_2 hydrogenation by changing composition of CuO–ZnO–ZrO_2 catalysts, Energy Convers. Manag. 118 (2016) 21–31, https://doi.org/10.1016/j.enconman.2016.03.075.

[271] K. Li, J.G. Chen, CO_2 hydrogenation to methanol over ZrO_2-containing catalysts: insights into ZrO_2 induced synergy, ACS Catal. 9 (2019) 7840–7861, https://doi.org/10.1021/acscatal.9b01943.

[272] J. Słoczyński, R. Grabowski, P. Olszewski, A. Kozłowska, J. Stoch, M. Lachowska, J. Skrzypek, Effect of metal oxide additives on the activity and stability of Cu/ZnO/ZrO_2 catalysts in the synthesis of methanol from CO_2 and H_2, Appl. Catal. A Gen. 310 (2006) 127–137, https://doi.org/10.1016/j.apcata.2006.05.035.

[273] J. Schumann, M. Eichelbaum, T. Lunkenbein, N. Thomas, M.C.Á. Galván, R. Schlögl, M. Behrens, Promoting strong metal support interaction: doping ZnO for enhanced activity of Cu/ZnO:M (M = Al, Ga, Mg) catalysts, ACS Catal. 5 (2015) 3260–3270, https://doi.org/10.1021/ACSCATAL.5B00188.

[274] A. Kornas, R. Grabowski, M. Śliwa, K. Samson, M. Ruggiero-Mikołajczyk, A. Żelazny, Dimethyl ether synthesis from CO_2 hydrogenation over hybrid catalysts: effects of preparation methods, React. Kinet. Mech. Catal. 121 (2017) 317–327, https://doi.org/10.1007/s11144-017-1153-7.

[275] M.M.-J. Li, Z. Zeng, F. Liao, X. Hong, S.C.E. Tsang, Enhanced CO_2 hydrogenation to methanol over CuZn nanoalloy in Ga modified Cu/ZnO catalysts, J. Catal. 343 (2016) 157–167, https://doi.org/10.1016/J.JCAT.2016.03.020.

[276] J. Toyir, P. Ramírez De La Piscina, J.L.G. Fierro, N. Homs, Highly effective conversion of CO_2 to methanol over supported and promoted copper-based catalysts: influence of support and promoter, Appl. Catal. B Environ. 29 (2001) 207–215, https://doi.org/10.1016/S0926-3373(00)00205-8.

[277] J. Toyir, P.R. De la Piscina, J.L.G. Fierro, N. Homs, Catalytic performance for CO_2 conversion to methanol of gallium-promoted copper-based catalysts: influence of metallic precursors, Appl. Catal. B Environ. 34 (2001) 255–266, https://doi.org/10.1016/S0926-3373(01)00203-X.

[278] W. Cai, P.R. De La Piscina, J. Toyir, N. Homs, CO_2 hydrogenation to methanol over CuZnGa catalysts prepared using microwave-assisted methods, Catal. Today 242 (2015) 193–199, https://doi.org/10.1016/J.CATTOD.2014.06.012.

[279] R. Ladera, F.J. Pérez-Alonso, J.M. González-Carballo, M. Ojeda, S. Rojas, J.L. G. Fierro, Catalytic valorization of CO_2 via methanol synthesis with Ga-promoted

Cu–ZnO–ZrO_2 catalysts, Appl. Catal. B Environ. 142–143 (2013) 241–248, https://doi.org/10.1016/J.APCATB.2013.05.019.
[280] P.B. Sanguineti, M.A. Baltanás, A.L. Bonivardi, Copper–gallia interaction in Cu–Ga_2O_3–ZrO_2 catalysts for methanol production from carbon oxide(s) hydrogenation, Appl. Catal. A Gen. 504 (2015) 476–481, https://doi.org/10.1016/J.APCATA.2014.11.021.
[281] J. Xiao, D. Mao, X. Guo, J. Yu, Methanol synthesis from CO_2 hydrogenation over CuO–ZnO–TiO_2 catalysts: the influence of TiO_2 content, Energy Technol. 3 (2015) 32–39, https://doi.org/10.1002/ENTE.201402091.
[282] L. Angelo, K. Kobl, L.M.M. Tejada, Y. Zimmermann, K. Parkhomenko, A.C. Roger, Study of CuZnMOx oxides (M = Al, Zr, Ce, CeZr) for the catalytic hydrogenation of CO_2 into methanol, Comptes Rendus Chim. 18 (2015) 250–260, https://doi.org/10.1016/J.CRCI.2015.01.001.
[283] E.L. Fornero, P.B. Sanguineti, D.L. Chiavassa, A.L. Bonivardi, M.A. Baltanás, Performance of ternary Cu–Ga_2O_3–ZrO_2 catalysts in the synthesis of methanol using CO_2-rich gas mixtures, Catal. Today 213 (2013) 163–170, https://doi.org/10.1016/J.CATTOD.2013.03.012.
[284] Y. Yang, M.G. White, P. Liu, Theoretical study of methanol synthesis from CO_2 hydrogenation on metal-doped Cu(111) surfaces, J. Phys. Chem. C 116 (2011) 248–256, https://doi.org/10.1021/JP208448C.
[285] S.L. Suib, New and future developments in catalysis : activation of carbon dioxide, Elsevier Science & Technology (2013), https://doi.org/10.1016/C2010-0-68687-1.
[286] N. Pasupulety, H. Driss, Y.A. Alhamed, A.A. Alzahrani, M.A. Daous, L. Petrov, Studies on Au/Cu–Zn–Al catalyst for methanol synthesis from CO_2, Appl. Catal. A Gen. 504 (2015) 308–318, https://doi.org/10.1016/J.APCATA.2015.01.036.
[287] O. Martin, C. Mondelli, D. Curulla-Ferré, C. Drouilly, R. Hauert, J. Pérez-Ramírez, Zinc-rich copper catalysts promoted by gold for methanol synthesis, ACS Catal. 5 (2015) 5607–5616, https://doi.org/10.1021/ACSCATAL.5B00877.
[288] N. Pasupulety, H. Driss, Y.A. Alhamed, A.A. Alzahrani, M.A. Daous, L. Petrov, Influence of preparation method on the catalytic activity of Au/Cu-Zn-Al catalyst for CO_2 hydrogenation to methanol, in: Chim. Cinétique Catal, 2015, pp. 1511–1518, https://doi.org/10.1007/978-3-319-61112-9_1.
[289] J.L.G. Fierro, I. Melián-Cabrera, M. López Granados, Reverse topotactic transformation of a Cu–Zn–Al catalyst during Wet Pd impregnation: relevance for the performance in methanol synthesis from CO_2/H_2 mixtures, J. Catal. 210 (2002) 273–284, https://doi.org/10.1006/JCAT.2002.3676.
[290] I. Melián-Cabrera, M.L. Granados, J.L.G. Fierro, Pd-Modified Cu–Zn catalysts for methanol synthesis from CO_2/H_2 mixtures: catalytic structures and performance, J. Catal. 210 (2002) 285–294, https://doi.org/10.1006/jcat.2002.3677.
[291] E.J. Choi, Y.H. Lee, D.W. Lee, D.J. Moon, K.Y. Lee, Hydrogenation of CO_2 to methanol over Pd–Cu/CeO_2 catalysts, Mol. Catal. 434 (2017) 146–153, https://doi.org/10.1016/J.MCAT.2017.02.005.
[292] L. Liu, F. Fan, M. Bai, F. Xue, X. Ma, Z. Jiang, T. Fang, Mechanistic study of methanol synthesis from CO_2 hydrogenation on Rh-doped Cu(111) surfaces, Mol. Catal. 466 (2019) 26–36, https://doi.org/10.1016/J.MCAT.2019.01.009.
[293] G. Prieto, J. Zečević, H. Friedrich, K.P. de Jong, P.E. de Jongh, Towards stable catalysts by controlling collective properties of supported metal nanoparticles, Nat. Mater. 12 (2012) 34–39, https://doi.org/10.1038/nmat3471.
[294] C. Zhang, P. Liao, H. Wang, J. Sun, P. Gao, Preparation of novel bimetallic CuZn-BTC coordination polymer nanorod for methanol synthesis from CO_2 hydrogenation, Mater. Chem. Phys. 215 (2018) 211–220, https://doi.org/10.1016/J.MATCHEMPHYS.2018.05.028.
[295] J. Wang, G. Li, Z. Li, C. Tang, Z. Feng, H. An, H. Liu, T. Liu, C. Li, A highly selective and stable ZnO-ZrO_2 solid solution catalyst for CO_2 hydrogenation to methanol, Sci. Adv. 3 (2017), e1701290, https://doi.org/10.1126/SCIADV.1701290.
[296] J. Wang, C.Y. Liu, T.P. Senftle, J. Zhu, G. Zhang, X. Guo, C. Song, Variation in the In_2O_3 crystal phase alters catalytic performance toward the reverse water gas shift reaction, ACS Catal. 10 (2020) 3264–3273, https://doi.org/10.1021/acscatal.9b04239.
[297] T.Y. Chen, C. Cao, T.B. Chen, X. Ding, H. Huang, L. Shen, X. Cao, M. Zhu, J. Xu, J. Gao, Y.F. Han, Unraveling highly tunable selectivity in CO_2 hydrogenation over bimetallic In-Zr oxide catalysts, ACS Catal. 9 (2019) 8785–8797, https://doi.org/10.1021/acscatal.9b01869.
[298] M.S. Frei, M. Capdevila-Cortada, R. García-Muelas, C. Mondelli, N. López, J. A. Stewart, D. Curulla Ferré, J. Pérez-Ramírez, Mechanism and microkinetics of methanol synthesis via CO_2 hydrogenation on indium oxide, J. Catal. 361 (2018) 313–321, https://doi.org/10.1016/j.jcat.2018.03.014.
[299] J. Ye, C. Liu, D. Mei, Q. Ge, Active oxygen vacancy site for methanol synthesis from CO_2 hydrogenation on In_2O_3 (110): a DFT study, ACS Catal. 3 (2013) 1296–1306, https://doi.org/10.1021/cs400132a.
[300] O. Martin, A.J. Martín, C. Mondelli, S. Mitchell, T.F. Segawa, R. Hauert, C. Drouilly, D. Curulla-Ferré, J. Pérez-Ramírez, Indium oxide as a superior catalyst for methanol synthesis by CO_2 hydrogenation, Angew. Chemie Int. Ed. 55 (2016) 6261–6265, https://doi.org/10.1002/ANIE.201600943.
[301] S. Wang, P. Wang, Z. Qin, W. Yan, M. Dong, J. Li, J. Wang, W. Fan, Enhancement of light olefin production in CO_2 hydrogenation over In_2O_3-based oxide and SAPO-34 composite, J. Catal. 391 (2020) 459–470, https://doi.org/10.1016/J.JCAT.2020.09.010.
[302] J. Wang, G. Zhang, J. Zhu, X. Zhang, F. Ding, A. Zhang, X. Guo, C. Song, CO_2 hydrogenation to methanol over In_2O_3-based catalysts: from mechanism to catalyst development, ACS Catal. 11 (2021) 1406–1423, https://doi.org/10.1021/acscatal.0c03665.
[303] S. Ghosh, J. Sebastian, L. Olsson, D. Creaser, Experimental and kinetic modeling studies of methanol synthesis from CO_2 hydrogenation using In_2O_3 catalyst, Chem. Eng. J. 416 (2021), 129120, https://doi.org/10.1016/j.cej.2021.129120.
[304] M.S. Frei, C. Mondelli, A. Cesarini, F. Krumeich, R. Hauert, J.A. Stewart, D. C. Ferré, J. Pérez-Ramírez, Role of zirconia in indium oxide-catalyzed CO_2 hydrogenation to methanol, ACS Catal. 10 (2019) 1133–1145, https://doi.org/10.1021/ACSCATAL.9B03305.
[305] C.-S. Li, G. Melaet, W.T. Ralston, K. An, C. Brooks, Y. Ye, Y.-S. Liu, J. Zhu, J. Guo, S. Alayoglu, G.A. Somorjai, High-performance hybrid oxide catalyst of manganese and cobalt for low-pressure methanol synthesis, Nat. Commun. 6 (2015) 1–5, https://doi.org/10.1038/ncomms7538.
[306] K. Stangeland, D.Y. Kalai, Y. Ding, Z. Yu, Mesoporous manganese-cobalt oxide spinel catalysts for CO_2 hydrogenation to methanol, J. CO2 Util. 32 (2019) 146–154, https://doi.org/10.1016/J.JCOU.2019.04.018.
[307] L. Wang, E. Guan, Y. Wang, L. Wang, Z. Gong, Y. Cui, X. Meng, B.C. Gates, F.-S. Xiao, Silica accelerates the selective hydrogenation of CO_2 to methanol on cobalt catalysts, Nat. Commun. 11 (2020) 1–9, https://doi.org/10.1038/s41467-020-14817-9.
[308] J. Xu, X. Su, X. Liu, X. Pan, G. Pei, Y. Huang, X. Wang, T. Zhang, H. Geng, Methanol synthesis from CO_2 and H_2 over Pd/ZnO/Al_2O_3: catalyst structure dependence of methanol selectivity, Appl. Catal. A Gen. 514 (2016) 51–59, https://doi.org/10.1016/J.APCATA.2016.01.006.
[309] N. Rui, Z. Wang, K. Sun, J. Ye, Q. Ge, C. Jun Liu, CO_2 hydrogenation to methanol over Pd/In_2O_3: effects of Pd and oxygen vacancy, Appl. Catal. B Environ. 218 (2017) 488–497, https://doi.org/10.1016/J.APCATB.2017.06.069.
[310] C. Wu, P. Zhang, Z. Zhang, L. Zhang, G. Yang, B. Han, Efficient hydrogenation of CO_2 to methanol over supported subnanometer gold catalysts at low temperature, ChemCatChem. 9 (2017) 3691–3696, https://doi.org/10.1002/CCTC.201700872.
[311] D.L. Chiavassa, S.E. Collins, A.L. Bonivardi, M.A. Baltanás, Methanol synthesis from CO_2/H_2 using Ga_2O_3-Pd/silica catalysts: kinetic modeling, Chem. Eng. J. 150 (2009) 204–212, https://doi.org/10.1016/j.cej.2009.02.013.
[312] O.A. Ojelade, S.F. Zaman, M.A. Daous, A.A. Al-Zahrani, A.S. Malik, H. Driss, G. Shterk, J. Gascon, Optimizing Pd:Zn molar ratio in PdZn/CeO_2 for CO_2 hydrogenation to methanol, Appl. Catal. A Gen. 584 (2019), 117185, https://doi.org/10.1016/J.APCATA.2019.117185.
[313] A.S. Malik, S.F. Zaman, A.A. Al-Zahrani, M.A. Daous, Turning CO_2 into di-methyl ether (DME) using Pd based catalysts – Role of Ca in tuning the activity and selectivity, J. Ind. Eng. Chem. 103 (2021) 67–79, https://doi.org/10.1016/J.JIEC.2021.07.019.
[314] H. Bahruji, M. Bowker, G. Hutchings, N. Dimitratos, P. Wells, E. Gibson, W. Jones, C. Brookes, D. Morgan, G. Lalev, Pd/ZnO catalysts for direct CO_2 hydrogenation to methanol, J. Catal. 343 (2016) 133–146, https://doi.org/10.1016/J.JCAT.2016.03.017.
[315] H. Bahruji, M. Bowker, W. Jones, J. Hayward, J.R. Esquius, D.J. Morgan, G. J. Hutchings, PdZn catalysts for CO_2 hydrogenation to methanol using chemical vapour impregnation (CVI), Faraday Discuss. 197 (2017) 309–324, https://doi.org/10.1039/C6FD00189K.
[316] Y. Hartadi, D. Widmann, R.J. Behm, CO_2 hydrogenation to methanol on supported Au catalysts under moderate reaction conditions: support and particle size effects, ChemSusChem. 8 (2015) 456–465, https://doi.org/10.1002/CSSC.201402645.
[317] Y. Hartadi, D. Widmann, R.J. Behm, Methanol formation by CO_2 hydrogena on Au/ZnO catalysts – effect of total pressure and influence of CO on the reaction characteristics, J. Catal. 333 (2016) 238–250, https://doi.org/10.1016/J.JCAT.2015.11.002.
[318] Y. Hartadi, D. Widmann, R.J. Behm, Methanol synthesis via CO_2 hydrogenation over a Au/ZnO catalyst: an isotope labelling study on the role of CO in the reaction process, Phys. Chem. Chem. Phys. 18 (2016) 10781–10791, https://doi.org/10.1039/C5CP06888F.
[319] D. Liu, C. Yao, J. Zhang, D. Fang, D. Chen, Catalytic dehydration of methanol to dimethyl ether over modified γ-Al_2O_3 catalyst, Fuel 90 (2011) 1738–1742, https://doi.org/10.1016/J.FUEL.2011.01.038.
[320] A. Ghorbanpour, J.D. Rimer, L.C. Grabow, Computational assessment of the dominant factors governing the mechanism of methanol dehydration over H-ZSM-5 with heterogeneous aluminum distribution, ACS Catal. 6 (2016) 2287–2298, https://doi.org/10.1021/acscatal.5b02367.
[321] M. Xu, J.H. Lunsford, D.W. Goodman, A. Bhattacharyya, Synthesis of dimethyl ether (DME) from methanol over solid-acid catalysts, Appl. Catal. A Gen. 149 (1997) 289–301, https://doi.org/10.1016/S0926-860X(96)00275-X.
[322] S.S. Akarmazyan, P. Panagiotopoulou, A. Kambolis, C. Papadopoulou, D. I. Kondarides, Methanol dehydration to dimethylether over Al_2O_3 catalysts, Appl. Catal. B Environ. 145 (2014) 136–148, https://doi.org/10.1016/j.apcatb.2012.11.043.
[323] X. Sun, S. Mueller, Y. Liu, H. Shi, G.L. Haller, M. Sanchez-Sanchez, A.C. Van Veen, J.A. Lercher, On reaction pathways in the conversion of methanol to hydrocarbons on HZSM-5, J. Catal. 317 (2014) 185–197, https://doi.org/10.1016/J.JCAT.2014.06.017.
[324] B. Şeker, A.K. Dizaji, V. Balci, A. Uzun, MCM-41-supported tungstophosphoric acid as an acid function for dimethyl ether synthesis from CO_2 hydrogenation, Renew. Energy 171 (2021) 47–57, https://doi.org/10.1016/J.RENENE.2021.02.060.
[325] D.F. Carvalho, G.C. Almeida, R.S. Monteiro, C.J.A. Mota, Hydrogenation of CO_2 to methanol and dimethyl ether over a bifunctional Cu·ZnO catalyst impregnated on modified γ-alumina, Energy Fuel 34 (2020) 7269–7274, https://doi.org/10.1021/ACS.ENERGYFUELS.0C00680.

[326] E. Catizzone, A. Aloise, M. Migliori, G. Giordano, Dimethyl ether synthesis via methanol dehydration: effect of zeolite structure, Appl. Catal. A Gen. 502 (2015) 215–220, https://doi.org/10.1016/j.apcata.2015.06.017.

[327] E. Catizzone, E. Giglio, M. Migliori, P.C. Cozzucoli, G. Giordano, The effect of zeolite features on the dehydration reaction of methanol to dimethyl ether: catalytic behaviour and kinetics, Materials (Basel). 13 (2020) 1–15, https://doi.org/10.3390/ma13235577.

[328] J. Ereña, R. Garoña, J.M. Arandes, A.T. Aguayo, J. Bilbao, Effect of operating conditions on the synthesis of dimethyl ether over a CuO-ZnO-Al_2O_3/NaHZSM-5 bifunctional catalyst, Catal. Today 107–108 (2005) 467–473, https://doi.org/10.1016/j.cattod.2005.07.116.

[329] L. Vanoye, A. Favre-Réguillon, P. Munno, J.F. Rodríguez, S. Dupuy, S. Pallier, I. Pitault, C. De Bellefon, Methanol dehydration over commercially available zeolites: effect of hydrophobicity, Catal. Today 215 (2013) 239–242, https://doi.org/10.1016/j.cattod.2013.01.012.

[330] M. Sánchez-Contador, A. Ateka, A.T. Aguayo, J. Bilbao, Behavior of SAPO-11 as acid function in the direct synthesis of dimethyl ether from syngas and CO_2, J. Ind. Eng. Chem. 63 (2018) 245–254, https://doi.org/10.1016/j.jiec.2018.02.022.

[331] J. Abu-Dahrieh, D. Rooney, A. Goguet, Y. Saih, Activity and deactivation studies for direct dimethyl ether synthesis using CuO–ZnO–Al_2O_3 with NH4ZSM-5, HZSM-5 or γ-Al_2O_3, Chem. Eng. J. 203 (2012) 201–211, https://doi.org/10.1016/j.cej.2012.07.011.

[332] S.M.K. Aboul-Fotouh, L.I. Ali, M.A. Naghmash, N.A.K. Aboul-Gheit, Effect of the Si/Al ratio of HZSM-5 zeolite on the production of dimethyl ether before and after ultrasonication, J. Fuel Chem. Technol. 45 (2017) 581–588, https://doi.org/10.1016/S1872-5813(17)30030-0.

[333] M. Cai, A. Palčić, V. Subramanian, S. Moldovan, O. Ersen, V. Valtchev, V. V. Ordomsky, A.Y. Khodakov, Direct dimethyl ether synthesis from syngas on copper–zeolite hybrid catalysts with a wide range of zeolite particle sizes, J. Catal. 338 (2016) 227–238, https://doi.org/10.1016/j.jcat.2016.02.025.

[334] A. García-Trenco, A. Martínez, Direct synthesis of DME from syngas on hybrid CuZnAl/ZSM-5 catalysts: new insights into the role of zeolite acidity, Appl. Catal. A Gen. 411–412 (2012) 170–179, https://doi.org/10.1016/j.apcata.2011.10.036.

[335] M.-H. Zhang, Z.-M. Liu, G.-D. Lin, H.-B. Zhang, Pd/CNT-promoted $CuZrO_2$/HZSM-5 hybrid catalysts for direct synthesis of DME from CO_2/H_2, Appl. Catal. A Gen. 451 (2013) 28–35, https://doi.org/10.1016/j.apcata.2012.10.038.

[336] J.M. Müller, G.C. Mesquita, S.M. Franco, L.D. Borges, J.L. De Macedo, J.A. Dias, S. C.L. Dias, Solid-state dealumination of zeolites for use as catalysts in alcohol dehydration, Microporous Mesoporous Mater. 204 (2015) 50–57, https://doi.org/10.1016/J.MICROMESO.2014.11.002.

[337] V.V. Ordomsky, M. Cai, V. Sushkevich, S. Moldovan, O. Ersen, C. Lancelot, V. Valtchev, A.Y. Khodakov, The role of external acid sites of ZSM-5 in deactivation of hybrid CuZnAl/ZSM-5 catalyst for direct dimethyl ether synthesis from syngas, Appl. Catal. A Gen. 486 (2014) 266–275, https://doi.org/10.1016/j.apcata.2014.08.030.

[338] Y. Wei, P.E. de Jongh, M.L.M. Bonati, D.J. Law, G.J. Sunley, K.P. de Jong, Enhanced catalytic performance of zeolite ZSM-5 for conversion of methanol to dimethyl ether by combining alkaline treatment and partial activation, Appl. Catal. A Gen. 504 (2015) 211–219, https://doi.org/10.1016/j.apcata.2014.12.027.

[339] S.M.K. Aboul-Fotouh, N.A.K. Aboul-Gheit, M.A. Naghmash, Dimethyletherproduction on zeolite catalysts activated by Cl−, F− and/or ultrasonication, J. Fuel Chem. Technol. 44 (2016) 428–436, https://doi.org/10.1016/S1872-5813(16)30022-6.

[340] K. Krim, A. Sachse, A. Le Valant, Y. Pouilloux, S. Hocine, One step dimethyl ether (DME) synthesis from CO_2 hydrogenation over hybrid catalysts containing Cu/ZnO/Al_2O_3 and nano-sized hollow ZSM-5 zeolites, Catal. Letters. 1 (2022) 1–12, https://doi.org/10.1007/S10562-022-03949-W/FIGURES/9.

[341] W. Dai, W. Kong, G. Wu, N. Li, L. Li, N. Guan, Catalytic dehydration of methanol to dimethyl ether over aluminophosphate and silico-aluminophosphate molecular sieves, Catal. Commun. 12 (2011) 535–538, https://doi.org/10.1016/j.catcom.2010.11.019.

[342] Z. Chen, X. Li, Y. Xu, Y. Dong, W. Lai, W. Fang, X. Yi, Fabrication of nano-sized SAPO-11 crystals with enhanced dehydration of methanol to dimethyl ether, Catal. Commun. 103 (2018) 1–4, https://doi.org/10.1016/j.catcom.2017.09.002.

[343] A.T. Aguayo, A.E.S. del Campo, A.G. Gayubo, A. Tarrío, J. Bilbao, Deactivation by coke of a catalyst based on a SAPO-34 in the transformation of methanol into olefins, J. Chem. Technol. Biotechnol. 74 (1999) 315–321, https://doi.org/10.1002/(SICI)1097-4660(199904)74:4<315::AID-JCTB34>3.0.CO;2-G.

[344] J. Zhong, J. Han, Y. Wei, Z. Liu, Catalysts and shape selective catalysis in the methanol-to-olefin (MTO) reaction, J. Catal. 396 (2021) 23–31, https://doi.org/10.1016/J.JCAT.2021.01.027.

[345] F. Frusteri, M. Migliori, C. Cannilla, L. Frusteri, E. Catizzone, A. Aloise, G. Giordano, G. Bonura, Direct CO_2-to-DME hydrogenation reaction: new evidences of a superior behaviour of FER-based hybrid systems to obtain high DME yield, J. CO2 Util. 18 (2017) 353–361, https://doi.org/10.1016/j.jcou.2017.01.030.

[346] L. Yao, X. Shen, Y. Pan, Z. Peng, Unravelling proximity-driven synergetic effect within CIZO-SAPO bifunctional catalyst for CO_2 hydrogenation to DME, Energy and Fuels. 34 (2020) 8635–8643, https://doi.org/10.1021/acs.energyfuels.0c01256.

[347] A. Ateka, M. Sánchez-Contador, J. Ereña, A.T. Aguayo, J. Bilbao, Catalyst configuration for the direct synthesis of dimethyl ether from CO and CO_2 hydrogenation on CuO–ZnO–MnO/SAPO-18 catalysts, React. Kinet. Mech. Catal. 124 (2018) 401–418, https://doi.org/10.1007/s11144-018-1344-x.

[348] G. Bonura, M. Cordaro, L. Spadaro, C. Cannilla, F. Arena, F. Frusteri, Hybrid Cu–ZnO–ZrO_2/H-ZSM5 system for the direct synthesis of DME by CO_2 hydrogenation, Appl. Catal. B Environ. 140–141 (2013) 16–24, https://doi.org/10.1016/j.apcatb.2013.03.048.

[349] G. Bonura, F. Frusteri, C. Cannilla, G. Drago Ferrante, A. Aloise, E. Catizzone, M. Migliori, G. Giordano, Catalytic features of CuZnZr–zeolite hybrid systems for the direct CO_2-to-DME hydrogenation reaction, Catal. Today 277 (2016) 48–54, https://doi.org/10.1016/j.cattod.2016.02.013.

[350] G. Bonura, M. Cordaro, C. Cannilla, A. Mezzapica, L. Spadaro, F. Arena, F. Frusteri, Catalytic behaviour of a bifunctional system for the one step synthesis of DME by CO_2 hydrogenation, Catal. Today 228 (2014) 51–57, https://doi.org/10.1016/j.cattod.2013.11.017.

[351] M. Sánchez-Contador, A. Ateka, A.T. Aguayo, J. Bilbao, Direct synthesis of dimethyl ether from CO and CO_2 over a core-shell structured CuO-ZnO-ZrO_2@SAPO-11 catalyst, Fuel Process. Technol. 179 (2018) 258–268, https://doi.org/10.1016/j.fuproc.2018.07.009.

[352] G. Yang, M. Thongkam, T. Vitidsant, Y. Yoneyama, Y. Tan, N. Tsubaki, A double-shell capsule catalyst with core–shell-like structure for one-step exactly controlled synthesis of dimethyl ether from CO_2 containing syngas, Catal. Today 171 (2011) 229–235, https://doi.org/10.1016/j.cattod.2011.02.021.

[353] Y. Wang, W. Wang, Y. Chen, J. Ma, J. Zheng, R. Li, Core–shell catalyst CuO–ZnO–Al_2O_3@Al_2O_3 for dimethyl ether synthesis from syngas, Chem. Lett. 42 (2013) 335–337, https://doi.org/10.1246/CL.121099.

[354] S. Guffanti, C.G. Visconti, G. Groppi, Model analysis of the role of kinetics, adsorption capacity, and heat and mass transfer effects in sorption enhanced dimethyl ether synthesis, Ind. Eng. Chem. Res. 60 (2021) 6767–6783, https://doi.org/10.1021/acs.iecr.1c00521.

[355] Y. Wang, W. Wang, Y. Chen, J. Ma, R. Li, Synthesis of dimethyl ether from syngas over core–shell structure catalyst CuO–ZnO–Al_2O_2@SiO_2–Al_2O_3, Chem. Eng. J. 250 (2014) 248–256, https://doi.org/10.1016/j.cej.2014.04.018.

[356] R. Phienluphon, K. Pinkaew, G. Yang, J. Li, Q. Wei, Y. Yoneyama, T. Vitidsant, N. Tsubaki, Designing core (Cu/ZnO/Al_2O_3)–shell (SAPO-11) zeolite capsule catalyst with a facile physical way for dimethyl ether direct synthesis from syngas, Chem. Eng. J. 270 (2015) 605–611, https://doi.org/10.1016/j.cej.2015.02.071.

[357] S. Guffanti, C.G. Visconti, G. Groppi, Model analysis of the effects of active phase distribution at the pellet scale in catalytic reactors for the direct dimethyl ether synthesis, Ind. Eng. Chem. Res. 59 (2020) 14252–14266, https://doi.org/10.1021/acs.iecr.0c01938.

[358] K. Pinkaew, G. Yang, T. Vitidsant, Y. Jin, C. Zeng, Y. Yoneyama, N. Tsubaki, A new core–shell-like capsule catalyst with SAPO-46 zeolite shell encapsulated Cr/ZnO for the controlled tandem synthesis of dimethyl ether from syngas, Fuel 111 (2013) 727–732, https://doi.org/10.1016/j.fuel.2013.03.027.

[359] M. Sánchez-Contador, A. Ateka, M. Ibáñez, J. Bilbao, A.T. Aguayo, Influence of the operating conditions on the behavior and deactivation of a CuO-ZnO-ZrO_2@SAPO-11 core-shell-like catalyst in the direct synthesis of DME, Renew. Energy 138 (2019) 585–597, https://doi.org/10.1016/j.renene.2019.01.093.

[360] R. Nie, H. Lei, S. Pan, L. Wang, J. Fei, Z. Hou, Core–shell structured CuO–ZnO@H-ZSM-5 catalysts for CO hydrogenation to dimethyl ether, Fuel 96 (2012) 419–425, https://doi.org/10.1016/j.fuel.2011.12.048.

[361] A. García-Trenco, A. Martínez, The influence of zeolite surface-aluminum species on the deactivation of CuZnAl/zeolite hybrid catalysts for the direct DME synthesis, Catal. Today 227 (2014) 144–153, https://doi.org/10.1016/j.cattod.2013.09.051.

[362] S. Mitchell, N.L. Michels, J. Pérez-Ramírez, From powder to technical body: the undervalued science of catalyst scale up, Chem. Soc. Rev. 42 (2013) 6094–6112, https://doi.org/10.1039/c3cs60076a.

[363] I. Melián-Cabrera, Catalytic materials: concepts to understand the pathway to implementation, Ind. & Eng. Chem. Res. 60 (2021) 18545–18559, https://doi.org/10.1021/acs.iecr.1c02681.

[364] F. Magzoub, X. Li, S. Lawson, F. Rezaei, A.A. Rownaghi, 3D-printed HZSM-5 and 3D-HZM5@SAPO-34 structured monoliths with controlled acidity and porosity for conversion of methanol to dimethyl ether, Fuel 280 (2020), 118628, https://doi.org/10.1016/J.FUEL.2020.118628.

[365] I. Pérez-Miqueo, O. Sanz, M. Montes, Highly conductive structured catalytic reactors for one-step synthesis of dimethyl ether, Ind. Eng. Chem. Res. 60 (2021) 6676–6686, https://doi.org/10.1021/acs.iecr.0c05821.

[366] F. Dadgar, R. Myrstad, P. Pfeifer, A. Holmen, H.J. Venvik, Catalyst deactivation during one-step dimethyl ether synthesis from synthesis gas, Catal. Lett. 1474 (147) (2017) 865–879, https://doi.org/10.1007/S10562-017-1971-2.

[367] A. Ateka, P. Pérez-Uriarte, I. Sierra, J. Ereña, J. Bilbao, A.T. Aguayo, Regenerability of the CuO–ZnO–MnO/SAPO-18 catalyst used in the synthesis of dimethyl ether in a single step, React. Kinet. Mech. Catal. 119 (2016) 655–670, https://doi.org/10.1007/s11144-016-1057-y.

[368] J. Ereña, I. Sierra, M. Olazar, A.G. Gayubo, A.T. Aguayo, Deactivation of a CuO-ZnO-Al_2O_3/γ-Al_2O_3 catalyst in the synthesis of dimethyl ether, Ind. Eng. Chem. Res. 47 (2008) 2238–2247, https://doi.org/10.1021/ie071478f.

[369] A. Ateka, J. Ereña, P. Pérez-Uriarte, A.T.A.T. Aguayo, J. Bilbao, Effect of the content of CO_2 and H_2 in the feed on the conversion of CO_2 in the direct synthesis of dimethyl ether over a CuO-ZnO-Al_2O_3/SAPO-18 catalyst, Int. J. Hydrog. Energy 42 (2017) 27130–27138, https://doi.org/10.1016/j.ijhydene.2017.09.104.

[370] A.T. Aguayo, J. Ereña, I. Sierra, M. Olazar, J. Bilbao, Deactivation and regeneration of hybrid catalysts in the single-step synthesis of dimethyl ether from syngas and CO_2, Catal. Today 106 (2005) 265–270, https://doi.org/10.1016/j.cattod.2005.07.144.

[371] R. Peláez, E. Bryce, P. Marín, S. Ordóñez, Catalyst deactivation in the direct synthesis of dimethyl ether from syngas over $CuO/ZnO/Al_2O_3$ and γ-Al_2O_3 mechanical mixtures, Fuel Process. Technol. 179 (2018) 378–386, https://doi.org/10.1016/J.FUPROC.2018.07.029.
[372] S. Asthana, C. Samanta, B. Saha, R. Kumar Voolapalli, K. Kishore Pant, Steering the aspects of MgO-induced structure sensitivity in Cu-based catalysts for CO_2-rich syngas conversion to dimethyl ether: Cu/Zn ratio and lattice parameters, Energy & Fuels 36 (2022) 2673–2687, https://doi.org/10.1021/acs.energyfuels.1c03945.
[373] S. Ren, X. Fan, Z. Shang, W.R. Shoemaker, L. Ma, T. Wu, S. Li, N.B. Klinghoffer, M. Yu, X. Liang, Enhanced catalytic performance of Zr modified $CuO/ZnO/Al_2O_3$ catalyst for methanol and DME synthesis via CO_2 hydrogenation, J. CO2 Util. 36 (2020) 82–95, https://doi.org/10.1016/J.JCOU.2019.11.013.
[374] Y. Luan, H. Xu, C. Yu, W. Li, S. Hou, Effects and control of steam in the systems of methanol and DME synthesis from syngas over Cu-based catalysts, Catal. Letters. 125 (2008) 271–276, https://doi.org/10.1007/S10562-008-9529-Y.
[375] Y. Wang, W. Gao, K. Li, Y. Zheng, Z. Xie, W. Na, J.G. Chen, H. Wang, Strong evidence of the role of H_2O in affecting methanol selectivity from CO_2 hydrogenation over Cu-ZnO-ZrO_2, Chem. 6 (2020) 419–430, https://doi.org/10.1016/J.CHEMPR.2019.10.023.
[376] X. Fan, S. Ren, B. Jin, S. Li, M. Yu, X. Liang, Enhanced stability of Fe-modified CuO-ZnO-ZrO_2-Al_2O_3/HZSM-5 bifunctional catalysts for dimethyl ether synthesis from CO_2 hydrogenation, Chinese, J. Chem. Eng. 38 (2021) 106–113, https://doi.org/10.1016/J.CJCHE.2020.11.031.
[377] X. Fan, B. Jin, S. Ren, S. Li, M. Yu, X. Liang, Roles of interaction between components in CZZA/HZSM-5 catalyst for dimethyl ether synthesis via CO_2 hydrogenation, AICHE J. 67 (2021), e17353, https://doi.org/10.1002/AIC.17353.
[378] X.D. Peng, B.A. Toseland, R.P. Underwood, A novel mechanism of catalyst deactivation in liquid phase synthesis gas-to-DME reactions, Stud. Surf. Sci. Catal. 111 (1997) 175–182, https://doi.org/10.1016/S0167-2991(97)80153-X.
[379] A. García-Trenco, A. Vidal-Moya, A. Martínez, Study of the interaction between components in hybrid CuZnAl/HZSM-5 catalysts and its impact in the syngas-to-DME reaction, Catal. Today 179 (2012) 43–51, https://doi.org/10.1016/j.cattod.2011.06.034.
[380] A. García-Trenco, A. Martínez, A rational strategy for preparing Cu–ZnO/H-ZSM-5 hybrid catalysts with enhanced stability during the one-step conversion of syngas to dimethyl ether (DME), Appl. Catal. A Gen. 493 (2015) 40–49, https://doi.org/10.1016/j.apcata.2015.01.007.